

EUMETSAT Satellite Application Facility on Climate Monitoring

The EUMETSAT
Network of
Satellite
Application
Facilities



CM SAF

Climate Monitoring

CM SAF Cloud, Albedo, Radiation dataset, AVHRR-based, Edition 1 (CLARA-A1)

Cloud Products

Validation Report

[DOI: 10.5676/EUM_SAF_CM/CLARA_AVHRR/V001](https://doi.org/10.5676/EUM_SAF_CM/CLARA_AVHRR/V001)

Fractional Cloud Cover

CM-05

Joint Cloud property histogram

CM-11

Cloud Top level

CM-17

Cloud Optical Thickness

CM-34

(Cloud Phase

CM-38

Liquid Water Path

CM-43

Ice Water Path

CM-47

Reference Number:

SAF/CM/SMHI/VAL/GAC/CLD

Issue/Revision Index:

1.2

Date:

30.04.2012

 	<p align="center">EUMETSAT SAF on CLIMATE MONITORING Validation Report Cloud product GAC Edition 1</p>	<p>Doc.No.:SAF/CM/SMHI/VAL/GAC/CLD Issue: 1.1 Date: 30.04.2012</p>
---	---	--

Document Signature Table

	Name	Function	Signature	Date
Author	Karl-Göran Karlsson	CM SAF scientist		30/05/2012
Editor	Rainer Hollmann	Science Coordinator		30/05/2012
Approval	Steering Group			26/09/2012
Release	Martin Werscheck	Project Manager		30/11/2012



Distribution List

Internal Distribution	
Name	No. Copies
DWD Archive	1
CM SAF Team	1

External Distribution		
Company	Name	No. Copies
PUBLIC		1

Document Change Record

Issue/Revision	Date	DCN No.	Changed Pages/Paragraphs
1.0	21/11/2011	SAF/CM/SMHI/VAL/GAC/CLD	First official version submitted for DRI5
1.1	30/04/2012	SAF/CM/SMHI/VAL/GAC/CLD	Revised version at DRI-5 Close-out
1.2	30/05/2012	SAF/CM/SMHI/VAL/GAC/CLD	Implementation of RIDs from DRI5 close-out. - editorial update of cover page to account for DOI number and edition name - editorial update of the introduction section of CM SAF

 	<p align="center">EUMETSAT SAF on CLIMATE MONITORING Validation Report Cloud product GAC Edition 1</p>	<p>Doc.No.:SAF/CM/SMHI/VAL/GAC/CLD Issue: 1.1 Date: 30.04.2012</p>
---	--	--

Applicable documents

Reference	Title	Code
AD 1	CM SAF Product Requirements Document	SAF/CM/DWD/PRD/1.7
AD 2	CM SAF Service Specification Document	SAF/CM/DWD/SeSp/1.9
AD 3	SYSTEMATIC OBSERVATION REQUIREMENTS FOR SATELLITE- BASED DATA PRODUCTS FOR CLIMATE - 2011 Update	GCOS-154

Reference Documents

Reference	Title	Code
RD 1	Product User Manual Cloud Products CLARA-A1	SAF/CM/DWD/PUM/GAC/CLD/1.2
RD 2	Algorithm Theoretical Basis Document Cloud products CLARA-A1	SAF/CM/DWD/ATBD/GAC/CLD/1.1
RD 3	Algorithm Theoretical Basis Document NWCSAF/PPP "Cloud mask"	SAF-NWC-CDOP-SMHI-PPS-SCI- ATBD-3_v2_3_3
RD 4	Algorithm Theoretical Basis Document NWCSAF/PPS "Cloud top Temperature, Pressure, Height"	SAF-NWC-CDOP-SMHI-PPS-SCI- ATBD-3_v2_3_1
RD 5	Algorithm Theoretical Basis Document Cloud physical products CLARA-A1	SAF/CM/KNMI/ATBD/GAC/PPP/1.1
RD 6	Algorithm Theoretical Basis Document Joint Cloud property Histograms AVHRR/SEVIRI	SAF/CM/SMHI/ATBD/JCH/1.1




 	<p align="center">EUMETSAT SAF on CLIMATE MONITORING Validation Report Cloud product GAC Edition 1</p>	<p>Doc.No.:SAF/CM/SMHI/VAL/GAC/CLD Issue: 1.1 Date: 30.04.2012</p>
---	---	--

Table of Contents

List of Figures	5
List of Tables	11
1 Executive Summary	14
2 The EUMETSAT SAF on Climate Monitoring	19
3 Introduction to the AVHRR GAC dataset	20
4 Cloud products and validation strategy	24
5 Data Sets for Comparison with GAC	28
5.1 Manual cloud observations from surface stations (SYNOP)	28
5.2 A-Train (CALIPSO-CALIOP)	29
5.3 Cloud liquid water observations from microwave imagers	32
5.4 PATMOS-x	32
5.5 ISCCP	34
5.6 MODIS	36
6 Evaluation of GAC Parameters	37
6.1 Macroscopical cloud products	37
6.2 Microphysical cloud products	96
6.3 Multi-parameter product representations	119
7 Decadal stability	123
8 Conclusions	128
Final Remarks	131
References	132

 	EUMETSAT SAF on CLIMATE MONITORING Validation Report Cloud product GAC Edition 1	Doc.No.:SAF/CM/SMHI/VAL/GAC/CLD Issue: 1.1 Date: 30.04.2012
---	---	---

List of Figures

Figure 3.1 <i>Historic overview of all NOAA satellites available in the covered period until 2009. (Courtesy of Andrew Heidinger, NOAA).</i>	21
Figure 3.2 <i>Visualisation of the used NOAA-satellites showing satellite numbers on Y-axis and the length of the observation period for each satellite. Notice that number 20 denotes Metop-A. Some data gaps are present but only for some isolated months for NOAA-7, NOAA-9, NOAA-12 and NOAA-14.</i>	22
Figure 3.3 <i>Local solar times at equator observations for all NOAA satellites from NOAA-7 to NOAA-19. Notice that the figure shows both ascending (northbound) and ascending (southbound) equator crossing times for each satellite separated 12 hours apart. (Courtesy of M. Foster, NOAA).</i>	23
Figure 5.1 <i>The Aqua-Train satellites. (Image credit: NASA)</i>	29
Figure 5.2 <i>CM SAF Level2b cloud top pressure (hPa) on July 1, 2001 from NOAA16 for the ASC (13:30 LT) overpass (top panel) and for the DES (01:30 LT) overpass (bottom panel).</i>	35
Figure 6.1 <i>Regional distribution of the number of Level 2 match-ups (left) and number of monthly means (Level 3) available (right) for the month of July 1982-2009.</i>	39
Figure 6.2 <i>Left: Regional distribution of the mean error (bias) of cloud fraction for Level 2 products. Right: Histogram of the difference in cloud coverage results between AVHRR-GAC and SYNOP.</i>	39
Figure 6.3 <i>Regional distribution of the bias in cloud coverage (AVHRR-GAC – SYNOP) for the individual satellites. The respective time period covered by the satellites ranges from 3 years for Metop-A to 10 years for NOAA-15. Notice that the left column of plots show afternoon-night satellites and the right column shows morning-evening satellites.</i>	40
Figure 6.4 <i>Time series of the mean error (bias) in cloud coverage for the month of July from for the period 1990 to 2009, separately for the individual satellites. The dashed line depicts the bias averaged over all satellites available.</i>	41
Figure 6.5 <i>Regional distribution of the bias calculated for the entire time period (1982-2009). Target accuracy is met by all grid boxes in yellow and green.</i>	42
Figure 6.6 <i>2D-scatter plot of the monthly mean cloud cover shown by AVHRR-GAC and SYNOP (right) and histogram of the difference between AVHRR-GAC and SYNOP (left) for the entire time period.</i>	42
Figure 6.7 <i>Time series of mean cloud cover for AVHRR-GAC (red) and SYNOP (green) (upper panel), mean error and bias-corrected RMS (middle panel) as well as the number of stations (lower panel) for the entire period 1982-2009.</i>	44
Figure 6.8 <i>Total coverage of matched CALIPSO-NOAA-18 orbits in the period October 2006 to December 2009. Different colours refer to different years.</i>	47
Figure 6.9 <i>Trajectory for one selected matched CALIPSO-NOAA-18 orbit from 6 October 2006 with first matched observation at 18:00 UTC (over South America).</i>	47
Figure 6.10 <i>Matched CALIPSO-CALIOP cloud mask (green) and CM SAF cloud top height values (blue, in meters) for the same global orbit as shown in Figure 6.9. Track position is given in number of GAC pixels (to be multiplied by 4 to get roughly the distance in km). Significant topographic features are seen in black at track positions 6000 (Antarctica) and 3000 (Russia/China).</i>	48

 	<p align="center">EUMETSAT SAF on CLIMATE MONITORING Validation Report Cloud product GAC Edition 1</p>	<p>Doc.No.:SAF/CM/SMHI/VAL/GAC/CLD Issue: 1.1 Date: 30.04.2012</p>
---	--	--

Figure 6.11 Variation of AVHRR (notice – wrong label in the upper right corner) satellite zenith angles for the match to the CALIPSO orbit as shown in Figure 6.9 and in Figure 6.10. Calculation distortions (rounding errors) occur close to the poles near positions 2000 and 6000. The optimal SNO position (within 12 seconds) is seen near position 3000..... 48

Figure 6.12 Daily mean cloud fraction for PATMOS-x (red line, top panel) and CM SAF (black line, top panel). Daily averages are computed from all (ascending/descending) overpasses from all NOAA satellites. The lower panel shows the satellite platform(s) from CM SAF Level 2b cloud fractions used to make daily averages. 52

Figure 6.13 Daily mean cloud fraction for PATMOS-x (red line, top panel) and CM SAF (black line, top panel) in the latitude band 60°N to 60°S. Daily averages are computed from all (ascending/descending) overpasses from all NOAA satellites. The lower panel shows the satellite platform(s) from CM SAF Level 2b cloud fractions used to make daily averages..... 53

Figure 6.14 Mean cloud fraction for January 1982-2008 for CM SAF (left) and PATMOS-x (middle) and the difference in cloud fraction (CM SAF – PATMOS-x, right). Top panels are for all ascending, afternoon overpasses from NOAA7, NOAA9, NOAA11, NOAA14, NOAA16 and NOAA18 for years 1982-2008; Lower panels are the descending, overnight overpasses for the same satellites for the same years..... 55

Figure 6.15 Daily mean Low-level and High-level cloud fraction for PATMOS-x and CM SAF. Fractions are relative to the total number of cloudy pixels with valid cloud top pressure estimations. Daily averages are computed from all (ascending/descending) overpasses from all NOAA satellites. The lower panel shows the satellite platform(s) from CM SAF Level 2b cloud fractions used to make daily averages. 56

Figure 6.16 Relative Global fractions of High-level (two leftmost plots) and Low-level (two rightmost plots) clouds for CM SAF and PATMOS-x for July in the period 1993-2008 and separated into four observation times (local solar time). See text for further description..... 57

Figure 6.17 Mean bias anomaly (MBA) for CM SAF (left panels) and PATMOS-x (middle panels). The top panels are calculated for the GEWEX-style inter-comparison (described in section 6.1.1.6) of NOAA-15 for 2005-2009, while the lower panels for NOAA-18 for 2006-2008. The right panels are the linearly regressed BA correlations between CM SAF and PATMOS-x for the NOAA-15 (top) and NOAA-18 (bottom). A correlation of 1 indicates the BA is positively correlated between CM SAF and PATMOS-x, while -1 indicates an anti-correlation in BA..... 59

Figure 6.18 Same as Figure 6.12but with CM SAF Level 3 values plotted as well (green line). 60

Figure 6.19 Global map of monthly mean cloud fractional coverage for CM SAF (NOAA-17 only, top row), MODIS (Terra only, middle row) and their differences (bottom row). Shown are January 2007 (left) and July 2007 (July). Regions without values are grey-shaded..... 63

Figure 6.20 Global map of monthly mean cloud fractional coverage for CM SAF (NOAA-18 only, top row), MODIS (Aqua only, middle row) and their differences (bottom row). Shown are January 2007 (left) and July 2007 (July). Regions without values are grey-shaded..... 64

Figure 6.21 Global map of monthly mean cloud fractional coverage for CM SAF (all satellites, top row), ISCCP (middle row) and their differences (bottom row). Shown are January 2007 (left) and July 2007 (right). Regions without values are grey-shaded..... 66

Figure 6.22 Time series of mean cloud fractional coverage of CM SAF (grey), ISCCP (green), MODIS/Terra (blue) and MODIS/Aqua (red). Shown are the global values (upper panel) and the separation into various latitude-bands. 67


 	EUMETSAT SAF on CLIMATE MONITORING Validation Report Cloud product GAC Edition 1	Doc.No.:SAF/CM/SMHI/VAL/GAC/CLD Issue: 1.1 Date: 30.04.2012
---	---	---

Figure 6.23 Time series of relative mean (dashed lines) and standard deviation (solid lines) of CFC of CM SAF compared to ISCCP (green), MODIS/Terra (blue) and MODIS/Aqua (red). Shown are the global values (upper panel) and the separation into various latitude-bands. 68

Figure 6.24 CM SAF cloud fraction differences for NOAA-18 ASC+DES overpasses for 2007 for five global cloud datasets. These are (from top to bottom): PATMOS-x, MODIS CERES Team (CE), MODIS Science Team (ST), ISCCP and CALIPSO Science Team (ST). (Ignore title of CM SAF MODIS-CE, it includes both ASC and DES overpasses.) 72

Figure 6.25 Zonal mean cloud fraction and zonal mean cloud fraction anomaly relative to CM SAF for the same datasets as in Figure 6.24. Northern Hemisphere latitudes are positive. 74

Figure 6.26 Zonal mean cloud fraction (top panels) and zonal mean cloud fraction anomalies (bottom panels) for NOAA-18 descending orbit (01:30, left panels) and ascending orbit (13:30, right panels) for CM SAF and five other global cloud datasets in 2007. 75

Figure 6.27 Zonal mean cloud fraction (top panel) for NOAA-15 2005-2009 ASC+DES orbits (thick) for PATMOS-x (red) and CM SAF (black). Thin solid line is the zonal mean cloud fraction for the ASC (19:30) orbit and thin dashed is for the DES (07:30) orbit. Lower panel: Zonal mean cloud fraction anomaly for PATMOS-x relative to CM SAF, thick line for ASC+DES, thin and dashed for ASC (19:30) and DES (07:30) orbits, respectively. 77

Figure 6.28 Same as in, Figure 6.27but for NOAA-18 for 2006-2008. 78

Figure 6.29 Mean cloud top pressure (arithmetic means, hPa) for afternoon satellites at 13:30 LT (top panels) and overnight satellites at 01:30 LT for January from 1982-2008. The left panels are CM SAF mean cloud top pressures and the right panels are PATMOS-x means. 83

Figure 6.30 Histograms (colors) of PATMOS-x cloud top pressure (hPa) against CM SAF cloud top pressure for afternoon 13:30 LT overpasses from 1982-2008 for January (left) and July (right). Only scenes where both PATMOS-x and CM SAF agree on cloud presence are included. 84

Figure 6.31 Cloud top pressure disagreement distribution for CM SAF and PATMOS-x in January (left) and July (right) for the period 1982-2008. See text for further explanation. 85

Figure 6.32 Global map of monthly mean cloud top pressure for CM SAF (NOAA-17 only, top row), MODIS (Terra only, middle row) and their differences (bottom row). Shown are January 2007 (left) and July 2007 (July). Regions without values are grey-shaded. 88

Figure 6.33 Global map of monthly mean cloud top pressure for CM SAF (NOAA-18 only, top row), MODIS (Aqua only, middle row) and their differences (bottom row). Shown are January 2007 (left) and July 2007 (July). Regions without values are grey-shaded. 89

Figure 6.34 Global map of monthly mean cloud top pressure for CM SAF (all satellites, top row), ISCCP (middle row) and their differences (bottom row). Shown are January 2007 (left) and July 2007 (July). Regions without values are grey-shaded. 91

Figure 6.35 Time series of mean cloud top pressure of CM SAF (grey), ISCCP (green), MODIS/Terra (blue) and MODIS/Aqua (red). Shown are the global values (upper panel) and the separation into various latitude-bands. 92

Figure 6.36 Time series of mean (dashed lines) and standard (solid lines) deviation of CTP of CM SAF compared to ISCCP (green), MODIS/Terra (blue) and MODIS/Aqua (red). Shown are the global values (upper panel) and the separation into various latitude-bands. 93


 	<p align="center">EUMETSAT SAF on CLIMATE MONITORING Validation Report Cloud product GAC Edition 1</p>	<p>Doc.No.:SAF/CM/SMHI/VAL/GAC/CLD Issue: 1.1 Date: 30.04.2012</p>
---	---	--

Figure 6.37 CPH for July 2006 expressed as the fraction liquid water clouds (of the total cloud amount) for CM SAF (upper left), PATMOS-x (upper right), MODIS Aqua (lower left), and ISCCP (lower right). For MODIS the optical properties cloud phase is shown. 97

Figure 6.38 Zonal mean liquid water cloud fraction for CM SAF, PATMOS-x, MODIS, and ISCCP for morning (left) and afternoon satellites (right) for July 2006. The lighter and darker shaded areas around the CM SAF curve denote the threshold and target accuracy, respectively. For MODIS the optical properties cloud phase is shown. 98

Figure 6.39 Time series of the liquid water cloud fraction averaged between 50°S and 50°N for CM SAF, PATMOS-x, MODIS, and ISCCP for the morning satellites (left, 2000 - 2009) and the afternoon satellites(right, 1982 – 2009).The lighter and darker shaded areas around the CM SAF curve denote the threshold and target accuracy, respectively. For MODIS the optical properties cloud phase is shown. 98

Figure 6.40 As Figure 6.39 but for the area between 50-90°S plus 50-90°N. Averages for each individual dataset were calculated based on those grid cells for which the CM SAF datasets had valid data available..... 99

Figure 6.41 Upper left: MODIS Aqua IR-derived liquid water cloud fraction for July 2006. Bottom: Mean liquid water cloud fraction. Upper right: Time series of liquid water cloud fraction between 50°S and 50°N from 2000 to 2009. The bottom and upper right panels show CM SAF (red) and MODIS IR-derived (blue) CPH for morning (dashed) and afternoon (solid) satellites..... 99

Figure 6.42 CM SAF bias (left) and RMSE (right) for liquid cloud fraction relative to PATMOS-x, MODIS, and ISCCP calculated between 50°S and 50°N. Bar colours correspond to the colours used in the time series plot. The numbers on the x-axis refer to the respective NOAA satellites, while 'aft' and 'mrn' refer to afternoon and morning, respectively. For MODIS both the IR-based ('MOD IR', pale blue) and optical properties ('MOD OPT', dark blue) cloud phase are presented. The solid and dashed horizontal lines indicate the threshold and target values from the PRT, respectively..... 100

Figure 6.43 All-cloud COT for July 2006 for CM SAF (upper left), PATMOS-x (upper right), MODIS Aqua (lower left), and ISCCP (lower right). 102

Figure 6.44 Zonal mean all-cloud COT for CM SAF, PATMOS-x, MODIS, and ISCCP for July 2006 for morning (left) and afternoon (right) satellites. The lighter and darker shaded areas around the CM SAF curve denote the threshold and target accuracy, respectively..... 102

Figure 6.45 Time series of liquid+ice COT averaged between 50°S and 50°N for CM SAF, PATMOS-x, MODIS, and ISCCP for the morning satellites (left, 2000 - 2009) and the afternoon satellites (right, 1982 – 2009). The lighter and darker shaded areas around the CM SAF curve denote the threshold and target accuracy, respectively. 103

Figure 6.46 As Figure 6.45 but for the area between 50-90°S plus 50-90°N. Averages for each individual dataset were calculated based on those grid cells for which the CM SAF datasets had valid data available..... 103

Figure 6.47 Relative Frequency Distribution (RFD) of cloud optical thickness for cases when CM SAF sees a cloud while PATMOS-x is clear (black) and vice versa (red) for January (left) and July (right) for afternoon satellites during 1982-2008. 104

Figure 6.48 CM SAF bias (left panel) and RMS (right panel) for all-cloud COT relative to PATMOS-x, MODIS, and ISCCP, calculated between 50°S and 50°N. Bar colours correspond to the colours used in the time series plot. The numbers on the x-axis refer to the respective NOAA satellites, while 'aft' and 'mrn' refer to afternoon and morning,

 	<p align="center">EUMETSAT SAF on CLIMATE MONITORING Validation Report Cloud product GAC Edition 1</p>	<p>Doc.No.:SAF/CM/SMHI/VAL/GAC/CLD Issue: 1.1 Date: 30.04.2012</p>
---	--	--

respectively. The solid and dashed horizontal lines indicate the threshold and target values from the PRT, respectively. 105

Figure 6.49 LWP for July 2006 for CM SAF (upper left), PATMOS-x (upper right), MODIS Aqua, (lower left) and ISCCP (lower right). 107

Figure 6.50 Zonal mean LWP for July 2006 for CM SAF, PATMOS-x, MODIS, and ISCCP for morning (left) and afternoon (right) satellites. The lighter and darker shaded areas around the CM SAF curve denote the threshold and target accuracy, respectively. 107

Figure 6.51 Time series of LWP covering 50°S - 50°N for CM SAF, PATMOS-x, MODIS, and ISCCP for the morning satellites (left, 2000 - 2009) and the afternoon satellites (right, 1982 - 2009). The lighter and darker shaded areas around the CM SAF curve denote the threshold and target accuracy, respectively. 108

Figure 6.52 As Figure 6.51 but for the area between 50-90°S plus 50-90°N. Averages for each individual dataset were calculated based on those grid cells for which the CM SAF datasets had valid data available. 109

Figure 6.53 CM SAF bias (left panel) and RMSE (right panel) for LWP relative to PATMOS-x, MODIS, and ISCCP, calculated between 50°S - 50°N. The numbers refer to the different NOAA satellites. The abbreviations 'aft' and 'mnn' refer to afternoon and morning, respectively. 109

Figure 6.54 The locations of the S-Atl, S-Pac and N-Pac validation areas. 110

Figure 6.55 GAC (solid coloured lines) and UWisc (dotted coloured lines) monthly mean LWP (left column) for 1989 - 2008 over the S-Atl (upper panels), S-Pac area (center panels), and N-Pac area (lower panels). The relative bias is shown in % in the right column. UWisc values were calculated using the mean diurnal fit parameters for the period 1988 - 2008 (see text for further details). The solid and dashed horizontal lines in the right panels denote threshold and target accuracies, respectively. 111

Figure 6.56 As Figure 6.55 but for the RMSE (in %). 112

Figure 6.57 Relative bias (left panel) and RMSE (right panel) of CM SAF LWP vs UWisc over the three areas and averaged over all areas. Bar colours correspond to those in Figure 6.55 and Figure 6.56, and the NOAA satellite numbers are given as tick marks on the horizontal axis. 112



Figure 6.58 IWP for July 2006 for CM SAF (upper left), PATMOS-x (upper right), MODIS Aqua (lower left), and ISCCP (lower right). 115

Figure 6.59 Zonal mean IWP for July 2006 for CM SAF, PATMOS-x, MODIS, and ISCCP for morning (left) and afternoon (right) satellites. The lighter and darker shaded areas around the CM SAF curve denote the threshold and target accuracy, respectively. 115

Figure 6.60 Time series of IWP covering 50°S - 50°N for CM SAF, PATMOS-x, MODIS, and ISCCP for the morning satellites (left, 2000 - 2009) and the afternoon satellites (right, 1982 - 2009). The lighter and darker shaded areas around the CM SAF curve denote the threshold and target accuracy, respectively. 116

Figure 6.61 As Figure 6.60 but for the area between 50-90°S plus 50-90°N. Averages for each individual dataset were calculated based on those grid cells for which the CM SAF datasets had valid data available. 116

Figure 6.62 CM SAF bias (left panel) and RMSE (right panel) for IWP relative to PATMOS-x, MODIS, and ISCCP, calculated between 50°S - 50°N. The numbers refer to the different

 	EUMETSAT SAF on CLIMATE MONITORING Validation Report Cloud product GAC Edition 1	Doc.No.:SAF/CM/SMHI/VAL/GAC/CLD Issue: 1.1 Date: 30.04.2012
---	---	---

NOAA satellites. The abbreviations ‘aft’ and ‘mn’ refer to afternoon and morning, respectively. 117

Figure 6.63 Pressure-tau histograms for afternoon 13:30 LT overpasses for January 1982-2008 for CM SAF (left) and PATMOS-x (right). All data, regardless of whether CM SAF and PATMOS-x agree on cloudy pixels, are shown. The magenta star is the arithmetic mean of CTP and COT for the specified month and years. 119

Figure 6.64 Same as Figure 6.63, except distributions are only shown for only observations when CM SAF and PATMOS-x both agree on cloud presence. 120


Figure 6.65 Pressure-tau histograms of CM SAF (left column), MODIS-AQUA (middle column), and ISCCP (right column) for liquid clouds (upper row), ice clouds (middle row) and all clouds (bottom row), all for March 2007. The histograms are presented in relative numbers. 122

Figure 7.1 Availability of SYNOP stations (red spots) with observations made during the entire AVHRR GAC period 1982-2009. 124

Figure 7.2 Time series of cloud fraction (CFC, top panel) and the mean error and the RMS error (bottom panel) compared to observations from SYNOP stations available for the full period 1982-2009 (see Figure 7.1). 124


Figure 7.3 Time series (same representation as in Figure 6.23) of relative mean and standard deviation of CFC of CM SAF compared to ISCCP (green), MODIS/Terra (blue) and MODIS/Aqua (red) but only for daytime CM SAF results . Shown are the global values (upper panel) and the separation into various latitude-bands. 126

Figure 7.4 Time series (same representation as in Figure 6.23) of relative mean and standard deviation of CFC of CM SAF compared to ISCCP (green), MODIS/Terra (blue) and MODIS/Aqua (red) but only for night-time CM SAF results . Shown are the global values (upper panel) and the separation into various latitude-bands. 127

 	<p align="center">EUMETSAT SAF on CLIMATE MONITORING Validation Report Cloud product GAC Edition 1</p>	<p>Doc.No.:SAF/CM/SMHI/VAL/GAC/CLD Issue: 1.1 Date: 30.04.2012</p>
---	--	--

List of Tables

Table 1.1 Summary of validation results compared to target accuracies for each cloud product. Notice that accuracies are given as Mean errors or Biases (both terms being equivalent) valid for both negative and positive deviations. Results from consistency checks (not totally independent) are marked in blue	16
Table 1.2 Summary of validation results compared to target precisions for each cloud product. Consistency checks marked in blue.....	17
Table 3.1 Spectral channels of the Advanced Very High Resolution Radiometer (AVHRR). The three different versions of the instrument are described as well as the corresponding satellites. Notice that channel 3A was only used continuously on NOAA-17 and Metop-1. For the other satellites with AVHRR/3 it was used only for shorter periods.	21
Table 3.2 Channel 3A and 3B operations for the AVHRR/3 instruments during daytime.	22
Table 4.1 CM SAF cloud products and their respective target requirements (defined in AD 1) for the GAC dataset of Level 3 monthly mean products. Notice that the requirement on mean error or bias for accuracy is valid for both negative and positive deviations.	25
Table 5.1 Cloud type categories according to the CALIOP Vertical Feature Mask product.....	30
Table 5.2 Some basic characteristics of the PATMOS-x retrieval methods.	33
Table 6.1 Detailed statistics, including mean error (bias), the bias corrected RMS (BC-RMS) as well as the mean absolute bias (abs. bias) calculated also separately for different illumination conditions, satellite viewing angles, regions and satellites.	41
Table 6.2 Compliance matrix of found global CFC monthly mean product characteristics with respect to the defined product requirements for accuracy and precision. Comparisons were made against SYNOP observations. Remark: The anticipated error of SYNOP observations is probably of the order of 10 %, i.e., close to the Target requirement.	45
Table 6.3 Total CFC statistics for 107 matched orbits in the period October 2006 – December 2009, including reduced CALIOP datasets after applying cloud optical thickness filtering.	49
Table 6.4 Total CFC statistics for 107 matched orbits in the period October 2006 – December 2009 sub-divided according to four different Earth surfaces.	49
Table 6.5 Mean error (%) separated according to latitude bands and illumination categories (defined in the text) and surface conditions. Statistics computed from 107 full globally matched NOAA-18 and CALIPSO orbits with a total of 781520 individual pixel matches. Red colour coding denotes positive deviations larger than 5 %, blue colour coding negative deviations between 5 and 10 % and bold blue colours denote negative deviations larger than 10 %.	50
Table 6.6 Compliance matrix of found global CFC monthly mean product characteristics with respect to the defined product requirements for accuracy and precision. Comparisons were made against CALIPSO observations. Observe that the Level 3 to Level 2 comparison made here is only theoretically valid for the Bias error and not for RMS errors. Remark: The anticipated error of CALIOP cloud amounts (underestimation) is estimated to less than 3 %.	51
Table 6.7 Globally integrated CFC differences compared to PATMOS-x over the entire period 1982-2008 calculated from Level 2b product representation. In addition, correlation is given as well as results over three specific periods. The latter corresponds to the initial period	

	<p align="center">EUMETSAT SAF on CLIMATE MONITORING Validation Report Cloud product GAC Edition 1</p>	<p>Doc.No.:SAF/CM/SMHI/VAL/GAC/CLD Issue: 1.1 Date: 30.04.2012</p>
---	--	--

with exclusively afternoon-night satellites, the inter-mediate period with one afternoon-night and one morning-evening satellite and the final period with more than two satellites..... 54

Table 6.8	<i>Globally integrated CFC differences compared to PATMOS-x separated into observation nodes (i.e., local solar times).....</i>	58
Table 6.9	<i>Mean deviation and bias-corrected RMS results with respect to PATMOS-x computed for the entire dataset 1982-2008. Results are sub-divided in two versions: 1. Based on the official CM SAF GAC product (computed from Level 2 products – column 1), 2. Calculated in the same way as PATMOS-x (i.e., computed from Level 2b products – column 2).</i>	60
Table 6.10	<i>Mean deviations and bias-corrected RMS for daily mean Level 3 products composed from Level 2b products compared to PATMOS-x.</i>	61
Table 6.11	<i>Compliance matrix of found global CFC monthly mean product characteristics with respect to the defined product requirements for accuracy and precision. Comparisons were made against PATMOS-x observations.....</i>	62
Table 6.12	<i>Compliance matrix of found global CFC monthly mean product characteristics with respect to the defined product requirements for accuracy and precision. Comparisons were made against MODIS observations (consistency check).....</i>	65
Table 6.13:	<i>Compliance matrix of found global CFC monthly mean product characteristics with respect to the defined product requirements for accuracy and precision. Comparisons were made against ISCCP observations (consistency check).</i>	70
Table 6.14	<i>Compliance matrix of found global CFC monthly mean product characteristics with respect to the defined product requirements for accuracy and precision. Comparisons were made against PATMOS-x, MODIS (Science Team and CERES team), ISCCP and CALIPSO observations in the time period 2005-2009. Only results from CALIPSO represent independent observations and the remaining results should be considered as consistency checks.</i>	76
Table 6.15	<i>Overall requirement compliance of the CM SAF GAC CFC product with respect to the Mean Error. Consistency checks marked in blue.....</i>	79
Table 6.16	<i>Overall requirement compliance of the CM SAF GAC CFC product with respect to the bias-corrected RMS error. Consistency checks marked in blue.....</i>	79
Table 6.17	<i>Total CTH statistics for 106 matched orbits in the period October 2006 – December 2009, including reduced CALIOP datasets after applying cloud optical thickness filtering.</i>	81
Table 6.18	<i>Total CTH statistics for 106 matched orbits in the period October 2006 – December 2009 – separated according to three vertical levels.....</i>	82
Table 6.19	<i>Compliance matrix of found global CTH monthly mean product characteristics with respect to the defined product requirements for accuracy and precision. Comparisons were made against CALIPSO observations. Observe that the Level 3 to Level 2 comparison made here is only theoretically valid for the Bias error and not for RMS errors.</i>	82
Table 6.20	<i>Mean errors (bias) for CM SAF CTP compared to PATMOS-x for all observation nodes in the period 1982-2008.</i>	86
Table 6.21	<i>Mean deviations and bias-corrected RMS for daily mean Level 3 CTP products composed from Level 2b products compared to PATMOS-x.</i>	86



 	<p align="center">EUMETSAT SAF on CLIMATE MONITORING Validation Report Cloud product GAC Edition 1</p>	<p>Doc.No.:SAF/CM/SMHI/VAL/GAC/CLD Issue: 1.1 Date: 30.04.2012</p>
---	--	--

Table 6.22 <i>Compliance matrix of found global CTP monthly mean product characteristics with respect to the defined product requirements for accuracy and precision. Comparisons were made against PATMOS-x observations (consistency check).</i>	87
Table 6.23 <i>Compliance matrix of found global CTP monthly mean product characteristics with respect to the defined product requirements for accuracy and precision. Comparisons were made against MODIS results (consistency check).</i>	90
Table 6.24 <i>Compliance matrix of found global CTP monthly mean product characteristics with respect to the defined product requirements for accuracy and precision. Comparisons were made against ISCCP results (consistency check).</i>	94
Table 6.25 <i>Overall requirement compliance of the CM SAF GAC CTP product with respect to the Mean Error. Consistency checks marked in blue.</i>	94
Table 6.26 <i>Overall requirement compliance of the CM SAF GAC CTP product with respect to the bias-corrected RMS error. Consistency checks marked in blue.</i>	95
Table 6.27 <i>Datasets, their version and instruments that were used for the evaluation of the CPP products.</i>	96
Table 6.28 <i>Overall requirement compliance of the CM SAF GAC CPH product with respect to the Mean Error. Observe that results refer to the success of estimating the frequency of water clouds. Consistency checks marked in blue.</i>	101
Table 6.29 <i>Overall requirement compliance of the CM SAF GAC CPH product with respect to the RMS error. Consistency checks marked in blue.</i>	101
Table 6.30 <i>Overall requirement compliance of the CM SAF GAC COT product with respect to the Mean Error. Consistency checks marked in blue.</i>	106
Table 6.31 <i>Overall requirement compliance of the CM SAF GAC COT product with respect to the RMS error. Consistency checks marked in blue.</i>	106
Table 6.32 <i>Overall requirement compliance of the CM SAF GAC LWP product with respect to the Mean Error. Consistency checks marked in blue.</i>	113
Table 6.33 <i>Overall requirement compliance of the CM SAF GAC LWP product with respect to the RMS error. Consistency checks marked in blue.</i>	114
Table 6.34 <i>Overall requirement compliance of the CM SAF GAC IWP product with respect to the Mean Error. Consistency checks marked in blue.</i>	118
Table 6.35 <i>Overall requirement compliance of the CM SAF GAC LWP product with respect to the RMS error. Consistency checks marked in blue.</i>	118
Table 7.1 <i>Target requirements on stability of product accuracies as expressed in the PRD (AD 1).</i>	123
Table 8.1 <i>Summary of validation results compared to target accuracies for each cloud product. Notice that accuracies are given as Mean errors or Biases (both terms being equivalent) valid for both negative and positive deviations. Consistency checks marked in blue.</i>	129
Table 8.2 <i>Summary of validation results compared to target precisions for each cloud product. Consistency checks marked in blue.</i>	130

	EUMETSAT SAF on CLIMATE MONITORING Validation Report Cloud product GAC Edition 1	Doc.No.:SAF/CM/SMHI/VAL/GAC/CLD Issue: 1.1 Date: 30.04.2012
---	---	---

1 Executive Summary

This CM SAF report provides information on the validation of the CM SAF GAC Edition 1 data sets derived from the Advanced Very High Resolution Radiometer (AVHRR) observations onboard the NOAA satellites. The covered time period ranges from 1982 (first satellite NOAA-7) to 2009 (last satellite NOAA-18). For the last years 2007-2009 also AVHRR data from the EUMETSAT METOP-A satellite has been used.

This report presents an evaluation of the following products:


Fractional Cloud Cover	CM-05 (CFC)
Cloud Top level	CM-17 (CTO)
Cloud Optical Thickness	CM-34 (COT)
Cloud Phase	CM-38 (CPH)
Liquid Water Path	CM-43 (LWP)
Ice Water Path	CM-47 (IWP)
Joint Cloud property histogram	CM-11 (JCH)

An extensive validation of cloud products from the CM SAF GAC Edition 1 dataset has been performed. The reference datasets were taken from completely independent and different observation sources (e.g. SYNOP, CALIPSO-CALIOP, SSM/I and AMSR-E) as well as from similar satellite-based datasets from passive visible and infrared imagery (MODIS, ISCCP and PATMOS-x). A distinction was made between results from completely independent references (SYNOP, CALIPSO-CALIOP, SSM/I and AMSR-E) and results from datasets based on similar satellite sensors (PATMOS-x, MODIS and ISCCP). Highest credibility was given to results from the first group while results from the second group were used as consistency checks. Studies were made based on a mix of Level 2 and Level 3 products, also addressing some specific aspects affecting inter-comparisons (e.g., cloud detection capabilities for very thin clouds). More in depth inter-comparisons were also made with the PATMOS-x dataset because of the close relation (being also based on AVHRR GAC data). A limited study inter-comparing several global datasets simultaneously utilizing datasets prepared within GEWEX was also accomplished for the period 2005-2009.

Table 1.1 and 1.2 below give an overview of all results with respect to the target accuracies and precisions.

Results show the following, product by product:

- **Fractional Cloud Cover (CFC)**
 - The CM SAF GAC CFC product fulfils the Threshold requirement when compared with all references
 - The product also fulfils the Target requirement in most cases (the only exception occurs when comparing with MODIS results)
 - Optimal requirements are fulfilled when comparing with SYNOP results, with filtered CALIPSO results (removing clouds with optical thickness < 0.3) and with PATMOS-x results
 - Consideration of existing uncertainties of reference observations (e.g., a few percent underestimation of CFC from CALIPSO-CALIOP) does not change these conclusions.

	<p align="center">EUMETSAT SAF on CLIMATE MONITORING Validation Report Cloud product GAC Edition 1</p>	<p>Doc.No.:SAF/CM/SMHI/VAL/GAC/CLD Issue: 1.1 Date: 30.04.2012</p>
---	--	--

- **Cloud Top level (CTO)**

- The CM SAF GAC CTO product fulfils all levels of requirements for all references
- However, an exception occurs when comparing with unfiltered CALIPSO results when none of the requirements is fulfilled
- The latter result is explained by the fact that for the thinnest detected clouds (with COT < 0.3), corrections for the semi-transparency effect is still a major issue
- CM SAF results compare particularly well with datasets from similar satellite sensors, partly suggesting similar uncertainty characteristics.

- **Cloud Thermodynamic Phase (CPH)**

- The CM SAF GAC CPH product fulfils threshold requirements against most references except against ISCCP
- Target or Optimal requirements are generally not fulfilled (except if comparing against the MODIS IR method)
- Results are here based exclusively on consistency checks since no independent data source was available. Also, adequate information about uncertainties for reference datasets was missing.

- **Cloud Optical Thickness (COT)**

- The CM SAF GAC COT product fulfils threshold and target requirements when compared to PATMOS-x and to MODIS
- However, differences are very large and not even within threshold requirements if comparing with ISCCP. Confusing here is that this conclusion remains even after taking into account reported uncertainty (10 %) in the ISCCP results.

- **Liquid Water Path (LWP)**

- The CM SAF GAC LWP product generally fulfils threshold requirements even if RMS threshold values are exceeded in some cases.
- Target requirements are fulfilled with respect to MODIS and UWisc datasets (for the latter when evaluating LWP products based on the 3.7 micron channel). Note that – as a consequence of necessary selections of the data – the validation with UWisc was restricted to oceanic, stratocumulus-dominated areas.
- Differences are very large if comparing to ISCCP (not even within threshold requirements for neither mean error nor RMS error)
- Uncertainties in the reference observations (15-30 %) make firm conclusions difficult considering a target requirement of 15 % for accuracy.



 	<p align="center">EUMETSAT SAF on CLIMATE MONITORING Validation Report Cloud product GAC Edition 1</p>	<p>Doc.No.:SAF/CM/SMHI/VAL/GAC/CLD Issue: 1.1 Date: 30.04.2012</p>
---	---	--

Table 1.1 Summary of validation results compared to target accuracies for each cloud product. Notice that accuracies are given as Mean errors or Biases (both terms being equivalent) valid for both negative and positive deviations. Results from consistency checks (not totally independent) are marked in *blue*.

Product		Accuracy requirement (Mean error or Bias)	Achieved accuracies
Cloud Fractional Cover	(CFC)	10 % (absolute)	3.6 % (SYNOP) -10 % (CALIPSO) -4.1 % (PATMOS-x) -10 % to -20 % (MODIS) 0 % to -12 % (ISCCP)
Cloud Top Height	(CTH)	1200 m	-2661 m (CALIPSO)
Cloud Top Pressure	(CTP)	110 hPa	-20 to 60 hPa (PATMOS-X) -40 to -50 hPa (MODIS) -20 to 60 hPa (ISCCP)
Cloud Optical Thickness	(COT)	15 %	3-20 % (PATMOS-x) -5 % to -10 % (MODIS) 50-60 % (ISCCP)
Cloud Phase	(CPH)	5 % (absolute)	7-15 % (PATMOS-x) 3-20 % (MODIS) 12-15 % (ISCCP)
Liquid Water Path	(LWP)	15 %	+15 % to -26 % (UWisc) 0-30 % (PATMOS-x) 15 % (MODIS) 30-50 % (ISCCP)
Ice Water Path	(IWP)	25 %	0 % to -120 % (PATMOS-x) 0 % to -80 % (MODIS) 30-50 % (ISCCP)
Joint Cloud Histogram	(JCH)	n/a	n/a



 	<p align="center">EUMETSAT SAF on CLIMATE MONITORING Validation Report Cloud product GAC Edition 1</p>	<p>Doc.No.:SAF/CM/SMHI/VAL/GAC/CLD Issue: 1.1 Date: 30.04.2012</p>
---	---	--

Table 1.2 Summary of validation results compared to target precisions for each cloud product. Consistency checks marked in blue.

Product	Precision requirement (RMS)	Achieved precisions
Cloud Fractional Cover (CFC)	20 % (absolute)	11 % (SYNOP) n/a (CALIPSO) 2.6 % (PATMOS-x) 20-27 % (MODIS) 10-20 % (ISCCP)
Cloud Top Height (CTH)	2000 m	n/a (CALIPSO)
Cloud Top Pressure (CTP)	130 hPa	40 hPa (PATMOS-x) 80 hPa (MODIS) 90 hPa (ISCCP)
Cloud Optical Thickness (COT)	30 %	25-45 % (PATMOS-x) 30 % (MODIS) 80-90 % (ISCCP)
Cloud Phase (CPH)	10 % (absolute)	15-20 % (PATMOS-x) 12-25 % (MODIS) 25 % (ISCCP)
Liquid Water Path (LWP)	30 %	25-40 % (UWisc) 50-140 % (PATMOS-x) 35-45 % (MODIS) 70-90 % (ISCCP)
Ice Water Path (IWP)	50 %	60-180 % (PATMOS-x) 45-90 % (MODIS) 90-110 % (ISCCP)
Joint Cloud Histogram (JCH)	n/a	n/a

	<p align="center">EUMETSAT SAF on CLIMATE MONITORING Validation Report Cloud product GAC Edition 1</p>	<p>Doc.No.:SAF/CM/SMHI/VAL/GAC/CLD Issue: 1.1 Date: 30.04.2012</p>
---	--	--

- **Ice Water Path (IWP)**

- The CM SAF GAC IWP product only fulfils threshold accuracy requirements for one reference (ISCCP) (although precision requirements are not fulfilled)
- For all other references, differences are too large.
- Large uncertainties in the reference observations (30-50 %) make firm conclusions even more difficult for this parameter considering a target requirement of 25 % for accuracy.

- **Joint Cloud property Histograms (JCH)**



- This product is excluded from specific requirement testing because of being composed by two already existing products (COT and CTP)
- Nevertheless, a demonstration of the product in inter-comparisons with PATMOS-x, MODIS and ISCCP products shows that it provides added value to the products by giving important clues on the statistical distribution of the involved parameters
- It is believed that the access to this product representation would greatly enhance the usefulness of the CM SAF GAC products in some applications (e.g., climate model evaluation)

The usefulness of the CM SAF GAC cloud dataset could be questioned in the light of the existence of several other and similar satellite-based datasets and also if considering the shortcomings that have been revealed in this report. However, this validation report (and also the upcoming GEWEX cloud assessment report – Stubenrauch et al., 2012) has shown that also the referenced datasets have features that could be questioned and discussed. In that sense, we believe that results from a large number of analyses (i.e., an ensemble) should have a better chance of providing confidence in results compared to when relying on just one single dataset. If taking the PATMOS-x dataset as an example it is clear that our study has indeed increased the confidence in the PATMOS-x results. At the same time, we have raised important questions regarding some of the features of PATMOS-x results that need further attention. In that sense, we believe that the CM SAF- NOAA cooperation on AVHRR GAC cloud datasets within the framework of SCOPE-CM will lead to mutual improvement of both datasets.

Finally, we also want to highlight some advantages of the CM SAF GAC cloud dataset compared to other datasets. In our opinion the added value of the CMSAF dataset is:

- Compared to MODIS: Much longer record (1982-2009)
- Compared to ISCCP: More homogeneous (no GEO used) and more spectral channels used
- Compared to PATMOS-x: Good to have two similar datasets produced with different algorithms to identify strengths /weaknesses of both approaches
- Compared to independent sensors (CALIPSO-CALIOP, SSM-I, AMSR-E): Different measurement principle, different variables measured and longer time frame.

In conclusion, we recommend the release of the CM SAF AVHRR GAC cloud dataset Edition 1. Results are good enough to allow starting to use the dataset; also taking into

 	<p align="center">EUMETSAT SAF on CLIMATE MONITORING Validation Report Cloud product GAC Edition 1</p>	<p>Doc.No.:SAF/CM/SMHI/VAL/GAC/CLD Issue: 1.1 Date: 30.04.2012</p>
---	--	--

account that many of the existing limitations will be taken care of in the next release (Edition 2) scheduled for 2015.

Further guidance on how to use the products is given in the product user manual [RD 1]. Basic accuracy requirements are defined in the product requirements document [AD 1], and the algorithm theoretical basis documents describes the individual parameter algorithms [RD 2 – RD 6].

2 The EUMETSAT SAF on Climate Monitoring

The importance of climate monitoring with satellites was recognized in 2000 by EUMETSAT Member States when they amended the EUMETSAT Convention to affirm that the EUMETSAT mandate is also to “contribute to the operational monitoring of the climate and the detection of global climatic changes”. Following this, EUMETSAT established within its Satellite Application Facility (SAF) network a dedicated centre, the SAF on Climate Monitoring (CM SAF, <http://www.cmsaf.eu>).

The consortium of CM SAF currently comprises the Deutscher Wetterdienst (DWD) as host institute, and the partners from the Royal Meteorological Institute of Belgium (RMIB), the Finnish Meteorological Institute (FMI), the Royal Meteorological Institute of the Netherlands (KNMI), the Swedish Meteorological and Hydrological Institute (SMHI), the Meteorological Service of Switzerland (MeteoSwiss), and the Meteorological Service of the United Kingdom (UK MetOffice). Since the beginning in 1999, the EUMETSAT Satellite Application Facility on Climate Monitoring (CM SAF) has developed and will continue to develop capabilities for a sustained generation and provision of Climate Data Records (CDR’s) derived from operational meteorological satellites.

In particular the generation of long-term data sets is pursued. The ultimate aim is to make the resulting data sets suitable for the analysis of climate variability and potentially the detection of climate trends. CM SAF works in close collaboration with the EUMETSAT Central Facility and liaises with other satellite operators to advance the availability, quality and usability of Fundamental Climate Data Records (FCDRs) as defined by the Global Climate Observing System (GCOS). As a major task the CM-SAF utilizes FCDRs to produce records of Essential Climate Variables (ECVs) as defined by GCOS. Thematically, the focus of CM SAF is on ECVs associated with the global energy and water cycle.

Another essential task of CM SAF is to produce data sets that can serve applications related to the new Global Framework of Climate Services initiated by the WMO World Climate Conference-3 in 2009. CM SAF is supporting climate services at national meteorological and hydrological services (NMHSs) with long-term data records but also with data sets produced close to real time that can be used to prepare monthly/annual updates of the state of the climate. Both types of products together allow for a consistent description of mean values, anomalies, variability and potential trends for the chosen ECVs. CM SAF ECV data sets also serve the improvement of climate models both at global and regional scale.

As an essential partner in the related international frameworks, in particular WMO SCOPE-CM (Sustained COordinated Processing of Environmental satellite data for Climate Monitoring), the CM SAF - together with the EUMETSAT Central Facility, assumes the role as main implementer of EUMETSAT’s commitments in support to global climate monitoring. This is achieved through:

	EUMETSAT SAF on CLIMATE MONITORING Validation Report Cloud product GAC Edition 1	Doc.No.:SAF/CM/SMHI/VAL/GAC/CLD Issue: 1.1 Date: 30.04.2012
---	---	---

- Application of highest standards and guidelines as lined out by GCOS for the satellite data processing,
- Processing of satellite data within a true international collaboration benefiting from developments at international level and pollinating the partnership with own ideas and standards,
- Intensive validation and improvement of the CM SAF climate data records,
- Taking a major role in data set assessments performed by research organisations such as WCRP. This role provides the CM SAF with deep contacts to research organizations that form a substantial user group for the CM SAF CDRs,
- Maintaining and providing an operational and sustained infrastructure that can serve the community within the transition of mature CDR products from the research community into operational environments.

A catalogue of all available CM SAF products is accessible via the CM SAF webpage, www.cmsaf.eu/. Here, detailed information about product ordering, add-on tools, sample programs and documentation is provided.

3 Introduction to the AVHRR GAC dataset

Measurements from the Advanced Very High Resolution Radiometer (AVHRR) radiometer onboard the polar orbiting NOAA satellites and the EUMETSAT METOP satellites have been performed since 1978. Figure 3.1 gives an overview over all satellites carrying the AVHRR instrument until 2009 (the final year covered by the new CM SAF GAC dataset). Notice that also data from NOAA-19 and Metop-A has been used for the last two years in the CM SAF dataset (not included in Figure 3.1). The instrument only measured in four spectral bands in the beginning (AVHRR/1) but from 1982 a fifth channel was added (AVHRR/2) and in 1998 even a sixth channel was made available (AVHRR/3), although only accessible if switched with the previous third channel at 3.7 micron. Table 3.1 describes the AVHRR instrument, its various versions and the satellites carrying them. The retrieval of cloud physical properties (in particular particle effective radius and liquid/ice water path) is sensitive to the shortwave infrared channel being used. Table 3.2 summarizes when either of the channels 3a and 3b have been active on the AVHRR/3 instruments. The AVHRR instrument measures at a horizontal resolution close to 1 km at nadir but only data at a reduced resolution of approximately 4 km are permanently archived and available with global coverage since the beginning of measurements. This dataset is denoted Global Area Coverage (GAC) AVHRR data.

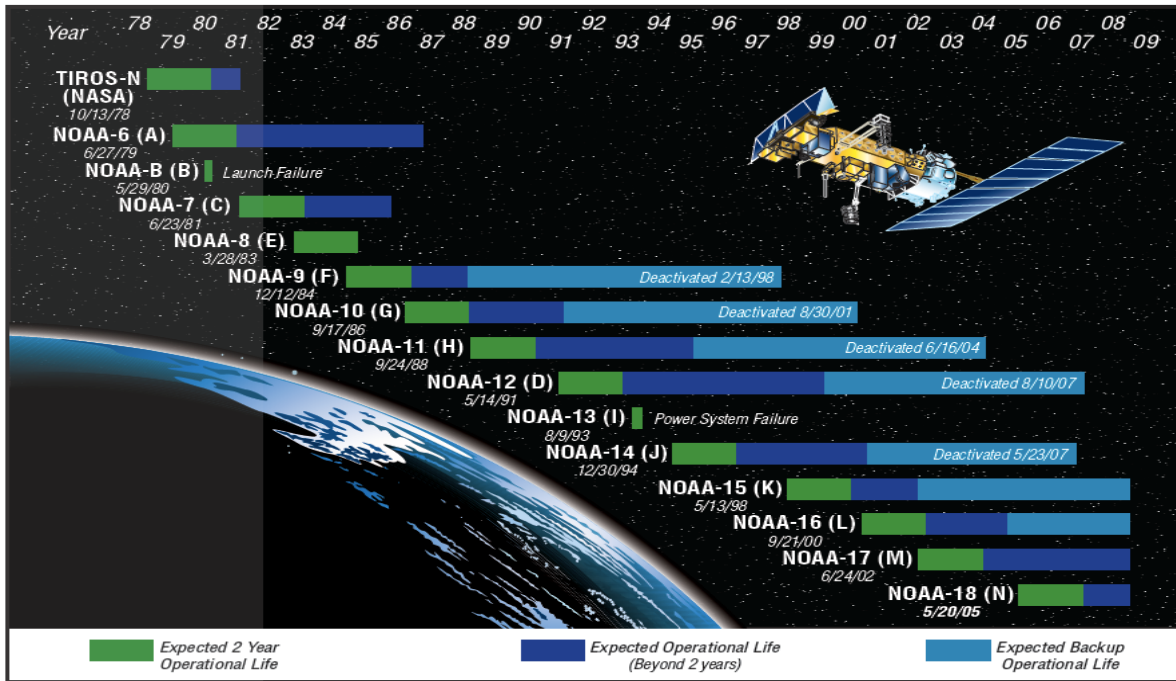


Figure 3.1 Historic overview of all NOAA satellites available in the covered period until 2009. (Courtesy of Andrew Heidinger, NOAA).

Table 3.1 Spectral channels of the Advanced Very High Resolution Radiometer (AVHRR). The three different versions of the instrument are described as well as the corresponding satellites. Notice that channel 3A was only used continuously on NOAA-17 and Metop-1. For the other satellites with AVHRR/3 it was used only for shorter periods.

Channel Number	Wavelength (micrometers) AVHRR/1 NOAA-6,8,10	Wavelength (micrometers) AVHRR/2 NOAA-7,9,11,12,14	Wavelength (micrometers) AVHRR/3 NOAA-15,16,17,18 NOAA-19, Metop-A
1	0.58-0.68	0.58-0.68	0.58-0.68
2	0.725-1.10	0.725-1.10	0.725-1.10
3A	-	-	1.58-1.64
3B	3.55-3.93	3.55-3.93	3.55-3.93
4	10.50-11.50	10.50-11.50	10.50-11.50
5	Channel 4 repeated	11.5-12.5	11.5-12.5

Table 3.2 Channel 3A and 3B operations for the AVHRR/3 instruments during daytime.

Satellite	Channel 3a active	Channel 3b active
NOAA-15		06/1998 – 12/2009
NOAA-16	10/2000 – 04/2003	05/2003 – 12/2009
NOAA-17	07/2002 – 12/2009	
NOAA-18		09/2005 – 12/2009
NOAA-19		06/2009 – 12/2009
Metop-A	09/2007 – 12/2009	

Figure 3.2 describes the coverage of observations for each individual satellite over the entire period. Notice that the limitations to the use of AVHRR/2 and AVHRR/3 instruments (excluding AVHRR/1) leads to poorer time sampling (i.e., only one satellite available for daily observations) between 1982 and 1991. On the other hand, from 2001 and onwards more than two satellites are available for daily observations.

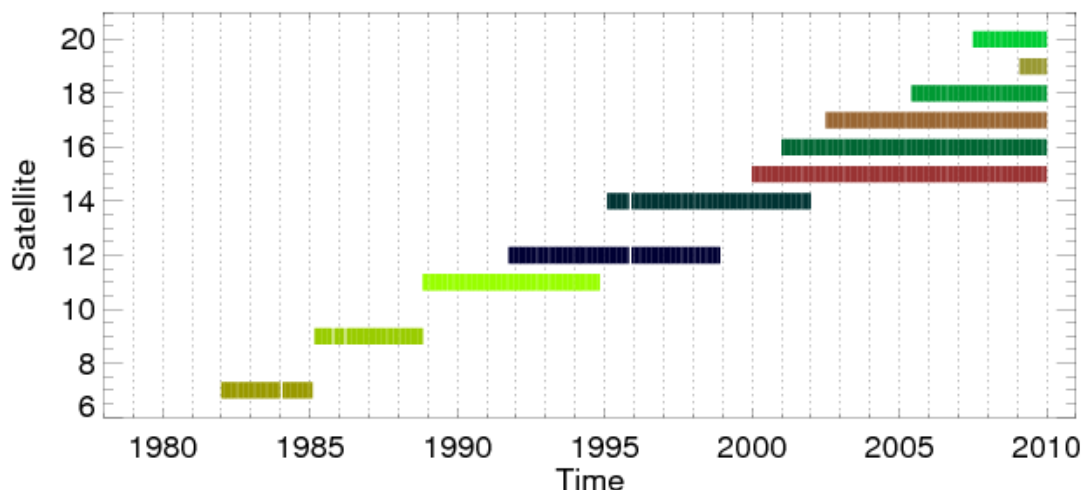



Figure 3.2 Visualisation of the used NOAA-satellites showing satellite numbers on Y-axis and the length of the observation period for each satellite. Notice that number 20 denotes Metop-A. Some data gaps are present but only for some isolated months for NOAA-7, NOAA-9, NOAA-12 and NOAA-14.

Observations from polar orbiting sun synchronous satellites are made at the same local solar time at each latitude band. Normally, satellites are classified into observation nodes according to the local solar time when crossing the equator during daytime (illuminated conditions). For the NOAA satellite observations, a system with one **morning observation node** and one **afternoon observation node** has been utilised as the fundamental polar orbiting observation system. This allows theoretically four equally distributed observations per day (if including the complementary observation times at night and in the evening when the satellite passes again 12 hours later). However, equator crossing times have varied slightly between satellites. Morning satellites have generally been confined to the local solar time interval 07:00-08:00 and afternoon satellites to the interval 13:30-14:30. However, a more significant deviation

	<p align="center">EUMETSAT SAF on CLIMATE MONITORING Validation Report Cloud product GAC Edition 1</p>	<p>Doc.No.:SAF/CM/SMHI/VAL/GAC/CLD Issue: 1.1 Date: 30.04.2012</p>
---	---	--

was introduced for the morning satellites NOAA-17 and Metop-A, now being defined in a so-called mid-morning orbit with equator crossing times close to 10:00. A specific problem with the observation nodes for the NOAA satellites has been the difficulty to keep observation times stable for each individual satellite (e.g., as described by Ignatov et al., 2004). This is illustrated further in Figure 3.3 for all NOAA satellites. Some compensation for this has been attempted in the CM SAF dataset but not for all parameters.

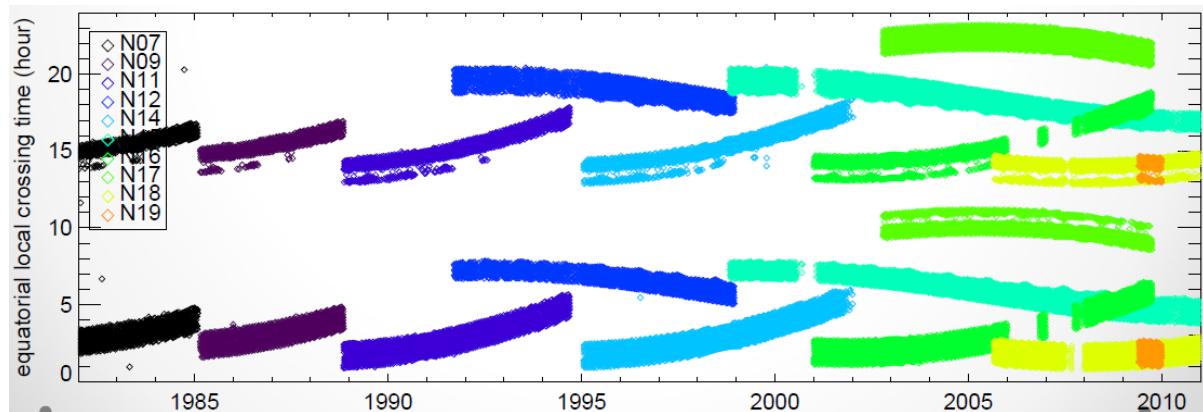



Figure 3.3 Local solar times at equator observations for all NOAA satellites from NOAA-7 to NOAA-19. Notice that the figure shows both ascending (northbound) and ascending (southbound) equator crossing times for each satellite separated 12 hours apart. (Courtesy of M. Foster, NOAA)

This validation report describes the efforts of validating global cloud products retrieved by CM SAF cloud retrieval methods from AVHRR GAC data spanning the time period 1982-2009. Retrieval methods have been dependent on the access to two infrared (split-window) channels at 11 and 12 microns meaning that only data from satellites carrying the AVHRR/2 or AVHRR/3 instruments have been used.

An important aspect for any product-based climate dataset (formally denoted Thematic Climate Data Records – TCDRs) is that retrieved products have been derived from accurately calibrated and homogenized radiances (formally denoted Fundamental Climate Data Records – FCDRs). For the CM SAF GAC dataset we have used an AVHRR FCDR prepared by NOAA (Heidinger et al., 2010). This FCDR was prepared for the compilation of the “NOAA Pathfinder Atmospheres – Extended” (PATMOS-x) dataset (for full description, see <http://cimss.ssec.wisc.edu/patmosx/overview.html>). This FCDR focussed in particular on homogenization of the AVHRR visible reflectances (now available for download at NOAA’s National Climate Data Centre, NCDC - see operational CDRs for 2010 at <http://www.ncdc.noaa.gov/cdr/operationalcdrs.html>). The calibration of infrared AVHRR channels is basically left untouched since the use of onboard blackbody calibration targets have been found to provide stable and reliable results. However, future upgrades of the AVHRR FCDR need to address remaining issues here also for the infrared channels (e.g., recognising the work of Mittaz et al., 2009).

The link to the work with PATMOS-x is also reflected in the CM SAF collaboration with NOAA within the SCOPE-CM initiative with particular focus on the derivation of TCDRs based on GAC AVHRR data. This explains also why a substantial part of this validation

	<p align="center">EUMETSAT SAF on CLIMATE MONITORING Validation Report Cloud product GAC Edition 1</p>	<p>Doc.No.:SAF/CM/SMHI/VAL/GAC/CLD Issue: 1.1 Date: 30.04.2012</p>
---	--	--

report deals with in-depth analyses of the similarities and differences between the CM SAF GAC dataset and PATMOS-x.

4 Cloud products and validation strategy

In this report, we evaluate results for the following six cloud products derived from AVHRR GAC data (with formal product numbers and abbreviations according to AD 1 given to the right):

Fractional Cloud Cover	CM-05 (CFC)
Cloud Top level	CM-17 (CTO)
Cloud Optical Thickness	CM-34 (COT)
Cloud Phase	CM-38 (CPH)
Liquid Water Path	CM-43 (LWP)
Ice Water Path	CM-47 (IWP)
Joint Cloud property histogram	CM-11 (JCH)

The theoretical basis for retrieval methods and compilation of TCDRs are described in RD 1. However, notice that RD 1 basically describes the methodology to prepare Level 1 datasets and to compile Level 3 products while individual retrieval methodologies are described in RD 2, RD 3, RD 4 and RD 5.

The purpose of the validation effort is to evaluate whether products comply with product requirements stated in AD 1. These requirements are summarised in Table 4.1.

The rationale for the chosen statistical parameters is that the overall SAF Product Requirements Table should include measures for both accuracy (i.e., how close to the truth is our estimation?) and precision (i.e., how stable is our estimation?).

Table 4.1 gives the target requirements for all CM SAF GAC cloud products. Observe that we describe two versions for the Cloud Top Level product (CM-17) since we will use reference measurements made in pressure as well as in geometric altitude coordinates. In addition, there are no specific requirements given for the JCH product since it is composed by individual products COT and CTP. Table 4.1 only lists the target requirements for the accuracy and precision parameters. Compliance with a more relaxed threshold requirement and a more demanding optimal requirement (as defined in AD 1) are also discussed further in each specific sub-section for every cloud product. Regarding corresponding requirements for Level 2 products, we notice that such requirements are still not defined (at least not for CM SAF products produced on the global area domain). However, a useful guideline here is to consider that accuracy requirements should theoretically be very similar (at least if neglecting problems due to specific sampling methodologies) while precision requirements would generally differ (i.e., higher variability is expected for Level 2 products).



	<p align="center">EUMETSAT SAF on CLIMATE MONITORING Validation Report Cloud product GAC Edition 1</p>	<p>Doc.No.:SAF/CM/SMHI/VAL/GAC/CLD Issue: 1.1 Date: 30.04.2012</p>
---	---	--

Table 4.1 CM SAF cloud products and their respective target requirements (defined in AD 1) for the GAC dataset of Level 3 monthly mean products. Notice that the requirement on mean error or bias for accuracy is valid for both negative and positive deviations.

Product	Accuracy requirement (mean error = bias))	Precision requirement (bias-corrected RMS for CFC,CTH and CTP, RMS for all others)
Cloud Fractional Cover (CFC)	10 % (absolute)	20 % (absolute)
Cloud Top Height (CTH)	1200 m	2000 m
Cloud Top Pressure (CTP)	110 hPa	130 hPa
Cloud Optical Thickness (COT)	15 %	30 %
Cloud Phase (CPH)	5 % (absolute)	10 % (absolute)
Liquid Water Path (LWP)	15 %	30 %
Ice Water Path (IWP)	25 %	50 %
Joint Cloud Histogram (JCH)	n/a	n/a

The requirement values listed in Table 4.1 are defined after taking into account requirements from different users and user groups. The most well-established reference here is the recommendations issued by the Global Climate Observation System - GCOS – community, see GCOS, 2006). However, values are also influenced by requirements from users working with regional climate monitoring and regional climate modelling applications (often having even stricter requirements than GCOS). All these requirements are rapidly changing (e.g., the GCOS requirements are currently under revision) but Table 4.1 gives the current basis used for the evaluation of the first edition of the CMSAF GAC cloud product dataset.

The CM SAF GAC dataset consists of daily and monthly mean (Level 3) products for the period 1982-2009. Thus, the validation task is to evaluate the quality of Level 3 products. However, we also have to take into account that inter-comparing with Level 3 products from other sources is much more difficult than to compare with instantaneous and simultaneous observations (i.e., the classical Level 2 validation process). The reason is that Level 3 products not only depend on the quality of Level 2 products but also on the method of compiling Level 3 products (i.e., in terms of the applied temporal and spatial sampling, criteria for including or excluding a measurement, averaging method, etc.). This means that it is not always that Level 3 product differences reflect true product differences in the same way as monitored by standard Level 2 validation activities. For this reason, we have tried to conduct both Level 2 and Level 3 validation (when applicable) in order to check the impact of different Level 3 methodologies. However, for practical reasons Level 2 studies have been limited in time and space compared to the task of evaluating the full CM SAF GAC dataset. In this context it should also be said that the validation of daily Level 3 products for a TCDR dataset spanning the time period 1982-2009 is a gigantic task. We have limited the study of daily mean products to an inter-comparison with surface observations for CFC products. For all other products there is simply a lack of suitable reference observations or, alternatively, the preparation and processing of corresponding reference products has not been possible to cope

 	EUMETSAT SAF on CLIMATE MONITORING Validation Report Cloud product GAC Edition 1	Doc.No.:SAF/CM/SMHI/VAL/GAC/CLD Issue: 1.1 Date: 30.04.2012
---	---	---

with regarding available staff and time resources. We believe that the mix of Level 2 (instantaneous) and Level 3(monthly mean) studies will also provide enough information about the expected quality of daily Level 3 products.

A perfectly valid validation exercise requires access to high quality and homogeneous observations which can be considered close to the truth and being independent from the observations or measurements being evaluated. For a global dataset of cloud products spanning a time period of 28 years these validation conditions do not exist, i.e., there is no high quality global observation dataset that is covering the entire 28 years in a homogeneous way. For that reason, we have been forced to use validation references that only partly fulfil the desired requirements.

The chosen validation references may be subdivided into two groups:

Group 1: Independent observations

- Cloud amount observations from surface stations (SYNOP)
(time period 1982-2009)
- Cloud amount and cloud top observations from the CALIPSO cloud lidar (CALIOP)
(time period 2006-2009)
- Cloud water measurements from microwave imagers (SSM/I and AMSR-E)
(time period 1988-2008)



Group 2: Similar observation datasets

- Cloud amount, cloud top, cloud phase, cloud optical thickness and cloud water observations from the NOAA AVHRR Pathfinder Atmospheres – Extended (PATMOS-x) dataset
(time period 1982-2009)
- Cloud amount, cloud top, cloud phase, cloud optical thickness and cloud water observations from the International Satellite Cloud Climatology Project (ISCCP)
(time period 1982-2008)
- Cloud amount, cloud top, cloud phase, cloud optical thickness and cloud water observations from the Moderate Resolution Imaging Spectroradiometer (MODIS)
(time period 2000-2009)

Notice also that the evaluation of the joint histogram product (JCH in Table 4.1) is based entirely on information provided by Group 2 above.

The first group of observations is definitely the most important group since it fulfils the condition that the observation reference must be independent. Thus, results achieved from comparisons with this group of observations will be given highest credibility.

However, as already stated, no reference is fulfilling the requirement of complete and homogeneous global and temporal coverage. Unfortunately, this concerns especially group 1. It forces us to use other kind of reference datasets to try to bridge existing gaps in the spatial and temporal domains, even if these datasets cannot be considered as being completely independent. When dealing with the latter we also have to use (when available) existing knowledge of the quality of these datasets. When such information is not easily found, we

 	<p align="center">EUMETSAT SAF on CLIMATE MONITORING Validation Report Cloud product GAC Edition 1</p>	<p>Doc.No.:SAF/CM/SMHI/VAL/GAC/CLD Issue: 1.1 Date: 30.04.2012</p>
---	--	--

can at least try to utilize results from inter-comparisons with results from group 1 for the limited periods and spatial domains that are offered. In conclusion, results based on observations from reference group 2 should be considered as results from **consistency checks** rather than as results from a true validation effort. This will be pointed out repeatedly in the remainder of this report. We also conclude that for some products (CPH, COT and IWP) we unfortunately must rely exclusively on consistency checks since we do not have access to completely independent observations.

The utilisation of the CALIPSO-CALIOP cloud observations in Group 1 above is worth a special statement. Despite the obvious limitations in both the temporal (i.e., only available for three years) and spatial (i.e., poor sampling since it only measures at nadir) domains, we are of the opinion that these observations must be utilised since they are probably the best cloud observations that has ever become available. The idea has been to try to inter-compare with a limited but optimised CALIPSO dataset to get the best possible information about the true CMSAF performance of two of the products, namely CFC and CTH. This could then be put into relation with the results from all other datasets during the same limited period. Furthermore, these results should then be used as a baseline for the discussion of sub-sequent studies inter-comparing results for Group 2 for years before the CALIPSO observation period. For the future, we also believe that this optimised CALIPSO dataset (described further in Section 6.1.1.2) can serve as a tool for benchmark testing of new GAC Editions planned during the next CDOP-2 project phase.

The inter-comparison with PATMOS-X results has also a special position in this report, explaining the comparatively large share of the text discussing this particular study. It is explained by the fact that there are specific links between the CMSAF and NOAA concerning a pilot study in the framework of the SCOPE-CM cooperation (initiated by the WMO Space Programme). This pilot study includes a detailed inter-comparison of CM SAF and PATMOS-X datasets. The results presented here represent a substantial part of this work. Furthermore, PATMOS-X is the only other dataset using exactly the same fundamental input data (AVHRR GAC FCDR) as the CMSAF dataset which make it natural to compare with it. Regarding the analysis of the consistency checks for observations in Group 2 and the ability of making of a deeper analysis, we must state that only in the case of PATMOS-x we have had access to all underlying products so that more detailed analyses could be undertaken. In all other cases we only have Level 3 datasets (monthly means) which limits the further analysis to some extent.

In the following, we will first introduce in Section 5 the various reference datasets we have used. Notice here that for each dataset a special statement on errors and uncertainties is given at the end of the description. Section 6 presents validation results product by product sorted according to three general product groups. Some aspects regarding the decadal stability of results are discussed in Section 7 followed by the main conclusions in Section 8.

	EUMETSAT SAF on CLIMATE MONITORING Validation Report Cloud product GAC Edition 1	Doc.No.:SAF/CM/SMHI/VAL/GAC/CLD Issue: 1.1 Date: 30.04.2012
---	---	---

5 Data Sets for Comparison with GAC

5.1 Manual cloud observations from surface stations (SYNOP)

Observations of total cloud cover made at meteorological surface stations (i.e. synoptic observations – hereafter called SYNOP) constitute one of the datasets used to evaluate the cloud fractional coverage estimates. At manned stations the total cloud cover is visually estimated by human observers. In contrast, ceilometers are used for that purpose at automatic stations. However, for data quality and consistency reasons, only those SYNOP reports provided by manned airport stations were taken into account (~1800 stations globally).


SYNOP total cloud cover observations are used for the evaluation of both Level-2 and Level-3 cloud cover estimates.

Uncertainty and error sources:

Manual cloud observations are affected by many sources of error. We list some of the most important in the following:

- The observation is subjective in nature, i.e., despite clear instructions on how to make an observation, differences will appear because of different interpretations from person to person. This introduces a random noise in global cloud amount observations but may also lead to geographical biases (reflecting some systematic behaviour related to the way people have been educated/trained).
- The human eye has a detection limit for when a cloud can be clearly discernible against a cloud-free sky. This limit is somewhere in the cloud optical thickness range of 0.5-1.0 (with some dependence on solar zenith angle, on which viewing angles clouds are observed and the degree of aerosol load or haze in the troposphere). Thus, many satellite sensors have a higher sensitivity to e.g. cirrus detection than SYNOP observations.
- At night, the random error in the observations increases. This is natural since the observer does not have a clear sky background against which a cloud can be observed (i.e., clouds are as dark as the cloud-free sky). However, accuracies improve in the presence of moonlight. Nevertheless, the overall effect is normally a negative bias (underestimated cloud amounts) since the observer is tempted to report cloud free conditions as soon as stars becomes visible, thus neglecting that large fractions of thin cirrus and other cloud types may still be present.
- A well-known deficiency of SYNOP observations is the scenery effect, i.e. overestimation of convective cloud towers at a slanted view (Karlsson, 2003). This effect is thus most pronounced in the summer season and for low to moderate cloud amounts when the overestimation easily can reach values of 20-30 % (1-2 octas).
- It is important to consider that most SYNOP stations are located at land stations and with higher density in developed countries. Thus, global averages tend to be biased towards land conditions in densely populated countries.

Since no rigorous study has been able to cover all those aspects in a quantitative manner (mainly because of lack of an absolute truth as reference) we can only make a very general statement about the overall quality. We would suggest that the accuracy of SYNOP

	<p align="center">EUMETSAT SAF on CLIMATE MONITORING Validation Report Cloud product GAC Edition 1</p>	<p>Doc.No.:SAF/CM/SMHI/VAL/GAC/CLD Issue: 1.1 Date: 30.04.2012</p>
---	---	--

observations vary between approximately +10 % (some overestimation) at daytime conditions changing to -10 % or worse (some underestimation) at nighttime. However, the variability (precision) probably reaches higher absolute values and it is largest during night conditions. This may lead to a strong seasonal variation in quality with the worst accuracy and precision features during the winter season (at least at middle and high latitudes including the Polar Regions).

It is worth noting that the increasing trend to replace manual cloud observations with automatic observations from ceilometers will change the accuracy and precision of cloud observations in several ways. This may possibly lead to improved accuracies at night time but there is also a considerable risk that the precision figures degrades, mainly as an effect of that ceilometers only observe a very small fraction of the sky.

Despite their subjective character and varying quality, SYNOP observations still provide a useful reference data set suitable for monitoring and validating space-based estimations of cloud coverage, especially due to their long-term availability.

5.2 A-Train (CALIPSO-CALIOP)

Measurements from space-born active instruments (radar + lidar) provide probably the most accurate information we can get about cloud presence in the atmosphere. The reason is the fact that the measured reflected radiation comes almost exclusively from cloud and precipitation particles and is therefore not “contaminated” by radiation from other surfaces or atmospheric constituents as is the case for measurements from most passive radiometers. In this validation study we have decided to utilise measurements from the CALIOP lidar instrument carried by the CALIPSO satellite (included in the A-Train series of satellites - Figure 5.1).



Figure 5.1 *The Aqua-Train satellites. (Image credit: NASA)*

The Cloud-Aerosol Lidar and Infrared Pathfinder Satellite Observation (CALIPSO) satellite was launched in April 2006 together with CloudSat. The satellite carries the Cloud-Aerosol Lidar with Orthogonal Polarization (CALIOP) and the first data became available in August 2006. CALIOP provides detailed profile information about cloud and aerosol particles and corresponding physical parameters.

	<p align="center">EUMETSAT SAF on CLIMATE MONITORING Validation Report Cloud product GAC Edition 1</p>	<p>Doc.No.:SAF/CM/SMHI/VAL/GAC/CLD Issue: 1.1 Date: 30.04.2012</p>
---	--	--

CALIOP measures the backscatter intensity at 1064 nm while two other channels measure the orthogonally polarized components of the backscattered signal at 532 nm. The horizontal resolution of each single FOV is 333 m and the vertical resolution is 30-60 m. The CALIOP cloud product we have used report observed cloud layers i.e., all layers observed until signal becomes too attenuated. In practice the instrument can only probe the full geometrical depth of a cloud if the total optical thickness is not larger than a certain threshold (somewhere in the range 6-10). For optically thicker clouds only the upper portion of the cloud will be sensed.

CALIOP products have been retrieved from the NASA Langley Atmospheric Science Data Centre (ASDC, <http://eosweb.larc.nasa.gov/JORDER/ceres.html>). We have used the Lidar Level 2 Cloud and Aerosol Layer Information product Version 3.01 with detailed characteristics found here:

http://eosweb.larc.nasa.gov/PRODOCS/calipso/Quality_Summaries/CALIOP_L2LayerProducts_3.01.html)

Also the associated information from the Lidar Level 2 Vertical Feature Mask product has been used. The associated details of this product are found here:


http://eosweb.larc.nasa.gov/PRODOCS/calipso/Quality_Summaries/CALIOP_L2VFMProducts_3.01.html

The latter product defines up to 10 cloud layers and each layer is classified into one of 10 cloud types according to Table 5.1. To be noticed here is that the ISCCP cloud type method has been used in the sense that the vertical separation of Low (categories 0-3), Medium (categories 4-5) and High (categories 6-7) clouds is defined by use of vertical pressure levels of 680 hPa and 440 hPa. However, the separation of thin and thick clouds is made using the information on whether the surface or lower layers below the current layer can be seen by CALIOP.

Table 5.1 *Cloud type categories according to the CALIOP Vertical Feature Mask product*

Category 0:	Low, overcast, thin (transparent St, StCu, and fog)
Category 1:	Low, overcast, thick (opaque St, StCu, and fog)
Category 2:	Transition stratocumulus
Category 3:	Low, broken (trade Cu and shallow Cu)
Category 4:	Altostratus (transparent)
Category 5:	Altostratus (opaque, As, Ns, Ac)
Category 6:	Cirrus (transparent)
Category 7:	Deep convective (opaque As, Cb, Ns)

The CALIOP products are defined in five different versions with respect to the along-track resolution ranging from 333 m (individual footprint resolution), 1 km, 5 km, 20 km and 80 km. The four latter resolutions are consequently constructed from several original footprints/FOVs. This allows a higher confidence in the correct detection and identification of cloud and aerosol layers compared to when using the original high resolution profiles. For example, the identification of very thin Cirrus clouds is more reliable in the 5 km dataset than in the 1 km dataset since signal-to-noise levels can be raised by using a combined dataset of several original profiles.

 	EUMETSAT SAF on CLIMATE MONITORING Validation Report Cloud product GAC Edition 1	Doc.No.:SAF/CM/SMHI/VAL/GAC/CLD Issue: 1.1 Date: 30.04.2012
---	---	---

We have also utilised here that the CALIOP datasets are delivered with some interesting auxiliary information attached related to the surface conditions under which the measurements took place. This information concerns land cover characterisation taken from the International Geosphere Biosphere Programme (IGBP) and ice and snow cover information taken from the National Snow and Ice Data Center (NSIDC).

We only give a quite general description of the CALIPSO datasets in this section. The details concerning the actual use of the datasets are elaborated further in the following sections 6.1.1.2 and 6.1.2.1.


Uncertainty and error sources:

It should be emphasized that the CALIOP measurement is probing the atmosphere very efficiently in the along-track direction since it is a nadir pointing instrument. Here, cloud dimensions down to the original FOV resolution (333 m) will be detected. However, it should be made clear that the across-track extension of the observation is still limited to 333 m. Thus, to compare CALIOP-derived results with the results of 4 km GAC AVHRR pixel data is not entirely consistent (i.e., CALIOP is only capable of covering the GAC pixel properly in one direction and not in the perpendicular direction). However, we believe that this deficiency is of marginal importance. Most cloud systems on the GAC scale will be detected, e.g., it is very unlikely to imagine elongated clouds with size and shapes below 0.3x4 km that might risk remaining undetected within a GAC pixel that coincides with a CALIOP measurement. Most clouds will have aspect ratios for the two horizontal directions that guarantee detection by CALIOP.

It is important to consider that the CALIOP lidar instrument is much more sensitive to cloud particles than the measurement from a passively imaging instrument. It means that a significant fraction of all CALIOP-detected clouds will not be detected by imagers. Thus, to get reasonable and justified results (i.e., saying something on the performance of the applied cloud detection method for clouds that should be theoretically detectable) one should consider filtering out the contributions from the very thinnest clouds. We have tested this approach in this validation study, both in the study of cloud amounts (CFC) and cloud top heights (CTO).

The cloud detection efficiency with CALIOP is slightly different day and night because of the additional noise from reflected solar radiation at daytime that can contaminate lidar backscatter measurements. However, Chepher et al. (2010) reports that this can introduce an artificial difference of not more than 1 % when comparing night time and daytime data. This is also confirmed by Kuehn (2012, personal communication) pointing out that this effect is negligible for optically thick clouds while it may introduce some artificial diurnal variation for optically very thin clouds (of which a large fraction is not detectable by passive imagers).

In the GAC DRI-5 context we have used the 5 km CALIOP dataset since this resolution is closest to the nominal AVHRR GAC resolution. However, we have learnt that the results in different datasets from CALIPSO, related to different horizontal resolutions (with the five options 333 m, 1 km, 5 km, 20 km and 80 km) are unfortunately not entirely consistent (Dave Winker, NASA, personal communication). It means that some of the thick (opaque) boundary layer clouds that are reported in fine resolution (333 m and 1 km) datasets are not reported in the higher resolution (5 km or higher) datasets. This has to do with the methodology to do

	<p align="center">EUMETSAT SAF on CLIMATE MONITORING Validation Report Cloud product GAC Edition 1</p>	<p>Doc.No.:SAF/CM/SMHI/VAL/GAC/CLD Issue: 1.1 Date: 30.04.2012</p>
---	--	--

averaging at the longer scales (5 km or higher) where contributions from strongly reflecting boundary layer clouds are removed from the original signal to facilitate detection of very thin cloud layers and aerosols. A recent study (Ralph Kuehn, SSEC, Madison, personal communication) estimated the loss of cloudy CALIOP5 km pixels to between 1-3 % because of this effect based on all orbits in the period 1-16 July 2006 when comparing with corresponding results based on 1 km CALIOP data. To our knowledge, this deficiency has not yet been reported in the literature.

In conclusion: Despite the fact that the CALIPSO cloud observations most likely are the best available cloud reference dataset being released so far, we might still see a negative bias of a few percent in the CALIOP-derived cloud cover when using the 5 km dataset. Other errors, e.g. due to mis-interpretation of heavy aerosol loads as clouds, are in this respect of minor importance when judging the effect on accumulated results based on a large number of full global orbits. This also concerns problems with reduced signal-to-noise ratios due to solar contamination during daytime.

5.3 Cloud liquid water observations from microwave imagers

Passive microwave imagers, such as the Special Sensor Microwave/Imager (SSM/I) series, can be used to retrieve column-integrated liquid water along with water vapour and surface wind speed. Because the microwave (MW) channels fully penetrate clouds, they provide a direct measurement of the total liquid (but not solid) cloud condensate amount. For precipitating clouds an estimate of the rain water path has to be made and subtracted from the total liquid water path to retrieve the cloud liquid water path.

For the GAC LWP evaluation the University of Wisconsin (UWisc) MW-based LWP climatology (O'Dell et al., 2008) was chosen as an independent reference dataset. The LWP climatology is based on retrievals from various microwave radiometer instruments, including the SSM/I series, the Tropical Rainfall Measurement Mission Microwave Imager (TMI), and the Advanced Microwave Scanning Radiometer – EOS (AMSR-E). The most recent version of the dataset that was used for the evaluation (version 3) spans the years 1988 – 2008.

Uncertainty and error sources:

Liquid water path estimates are reported to have an accuracy of 15-30% (O'Dell et al., 2008).

Two remarks have to be made regarding the validation. First, the MW LWP measurements are only possible over ocean, so the validation is restricted to marine clouds. Second, since the MW measurements are sensitive to ice, care has to be taken to select for the validation only those GAC grid cells with a sufficiently low monthly mean ice cloud fraction.

5.4 PATMOS-x

The most appropriate satellite-derived climatology to compare with is the PATMOS-x dataset. The acronym stands for “AVHRR Pathfinder Atmospheres – Extended” and the corresponding cloud products have been derived using the CLAVR-X method (Clouds from AVHRR – Extended, see Heidinger et al, 2005, Pavolonis et al., 2005, Thomas et al., 2004 and Hedinger and Pavolonis, 2009). As for the CM SAF PPS method, AVHRR radiances in all available spectral channels have been used to derive global cloud and radiation products

	<p align="center">EUMETSAT SAF on CLIMATE MONITORING Validation Report Cloud product GAC Edition 1</p>	<p>Doc.No.:SAF/CM/SMHI/VAL/GAC/CLD Issue: 1.1 Date: 30.04.2012</p>
---	--	--

over the entire lifetime of the AVHRR sensor. Some basic information about the used methodology for the derivation of various parameters is given in Table 5.2. To notice is that the cloud screening methodology of CLAVR-X has undergone a substantial revision lately compared to the method described above by the cited references. The previous multispectral threshold approach has been replaced by a probabilistic methodology (naïve Bayesian classifier – described in a new paper by Heidinger et al., 2012). We have compared CM SAF results against the results produced by this new method.

Table 5.2 *Some basic characteristics of the PATMOS-x retrieval methods.*

Product	Methodology
Cloud amount	Computed from results of a statistical naïve Bayesian cloud mask trained from CALIPSO-CALIOP cloud information
Cloud top level	Optimum Estimation (OE) retrieval
Cloud phase	Infrared-based OE retrieval
Cloud optical thickness	OE retrieval (with look-up tables as CMSAF but with different radiative transfer models and ice particle definitions)
Cloud liquid water path	Calculated from optical thickness and effective radius (Stephens' parameterization – same as CMSAF)
Cloud ice water path	Calculated from optical thickness and effective radius (Stephens' parameterisation – same as CMSAF)

The PATMOS-x dataset is prepared exclusively as so-called Level 2b products. This means that, for each satellite, data from all orbits during one day have been sub-sampled to produce only two global products per day valid for the nominal local solar time for both the descending (southbound) and ascending (northbound) observation nodes.

Level2b cloud products have been created for the CM SAFGAC dataset in a similar manner as the PATMOS-x Level2b dataset. A global lat-lon grid at 0.1x0.1 degree resolution was created, and Level2 products were transformed onto this global grid. The idea of the Level2b dataset is that only one high-quality observation should be used at each lat-lon grid box and for each observation node (ascending or descending). This observation is chosen by selecting pixels belonging to the grid point (using the nearest neighbour criterion) and picking the pixel with the lowest observation angle (i.e., satellite zenith angle). The latter criterion is needed outside of the tropics where the same grid point may be observed from several adjacent orbits.

Examples of CM SAF Level2b cloud top pressures from NOAA16 for July 1, 2001 are shown in Figure 5.2. The upper panel shows the cloud top pressures for the ascending orbit (13:30 LT) and the lower panel for the descending orbit (01:30 LT).

Due to the very close relationship between the CM SAF GAC dataset and PATMOS-x, we will spend a substantial part of the validation report inter-comparing the results of the two datasets. This includes an evaluation of the impact and difference caused by the fact that Level 2b datasets (like PATMOS-x) only contains a fraction of the complete GAC dataset while the official CM SAF GAC Level 3 products will be based on the complete GAC dataset (i.e., data from all orbits).

 	<p align="center">EUMETSAT SAF on CLIMATE MONITORING Validation Report Cloud product GAC Edition 1</p>	<p>Doc.No.:SAF/CM/SMHI/VAL/GAC/CLD Issue: 1.1 Date: 30.04.2012</p>
---	--	--

Uncertainty and error sources:

Stubenrauch et al. (2012) reports the following uncertainties for PATMOS-x based on comparisons with CALIPSO-CALIOP cloud layer information:

CFC: Probability of detection (POD) varies between 70-75 % over Polar Regions and snow-covered land surfaces to roughly 90 % over all other surfaces. Deviations with respect to ISCCP and MODIS Level 3 datasets are reported to be less than 5 % over most global regions.

CTO: Cloud heights for high cloud layers are overestimated by approximately 0.5 km while low level cloud heights are underestimated by 0.8 km.

CPH: Uncertainty measures not given.

COT: Estimated to within 20 % for liquid clouds and within 30 % for ice clouds.

LWP: Estimated to within 30 %.

IWP: Estimated to within 50 %.

5.5 ISCCP

The International Satellite Cloud Climatology Project (ISCCP) provides cloud properties over a period of more than 25 years (Rossow and Schiffer, 1991; Rossow et al., 1996; Rossow and Schiffer, 1999). This project was established in 1982 as part of WCRP to collect weather satellite radiance measurements (from geostationary and polar orbiting satellites) and to analyze them to infer the global distribution of clouds, their properties, and their diurnal, seasonal and inter-annual variations. The resulting datasets and analysis products are being used to study the role of clouds in climate, both their effects on radiative energy exchanges and their role in the global water cycle. This project and its results are considered to be the state of the art today on what can be derived from routine weather satellite data. ISCCP is the only other existing TCDR for cloud physical property products (here we mean products CPH, COT, LWP and IWP). However, it has the disadvantage that it is based on different satellite types – polar and geostationary – of which most of the latter do not contain the necessary narrow-band channels for accurate retrieval of LWP and IWP.

Uncertainty and error sources:

Stubenrauch et al. (2012) reports the following uncertainties for the ISCCP dataset:

CFC: Within 10 %.

CTO: Within 100 hPa.

CPH: No uncertainty information given (method just based on 11 micron brightness temperature threshold at 260 K).

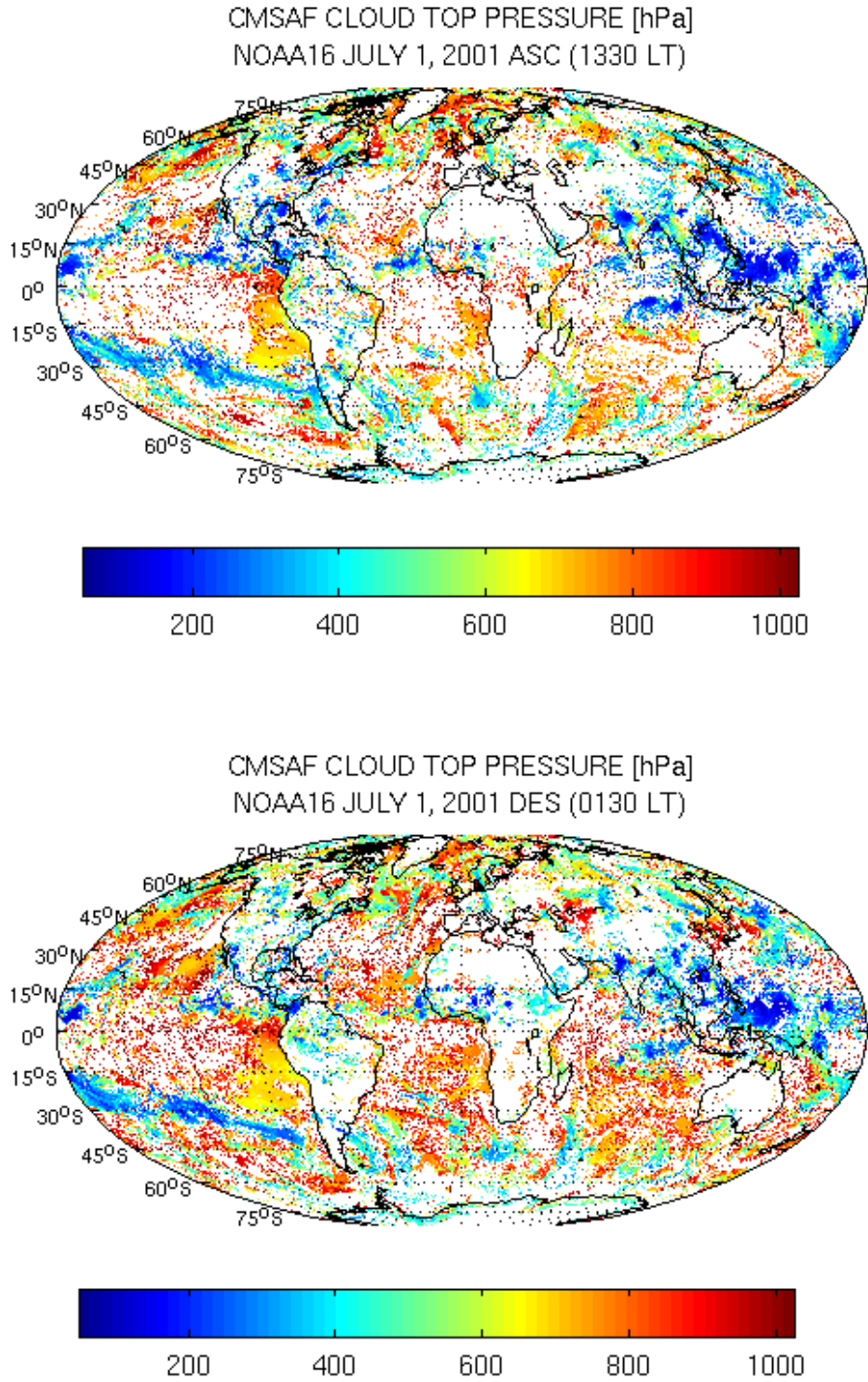


Figure 5.2 CM SAF Level2b cloud top pressure (hPa) on July 1, 2001 from NOAA16 for the ASC (13:30 LT) overpass (top panel) and for the DES (01:30 LT) overpass (bottom panel).

	<p align="center">EUMETSAT SAF on CLIMATE MONITORING Validation Report Cloud product GAC Edition 1</p>	<p>Doc.No.:SAF/CM/SMHI/VAL/GAC/CLD Issue: 1.1 Date: 30.04.2012</p>
---	--	--

COT: Estimated to within 10 % for monthly means.

LWP: Estimated to within 30 %.

IWP: Estimated to within 30 %.

5.6 MODIS

MODIS (or Moderate Resolution Imaging Spectroradiometer) is an advanced imaging instrument onboard the Terra (EOS AM) and Aqua (EOS PM) polar satellites (see <http://modis-atmos.gsfc.nasa.gov/index.html>). Terra's orbit around the Earth is sun synchronous and timed so that it passes from north to south across the equator in the morning (local solar time 10:30), while Aqua passes south to north over the equator in the afternoon (local solar time 13:30). Terra MODIS and Aqua MODIS are viewing the entire Earth's surface every 1 to 2 days, acquiring data in 36 spectral bands or groups of wavelengths.

Since the Terra and Aqua satellites pass in very similar orbits (at least the afternoon orbit of Aqua) as the NOAA and Metop-A satellites and since MODIS observes with as much as 36 spectral channels (including all the AVHRR-like channels), corresponding cloud products from MODIS should serve as a top quality reference for corresponding cloud products retrieved from AVHRR data. The only limitation is the relatively short duration of the observation period, starting in 2000. We have used the level-3 MODIS gridded atmosphere monthly global products - MOD08_M3 (Terra) and MYD08_M3 (Aqua). They contain monthly 1 x 1 degree grid average values of atmospheric parameters related to atmospheric aerosol particle properties, total ozone burden, atmospheric water vapour, cloud optical and physical properties, and atmospheric stability indices. Statistics are sorted into 1x1 degree cells on an equal-angle grid that spans a (calendar) monthly interval and then summarized over the globe. For this particular study we have used data from Terra & Aqua Collection 5.1 (with errors in the original Collection 5.0 dataset being corrected).

Uncertainty and error sources:

Stubenrauch et al. (2012) reports the following uncertainties for MODIS data (Science Team = ST, CERES = CE), mainly based on comparisons with CALIPSO-CALIOP cloud layer information:

CFC: For MODIS ST, probability of detection (POD) varies between 70-75 % over Polar Regions in the Polar night to roughly 90 % over all other surfaces (including Polar Regions in the Polar summer). No specific figures are given for MODIS CE but the same basic characteristics (e.g. problems in Polar Regions) are mentioned.

CTO: MODIS ST results show 1.5 km underestimation for high-level clouds and 1-2 km overestimation for low-level clouds. MODIS CE shows approximately the same, possibly with less overestimation of low-level cloud heights.

CPH: No uncertainty information given.

	<p align="center">EUMETSAT SAF on CLIMATE MONITORING Validation Report Cloud product GAC Edition 1</p>	<p>Doc.No.:SAF/CM/SMHI/VAL/GAC/CLD Issue: 1.1 Date: 30.04.2012</p>
---	--	--

COT: For MODIS ST estimated to within 10 % for optical thicknesses above 10. Uncertainties increase for lower values reaching 50-300 % for optical thicknesses below 1.0 (largest over land surfaces). For MODIS CE estimated to a small underestimation of COT for low-level water clouds (-5 % to 0 %) and some overestimation of COT for Cirrus clouds (10-40 %).

LWP: Estimated to within 30 % for MODIS ST and within 10 % for MODIS CE.

IWP: Estimated to within 30 % for MODIS ST and in the range 0-20 % for MODIS CE.

6 Evaluation of GAC Parameters

The presentation of validation results has been subdivided according to the following three sub-groups:

1. Macroscopical cloud products
2. Microphysical cloud products
3. Multi-parameter product representations.

The first group of cloud products (consisting of cloud amount and cloudtop level) represents the general three-dimensional occurrence of clouds as described by the horizontal and vertical extension of cloud layers. The second group (cloud phase, cloud optical thickness, cloud water path and cloud ice path) represents properties which are related to individual cloud particles and their density distribution. Finally, the third group (joint histograms) represents condensed forms for presentation of cloud information involving both of the previous two groups.

For some products, several validation approaches have been conducted and they are consequently described in specific sub-sections. Especially the performance of cloud screening or cloud detection is studied in depth in section 6.1.1 because of the importance for subsequent estimations of other cloud products.

To facilitate the reading of the document, each sub-section associated with a particular study ends with conclusions in a bullet list and a requirements compliance table or (if results are sub-divided in many aspects) compliance figure. In addition, for each cloud product a summarizing section with compliance tables is presented at the end of individual sections.

6.1 Macroscopical cloud products

6.1.1 Fractional cloud cover (CFC)

6.1.1.1 Evaluation against SYNOP

SYNOP total cloud cover observations are used for the evaluation of both Level-2 and Level-3 cloud cover estimates which makes it possible, as already mentioned earlier, to check the impact of spatial and temporal sampling. For both the Level 2 and the Level 3 comparison the available number of the match-ups and monthly mean, respectively, reflect the known geographically unbalanced distribution of the synoptic stations (see Figure 6.1): the majority of the stations are located in the northern mid-latitudes while there are fewer stations over large parts of Africa and the Northern part of South America. This uneven distribution has to

 	EUMETSAT SAF on CLIMATE MONITORING Validation Report Cloud product GAC Edition 1	Doc.No.:SAF/CM/SMHI/VAL/GAC/CLD Issue: 1.1 Date: 30.04.2012
---	---	---

be kept in mind when looking at accumulated statistics. For visualization purposes, all regional results have been aggregated to 5°x5° grid boxes.

In order to evaluate the performance of the AVHRR-GAC cloud fraction both mean error (accuracy parameter) and bias-corrected Root Mean Square errors (precision parameter) have been calculated and then compared to the defined target requirements as specified in Table 4.1. To remember here is that especially for the precision parameter higher values are to be expected when comparing Level 2 estimates. For the Mean Error, target requirements are the same for Level 2 and 3 products.

Level 2 comparison

For the Level 2 comparison AVHRR-GAC cloud mask estimates are compared against collocated total cloud cover observation made at SYNOP stations for all months of July during the entire time period (1982 -2009). The study is limited to the month of July because of the absolutely overwhelming task to do this type of comparison for all months. The AVHRR-GAC cloud fraction is computed as fraction of the 3x3 pixels around each station that have been labelled as either fully cloudy or cloud contaminated. The maximum time difference allowed between SYNOP and satellite observations is 20 minutes.

Figure 6.1 shows the regional distribution of the bias for the month of July calculated for the entire time period (1982-2009). In addition, the same results but separated for all individual satellites are shown in Figure 6.3. In general a good agreement is found between the two datasets. In most regions the mean bias remains within +/- 10 % cloud amount (yellow and green colors) and thereby within the target accuracy. Higher positive deviations can be found though over semi-arid areas: central Asia, Middle East and other semi-arid regions. These differences are noticeably higher for the afternoon satellites (i.e. NOAA-11, NOAA-14, NOAA-16, NOAA-18 - Figure 6.3, left column of plots) compared to morning satellites (i.e. NOAA-15, -NOAA17 and Metop-A - Figure 6.3, right column of plots). The histogram in Figure 6.2 (to the right) shows the distribution of the differences for all match-ups. Table 6.1 provides detailed statistics both averaged over all matchups and for different illumination and viewing angle conditions as well as for the different satellites. The overall difference between AVHRR-GAC and SYNOP is approximately 3% cloud amount with a bias-corrected RMS of 30% cloud amount. The mean error calculated separately for the different satellites range from -2 % (NOAA-15) to +10% (NOAA-19). The respective time period covered by the satellites ranges from 3 years for Metop-A to 10 years for NOAA-15.

Figure 6.4 shows the time series of the bias calculated over all stations for all months of July of the entire period 1982-2009 separately for the different satellites. The bias remains fairly stable over time for the different satellites and lies within +/- 10% cloud amount with the exception of the year 1983. Except for NOAA-15 all satellites show positive biases.

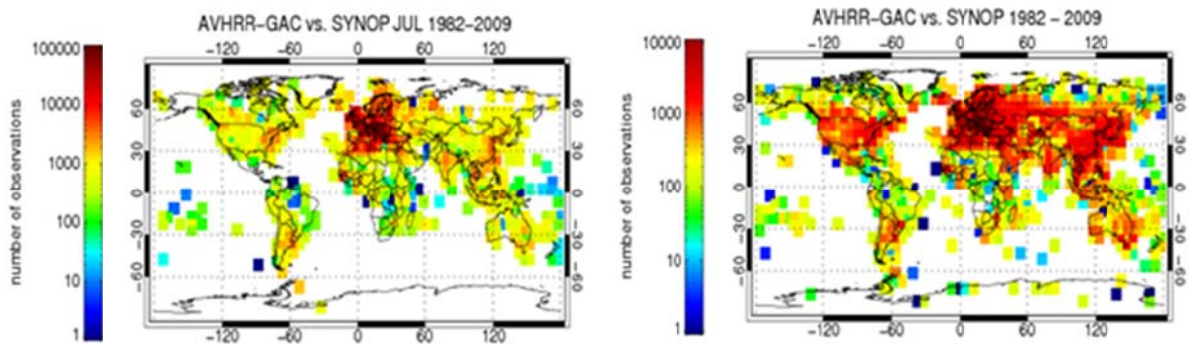


Figure 6.1 Regional distribution of the number of Level 2 match-ups (left) and number of monthly means (Level 3) available (right) for the month of July 1982-2009.

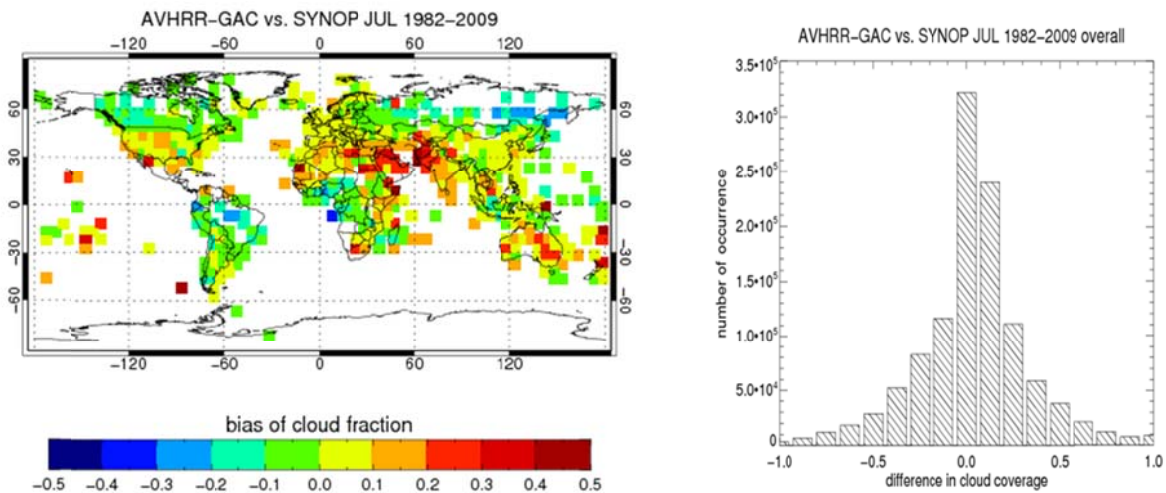


Figure 6.2 Left: Regional distribution of the mean error (bias) of cloud fraction for Level 2 products. Right: Histogram of the difference in cloud coverage results between AVHRR-GAC and SYNOP.

Level 3 comparison

For the Level 3 comparison the AVHRR-GAC monthly mean product generated from all the satellites available was compared against SYNOP monthly mean cloud cover calculated based on daily means. Only those stations and months were taken into account where at least 6 observations per day at 20 days of the respective month are available.

In Figure 6.5 the regional distribution of the bias calculated over the entire time period is depicted. For most regions the bias lies well below 10 % and thereby within the target accuracy defined for the CFC monthly mean product. Higher deviations are found again in semi-arid regions of the Middle East and Australia, western United States and over the snow-covered regions of Asia.

The good agreement found in general can also be seen in Figure 6.6 where the 2D-histogram of the cloud cover given by AVHRR-GAC and SYNOP is shown and where most of the samples align well on the 1:1 line. It also shows that for lower cloud cover values AVHRR-GAC is higher than SYNOP – reflecting the observed overestimation of cloud cover over semi-arid regions.

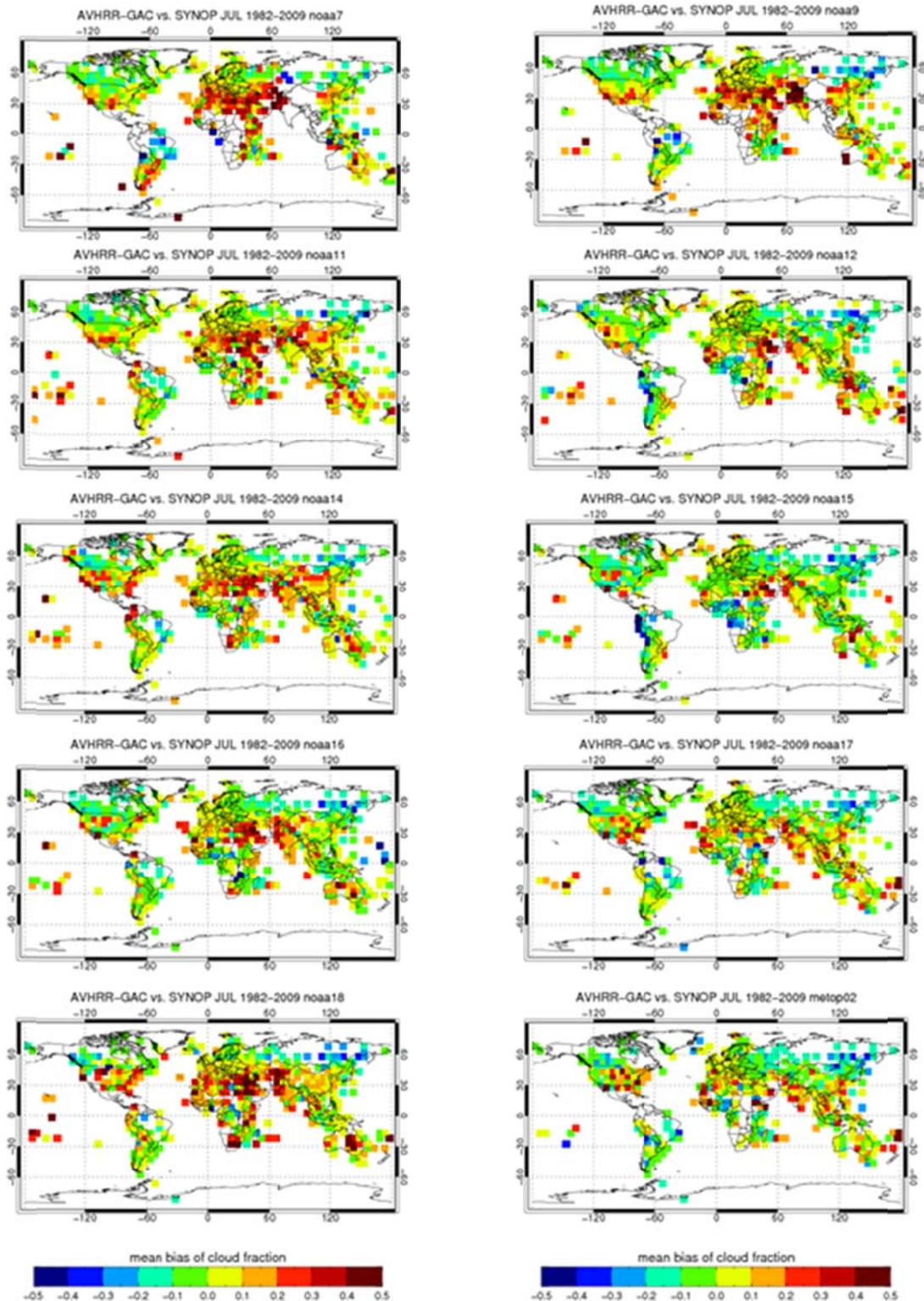


Figure 6.3 Regional distribution of the bias in cloud coverage (AVHRR-GAC – SYNOP) for the individual satellites. The respective time period covered by the satellites ranges from 3 years for Metop-A to 10 years for NOAA-15. Notice that the left column of plots show afternoon-night satellites and the right column shows morning-evening satellites.

Table 6.1 Detailed statistics, including mean error (bias), the bias corrected RMS (BC-RMS) as well as the mean absolute bias (abs. bias) calculated also separately for different illumination conditions, satellite viewing angles, regions and satellites.

SIT.	MATCH-UPS	MEAN GAC	MEAN SYN	BIAS	ABS. BIAS	BC-RMS
overall	1141738	0.57	0.54	0.03	0.21	0.30
europa	639488	0.57	0.52	0.04	0.20	0.27
trop_n	110521	0.68	0.62	0.06	0.23	0.33
trop_s	63194	0.48	0.47	0.02	0.23	0.34
midlat_n	828084	0.55	0.52	0.04	0.21	0.29
midlat_s	31016	0.52	0.51	0.02	0.21	0.32
polar_s	2328	0.55	0.56	-0.01	0.32	0.44
polar_n	106202	0.66	0.70	-0.03	0.18	0.26
day	804234	0.60	0.56	0.04	0.21	0.29
night	278220	0.51	0.48	0.03	0.22	0.32
twilight	59035	0.50	0.56	-0.06	0.22	0.31
sza_lt40	537020	0.55	0.54	0.01	0.21	0.30
sza_gt40	604718	0.59	0.54	0.05	0.21	0.29
noaa7	45204	0.60	0.52	0.07	0.22	0.30
noaa9	75207	0.62	0.56	0.06	0.21	0.30
noaa11	121161	0.60	0.54	0.06	0.21	0.30
noaa12	150491	0.56	0.55	0.01	0.19	0.28
noaa14	152874	0.63	0.57	0.06	0.21	0.30
noaa15	167536	0.52	0.54	-0.02	0.20	0.29
noaa16	151006	0.56	0.53	0.02	0.21	0.30
noaa17	129513	0.55	0.51	0.03	0.21	0.30
noaa18	83901	0.60	0.53	0.07	0.23	0.31
noaa19	15864	0.61	0.52	0.10	0.25	0.33
metop02	48981	0.51	0.50	0.01	0.20	0.29

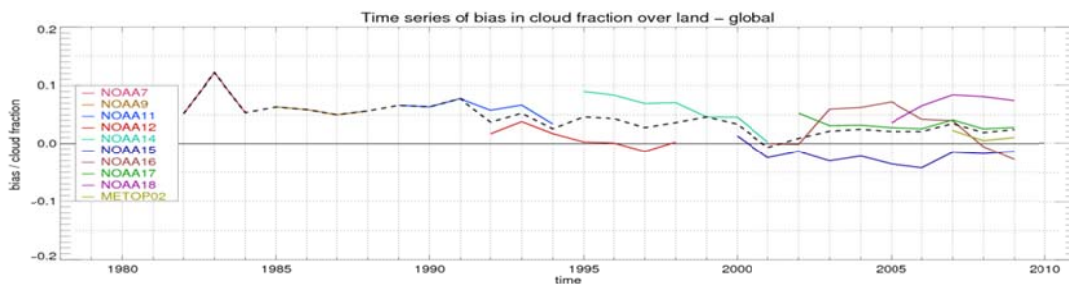


Figure 6.4 Time series of the mean error (bias) in cloud coverage for the month of July from for the period 1990 to 2009, separately for the individual satellites. The dashed line depicts the bias averaged over all satellites available.

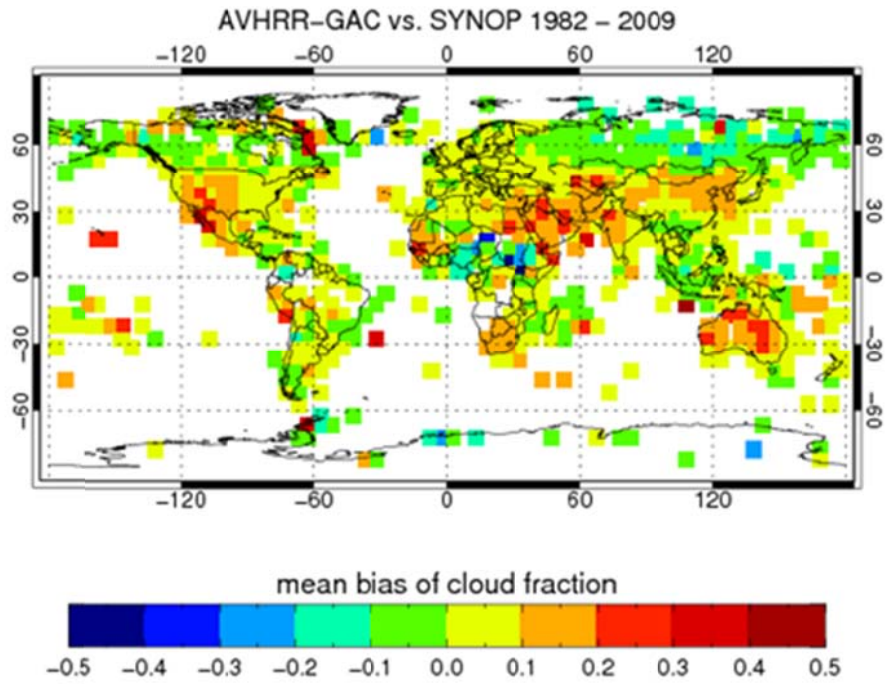


Figure 6.5 Regional distribution of the bias calculated for the entire time period (1982-2009). Target accuracy is met by all grid boxes in yellow and green.

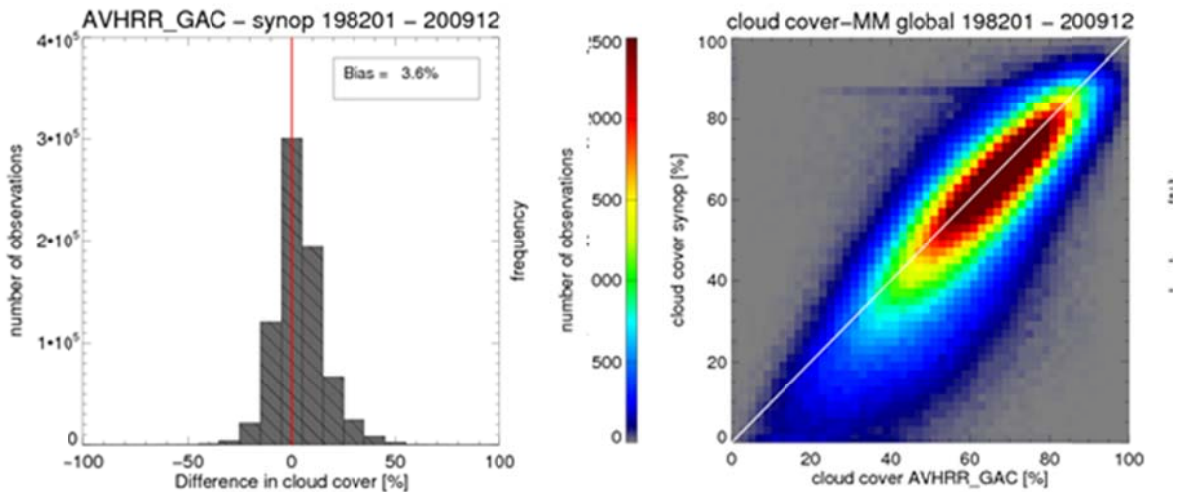



Figure 6.6 2D-scatter plot of the monthly mean cloud cover shown by AVHRR-GAC and SYNOP (right) and histogram of the difference between AVHRR-GAC and SYNOP (left) for the entire time period.

	EUMETSAT SAF on CLIMATE MONITORING Validation Report Cloud product GAC Edition 1	Doc.No.:SAF/CM/SMHI/VAL/GAC/CLD Issue: 1.1 Date: 30.04.2012
---	---	---

In Figure 6.7 the time series of the monthly mean cloud cover averaged over all stations available are shown for both AVHRR-GAC (red) and SYNOP (green). Both datasets show good agreement with the mean error and the bias-corrected RMS staying well below the target requirements of 10 % and 20% cloud amount respectively (Figure 6.7, middle panel). The seasonal cycle with higher cloud cover in Northern Hemisphere winter and lower in summer is also well reproduced by the AVHRR-GAC. Whereas the SYNOP time series stays stable over time between 50 to 60 % cloud amounts, AVHRR-GAC shows a decreasing trend over the time. This can be explained by the changes in the temporal sampling over the years. While only one satellite is available at the beginning of the time series, more and more satellites contribute to the monthly mean towards the end over the years. The additional satellites are mainly morning-evening satellites, thus often observing at twilight conditions. Twilight conditions often leads to underestimated cloud cover in the satellite analysis, thus providing a plausible explanation to the decreasing trend in overall cloud amounts over time. This also explains the decreasing variability observed in case of the AVHRR-GAC time series. Another feature that can be observed is that the bias-corrected RMS stays stable over the entire time series with values around 12% while the bias shows a seasonal cycle with lower differences in Northern Hemisphere summer/autumn and higher values in winter/spring.

The reason for the seasonal cycle of the mean error is not entirely obvious. It certainly may depend on the fact that we have more land masses over the Northern Hemisphere and that we therefore have different characters of the formed cloud fields over the Northern and Southern hemispheres over the different seasons. However, it could also be a sign of that the indicated CM SAF GAC problems of overestimating cloud cover over semi-arid regions (which represents rather large areas globally – e.g., as seen in Figure 6.5) have a seasonal variation with a maximum error occurring in Northern Hemisphere winter and spring. This has to be examined further. It is also a fact that the quality of SYNOP observations varies with varying solar illumination (night observations are indisputably less reliable). In section 5.1 we mentioned that we anticipate a seasonal cycle in the quality of SYNOP observations of clouds since cloud amounts are generally overestimated during daytime and underestimated during night. Such a cycle in the reference observation will naturally be seen in the results since for summer and winter seasons the daytime and night time observations dominate, respectively. A dominance of results for the Northern Hemisphere winter due to the fact that observation density is highest over mid- and high-latitude areas in Europe may also influence results further. Thus, there are several plausible causes indicating that a seasonal cycle in the bias can be expected but it is currently not possible to make firm conclusions about the relative importance of them.

The outlier found in January/February 1989 can be explained by the fact that due to some technical problems while extracting the data from the database there are only cloud observations available for one single station in these months (most clearly seen in the lowermost panel in Figure 6.7).

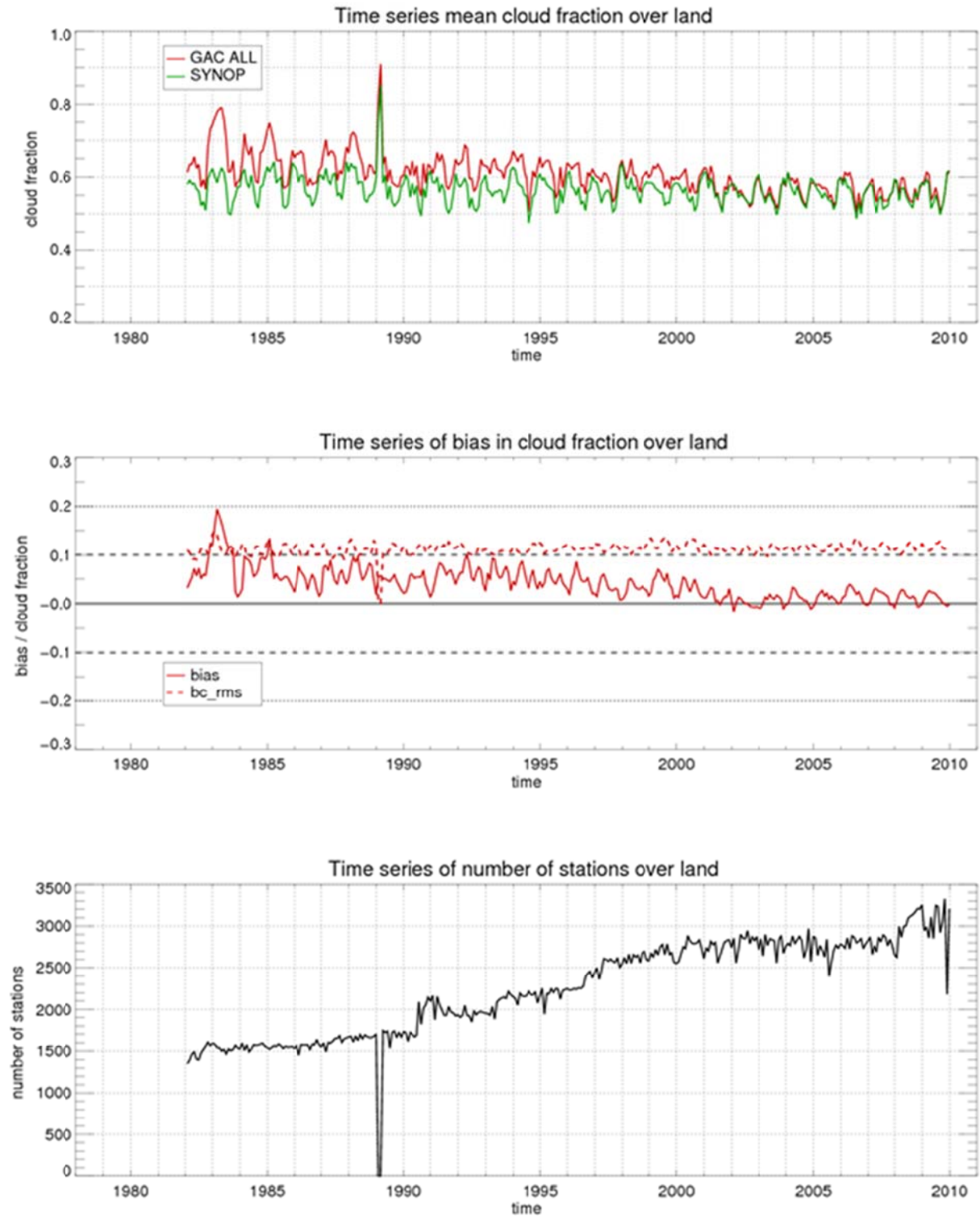



Figure 6.7 Time series of mean cloud cover for AVHRR-GAC (red) and SYNOP (green) (upper panel), mean error and bias-corrected RMS (middle panel) as well as the number of stations (lower panel) for the entire period 1982-2009.

 	<p align="center">EUMETSAT SAF on CLIMATE MONITORING Validation Report Cloud product GAC Edition 1</p>	<p>Doc.No.:SAF/CM/SMHI/VAL/GAC/CLD Issue: 1.1 Date: 30.04.2012</p>
---	--	--

Summary of results

- Compliances with requirements are summarized in Table 6.2
- Good agreement in general: in most regions the absolute bias found lies within 20% cloud amount (~ 2 octa) for Level 2 products
- Higher and positive deviations are found over semi-arid regions (e.g., Australia, Pakistan, Saudi-Arabia and western parts of the US)
- More pronounced (positive) deviations are found for afternoon satellites (i.e. NOAA-11, NOAA-14, NOAA-16, NOAA-18)
- Mean error and absolute bias between AVHRR-GAC and SYNOP Level 2 products for the entire 20 year time period are 3% and 20 % cloud amount, respectively
- The overall mean error calculated for all stations remains relatively stable over time and lies within the target accuracy of +/- 10% cloud amount (exception only in 1983)
- Corresponding values for Level 3 products are for bias 3.6 % and for bias-corrected RMS approximately 11 % absolute (target value 20 %)
- Unfortunately, the anticipated accuracy of SYNOP observations is probably not better than 10 %. Consequently, considering also the influence of the varying quality day and night and the uneven distribution of stations globally, the accuracy estimates above are likely to be quite uncertain in a global perspective.
- Considering the dominance of SYNOP observations over Europe, the results shown here are more representative for mid- and high-latitude land areas than for any other part of the Earth.

Table 6.2 Compliance matrix of found global CFC monthly mean product characteristics with respect to the defined product requirements for accuracy and precision. Comparisons were made against SYNOP observations. **Remark:** The anticipated error of SYNOP observations is probably of the order of 10 %, i.e., close to the Target requirement.

	CFC product requirements Level 3 (MM)			SYNOP Level 3 (1982-2009)	SYNOP Level 2 (July 1982-2009)
	Threshold	Target	Optimal		
Bias	20%	10%	10%	3.6 %	3 %
bc-RMS	40%	20%	15%	11 %	30 %

	<p align="center">EUMETSAT SAF on CLIMATE MONITORING Validation Report Cloud product GAC Edition 1</p>	<p>Doc.No.:SAF/CM/SMHI/VAL/GAC/CLD Issue: 1.1 Date: 30.04.2012</p>
---	--	--

6.1.1.2 Evaluation against A-Train (CALIPSO-CALIOP)

Following the approach by Karlsson and Dybbroe (2010), we have conducted a limited comparison with high-quality cloud observations from the CALIPSO-CALIOP sensor. Even though it is not possible to collect anything that is even close to a comparable Level 3 dataset from CALIPSO, we believe that extensive Level 2 comparisons will anyway provide an important snapshot of the behaviour and performance of the CM SAF GAC dataset. In addition, since the CALIOP dataset also provides valuable information about the optical thickness of the very thinnest detected clouds we believe it will be possible to better judge the limitations of the AVHRR cloud detection using the CM SAF methods in relation to e.g. other datasets.

We adopted the following strategy for this study:

- Select the best complete matches (i.e., entire global orbits) between NOAA-18 and A-Train/CALIPSO for every month where we have CALIPSO data available (i.e., October 2006-December 2009)
- Compile statistics for the total dataset as well as for selected regions (depending on latitude and surface conditions) and illumination conditions (day, night, twilight)
- Try to compare results (also including estimating the effect of thresholding the cloud optical thickness) with corresponding overall results for the other datasets (e.g. SYNOP, PATMOS-x, MODIS and ISCCP) evaluated during the same period (however, notice that the bulk of this comparison is made later in section 6.1.1.7).

Observe that the choice of NOAA-18 is explained by the fact that this satellite is placed in almost the same orbital plane as the Aqua-Train satellites with approximately the same equator crossing time. Thus, if choosing matches where the orbital tracks crosses simultaneously (denoted Simultaneous Nadir Observations – SNOs) - in this case occurring within only 12 seconds, we can get measurements matched in near nadir observation conditions for an entire global orbit and with a maximum time difference between observations of less than 2 minutes. Using this criterion we may theoretically get close to 3 such optimal matches each month. However, due to some losses of data we ended up with a total of 107 global orbits evenly distributed over the period (see total coverage in Figure 6.8). The geographical coverage is good but we can see that for some regions (e.g., over South America, North Atlantic Ocean, Africa and parts of the Pacific Ocean) the orbit coverage is less frequent than over other regions. An example of one of the resulting orbits is shown in Figure 6.9 and the corresponding plot of cloud mask results is given in Figure 6.10. Notice that only small deviations (less than 10 degrees) from the nadir view are achieved for the matched AVHRR observations during such an orbit (Figure 6.11).

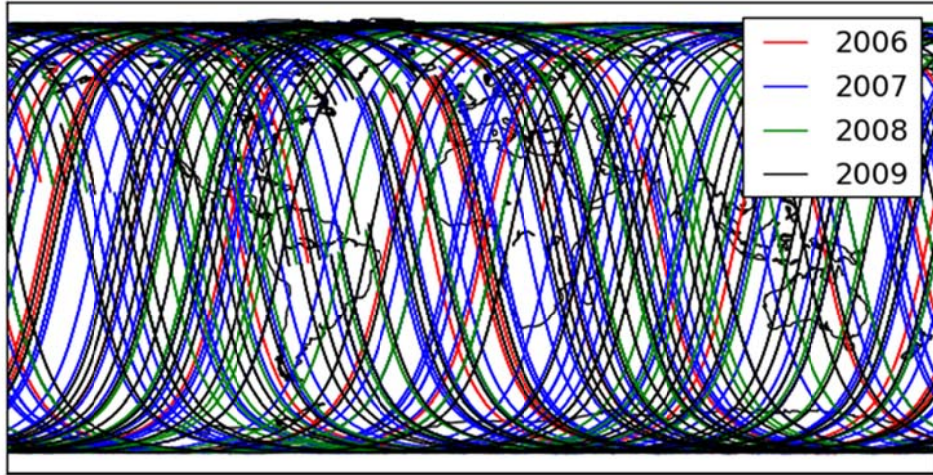


Figure 6.8 Total coverage of matched CALIPSO-NOAA-18 orbits in the period October 2006 to December 2009. Different colours refer to different years.

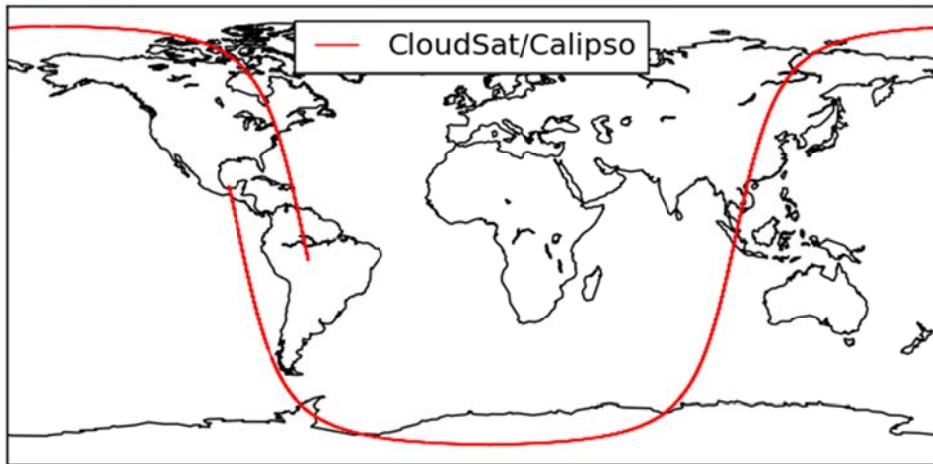


Figure 6.9 Trajectory for one selected matched CALIPSO-NOAA-18 orbit from 6 October 2006 with first matched observation at 18:00 UTC (over South America).

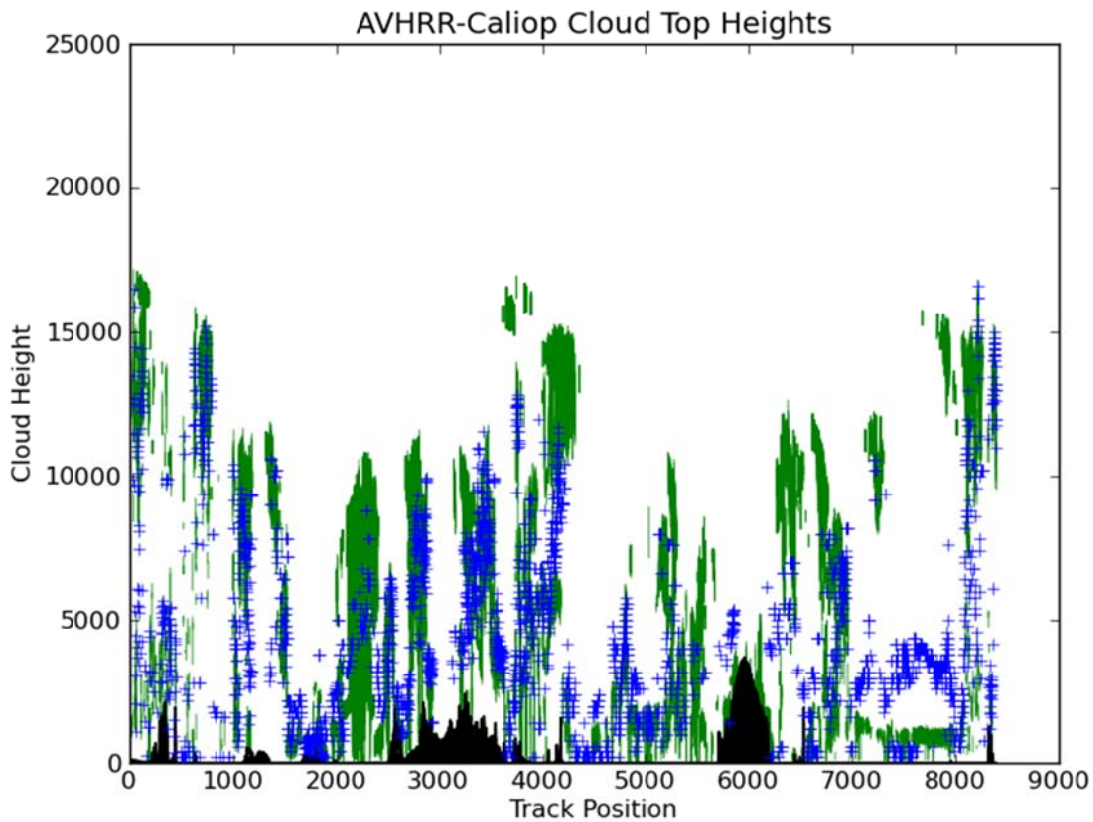


Figure 6.10 Matched CALIPSO-CALIOP cloud mask (green) and CM SAF cloud top height values (blue, in meters) for the same global orbit as shown in Figure 6.9. Track position is given in number of GAC pixels (to be multiplied by 4 to get roughly the distance in km). Significant topographic features are seen in black at track positions 6000 (Antarctica) and 3000 (Russia/China).

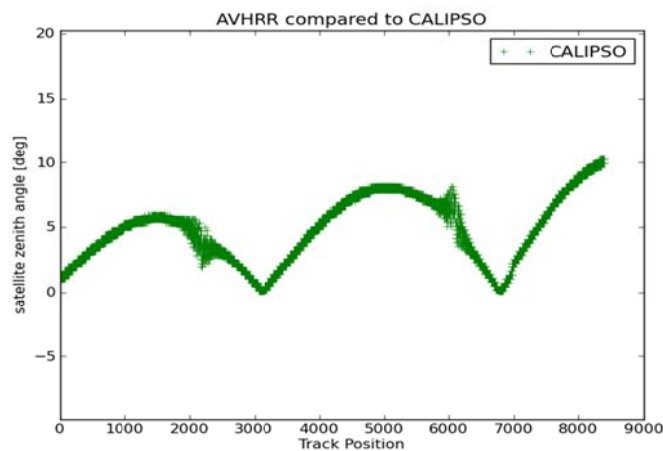




Figure 6.11 Variation of AVHRR (notice – wrong label in the upper right corner) satellite zenith angles for the match to the CALIPSO orbit as shown in Figure 6.9 and in Figure 6.10. Calculation distortions (rounding errors) occur close to the poles near positions 2000 and 6000. The optimal SNO position (within 12 seconds) is seen near position 3000.

 	EUMETSAT SAF on CLIMATE MONITORING Validation Report Cloud product GAC Edition 1	Doc.No.:SAF/CM/SMHI/VAL/GAC/CLD Issue: 1.1 Date: 30.04.2012
---	---	---

The study will here be limited to only looking at the two used scores for accuracy (mean error) and precision (RMS error) for the CFC product in the PRD (*AD 1*). To present and discuss additional verification scores, even if they were indeed calculated (like probabilities of detection, false alarm rates, hit rates and Kuiper's Skill Scores), would have required too much space in this report. A further analysis has to be left for potential follow-on publications.

We first look at the total statistics in Table 6.3. Results are also subdivided into two additional categories where CALIPSO observations of clouds have been filtered using total vertically integrated optical thickness thresholds of 0.5 and 0.3, respectively. The meaning of this is that CALIPSO cloud observations where optical thicknesses are below this threshold have been treated as if they were instead cloud-free.

Results show that without filtering we get an overall global bias of -10.1 %. However, when removing cases with cloud optical thicknesses less than 0.3 the bias becomes positive (+5.2 %). The bias increases to 8 % if applying a COT threshold of 0.5. Results indicate that the apparent CM SAF cloud detection limit might be slightly lower than COT = 0.3. However this conclusion is only valid provided that we do not have other cloud masking problems than just the identification of very thin clouds.

We now look at results sub-divided according to several different Earth surface categories in Table 6.4. Here we notice that cloud detection problems appear to be much worse over ice- and snow-covered surfaces. Consequently, the CM SAF GAC dataset evidently lack a substantial part of all existing clouds over ice- and snow-covered surfaces (i.e., generally over the Polar Regions in the Polar winter).

Table 6.3 *Total CFC statistics for 107 matched orbits in the period October 2006 – December 2009, including reduced CALIOP datasets after applying cloud optical thickness filtering.*

	CFC results Total dataset	CFC results COT threshold 0.3	CFC results COT threshold 0.5
Samples	781520	781520	774549
Bias (%)	-10.2	5.2	8.0
RMS (%)	48.7	45.7	46.3

Table 6.4 *Total CFC statistics for 107 matched orbits in the period October 2006 – December 2009 sub-divided according to four different Earth surfaces.*

	CFC results Ice-free ocean	CFC results Ice-covered Ocean	CFC results Snow-free land	CFC results Snow-covered land
Samples	44432	77541	125966	98424
Bias (%)	-5.0	-21.3	-8.0	-26.4
RMS (%)	44.1	51.0	51.6	56.4

 	<p align="center">EUMETSAT SAF on CLIMATE MONITORING Validation Report Cloud product GAC Edition 1</p>	<p>Doc.No.:SAF/CM/SMHI/VAL/GAC/CLD Issue: 1.1 Date: 30.04.2012</p>
---	---	--



Finally, we will now look at even more detailed results sub-divided according to main latitude bands and different illumination conditions. Leaving out RMS error results, we present a summary of how the mean error varies for all possible combinations in Table 6.5. Notice here that the **TWILIGHT** category is defined as solar zenith angles between 80 and 95 degrees with **DAY** and **NIGHT** categories either being lower or higher, respectively. The latitude bands chosen are the following:

TROPICAL: Latitudes (+/-) 0-15 degrees
SUB-TROPICAL: Latitudes (+/-) 15-45 degrees
HIGH-LATITUDE: Latitudes (+/-) 45-75 degrees
POLAR: Latitudes (+/-) 75-90 degrees

Results in Table 6.5 reveal substantial differences in performance over different regions and for different conditions. We notice in particular the large underestimation of cloud amounts over all surfaces in the **POLAR** category. In some cases not even 50 % of all clouds are detected here considering that total cloud amounts are around 60-80 % in this region according to CALIPSO. Noteworthy are also almost similar underestimations over land for the **HIGH-LATITUDE** category at night and in twilight. As already has been seen in comparisons with SYNOP in the previous section, we also notice a substantial overestimation of cloud amounts over the land portion of the **SUB-TROPICAL** category at daytime. There is even a sign of overestimation over the ocean portion of the same category. The overall conclusion is that there is a substantial difference in how cloud detection works during **DAY** (small underestimation except for some overestimation over **SUB-TROPICAL** region) in comparison to during **TWILIGHT/NIGHT** (generally large underestimation).

Table 6.5 Mean error (%) separated according to latitude bands and illumination categories (defined in the text) and surface conditions. Statistics computed from 107 full globally matched NOAA-18 and CALIPSO orbits with a total of 781520 individual pixel matches. Red colour coding denotes positive deviations larger than 5 %, blue colour coding negative deviations between 5 and 10 % and bold blue colours denote negative deviations larger than 10 %.

	DAY	TWILIGHT	NIGHT
TROPICAL Ocean	-4.8	-	-15.4
TROPICAL Land	1.5	-	-22.7
SUB-TROPICAL Ocean	1.9	-	-5.5
SUB-TROPICAL Land	6.9	-	-14.4
HIGH-LATITUDE Ocean	0.0	-14.9	-12.1
HIGH-LATITUDE Snow-free Land	-3.1	-27.9	-26.0
HIGH-LATITUDE Snow-cover Land	-16.6	-37.6	-33.3
POLAR Ice-free Ocean	-5.1	-22.2	-34.0
POLAR Ice-cover Ocean	-13.2	-13.1	-36.7
POLAR Snow-cover Land	-16.9	-36.5	-23.5
POLAR Snow-free Land	-19.7	-41.3	-33.8

 	EUMETSAT SAF on CLIMATE MONITORING Validation Report Cloud product GAC Edition 1	Doc.No.:SAF/CM/SMHI/VAL/GAC/CLD Issue: 1.1 Date: 30.04.2012
---	---	---

A final comment is that, according to what was written about the uncertainty of CALIPSO cloud amounts in the 5 km dataset in Section 5.2, it is likely that underestimations/overestimations are a few % larger/smaller than what is shown in Table 6.5. However, we also have to remember that all results here are based on the unfiltered CALIPSO dataset. This means that a substantial part of the cloudy CALIPSO dataset should/could theoretically be interpreted as cloud-free since many clouds would not be detectable at all by the AVHRR sensor. All in all, this means that if we were able to take these effects into account the negative deviations in Table 6.5 would possibly be smaller and in better agreement with the overall results provided by e.g. the middle column in Table 6.3. On the other hand, the positive deviations for some areas in the tropics and sub-tropics would then probably be even larger clearly pointing out some serious cloud masking problems (i.e., mis-interpretation of land surfaces as being clouds) over some regions.

Summary of results

- Compliances with requirements are summarized in Table 6.6
- Total global CFC results indicate underestimation of -10 %
- However, if excluding (i.e., interpreting as cloud-free) cases when the vertically integrated cloud optical thickness is less than 0.3 the global agreement is improved (+ 5.2 %) and more comparable with previous results from SYNOP
- With optical thickness limit of 0.5 we instead get an overestimation of 8 %
- Underestimations are particularly found over snow- and ice-covered surfaces (i.e., polar areas in polar winter) where unfiltered results indicate biases down to -31 %.
- Whereas general results indicate an overall underestimation of global cloud amounts, an exception is found during daytime in the sub-tropical region over land areas where cloud amounts are overestimated (+6.9 %)
- Also over ocean parts of the sub-tropical region we notice a small overestimation (+1.9 %) during daytime
- When accounting for the effect of a presumed negative bias of a few percent in the CALIPSO-CALIOP cloud amount observations the overall agreement after filtering sub-visible clouds improves slightly. However, the large underestimations in the Polar Regions (especially in Polar winter) and during night conditions, and some overestimation over sub-tropical land areas remains as very robust features of the cloud detection performance.

Table 6.6 Compliance matrix of found global CFC monthly mean product characteristics with respect to the defined product requirements for accuracy and precision. Comparisons were made against CALIPSO observations. Observe that the Level 3 to Level 2 comparison made here is only theoretically valid for the Bias error and not for RMS errors. **Remark:** The anticipated error of CALIOP cloud amounts (underestimation) is estimated to less than 3 %.

	CFC product requirements Level 3 (MM)			CALIPSO Level 2 (Oct 2006-2009)	CALIPSO Level 2 (Oct 2006-2009) COT > 0.3
	Threshold	Target	Optimal		
Bias	20 %	10 %	10 %	-10 %	5 %
bc-RMS	40 %	20 %	15 %	49 % (RMS)	46 % (RMS)

6.1.1.3 Evaluation against PATMOS-x

The evaluation of the CFC products has basically been made based on inter-comparisons of individual Level 2b products (i.e., after conversion of CM SAF products to Level 2b representation – introduced in Section 4 and exemplified in Figure 5.2. Accumulated statistics have been produced and compared to target requirements (where applicable). In this context we should remember that the mean error parameter (our primary accuracy parameter) should principally be the same for both Level 2 and Level 3 products while the precision parameter (bias-corrected RMS) is different (much lower values to be expected for Level 3). We estimate the precision parameter for Level 3 data by converting Level 2b results to Level 3 results. At the same time, we also examine the differences in results if we make the PATMOS-x comparison with CM SAF Level 3 products being composed from Level 2b product versions or, alternatively, from original Level 2 products (i.e., with no sub-sampling and thus representing the official CM SAF Level 3 product).

Figure 6.12 shows the time series of the global mean of cloud cover for CM SAF and for PATMOS-x computed from daily cloud fraction over the observation period 1982-2008¹.

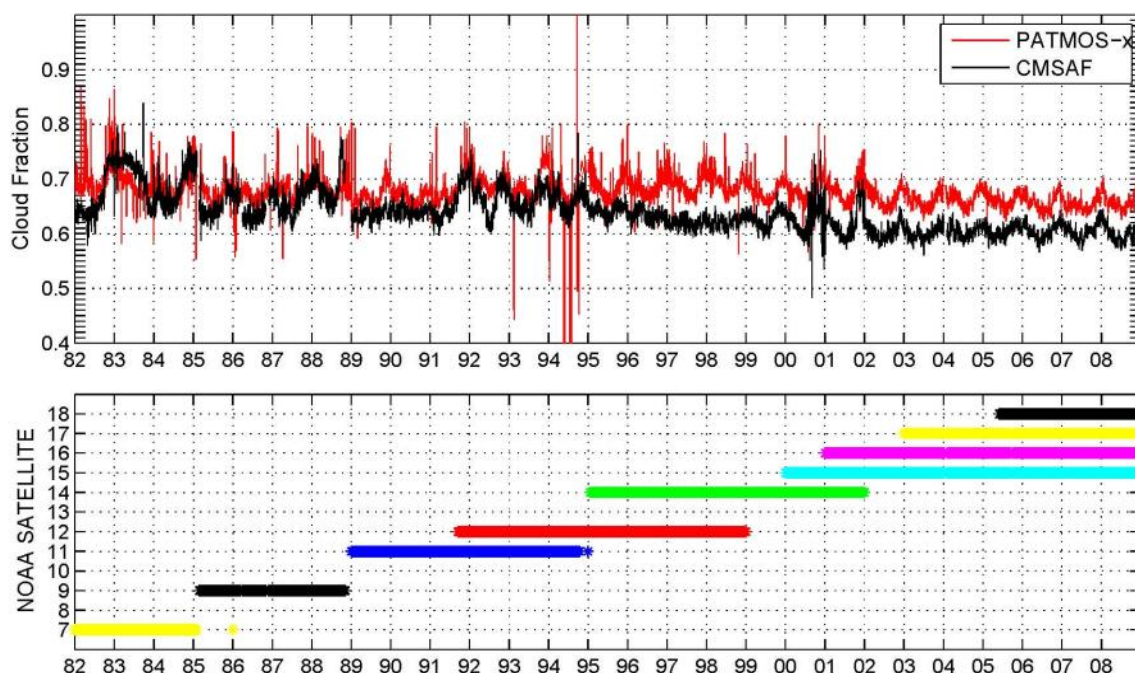


Figure 6.12 Daily mean cloud fraction for PATMOS-x (red line, top panel) and CM SAF (black line, top panel). Daily averages are computed from all (ascending/descending) overpasses from all NOAA satellites. The lower panel shows the satellite platform(s) from CM SAF Level2b cloud fractions used to make daily averages.

¹Results for 2009 from PATMOS-x were not accessible when the GAC DRI-5 validation work started. It has been made available later but due to time constraints we left it out.

For the daily cloud fraction, CFC was calculated in a latitude-longitude grid with grid resolution of 0.1 degrees (i.e., approximately 10 km at the equator) in accordance with how the PATMOS-x dataset was defined. Notice also that results are latitude-weighted in order to compensate for the decreasing geometric grid resolution at increasing latitudes.

We notice that global CFC values generally vary between 0.6 and 0.7. Fluctuations are large in the beginning of the period, largely explained by the fact that during the period 1982-1991 we only have access to one satellite (with two daily observations) for definition of the global mean. As time goes by, more and more satellites are available simultaneously and during the last eight years there are three or four satellites (with 6-8 daily observations) available simultaneously explaining the lower variability towards the end of the time period.

Some evidence of specific technical or sampling problems can be seen. Results are rather noisy in autumn 1994 due to the loss of the NOAA-11 satellite. Furthermore, initial observations from NOAA-15 during the second half of year 2000 were at times limited due to scanning problems leading to a loss of a significant fraction of all scan lines.

The most remarkable feature of the results in Figure 6.12 is the systematically lower CFC values for CM SAF, especially in the observation period after 1995 when often there is more than one satellite platform contributing to CFC. The difference amounts to 7-10 % CFC in absolute terms. Figure 6.13, showing results as zonal mean between latitudes 60°S and 60°N,

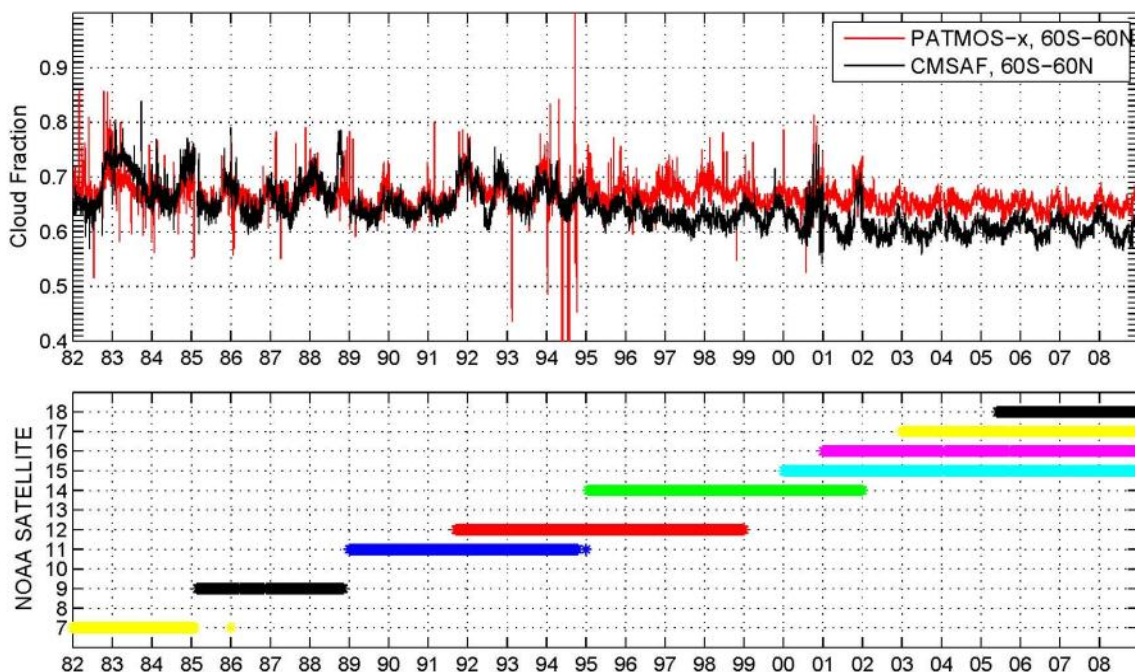


Figure 6.13 Daily mean cloud fraction for PATMOS-x (red line, top panel) and CM SAF (black line, top panel) in the latitude band 60°N to 60°S. Daily averages are computed from all (ascending/descending) overpasses from all NOAA satellites. The lower panel shows the satellite platform(s) from CM SAF Level2b cloud fractions used to make daily averages.

	EUMETSAT SAF on CLIMATE MONITORING Validation Report Cloud product GAC Edition 1	Doc.No.:SAF/CM/SMHI/VAL/GAC/CLD Issue: 1.1 Date: 30.04.2012
---	---	---

reveals that this difference decreases to 2-5 % if excluding the polar regions. In conclusion, CM SAF CFC values are generally lower than PATMOS-x with the largest deviations occurring in the Polar Regions. Table 6.7 summarizes results integrated globally over the whole observation period.

We notice the total mean deviation of -3.9 % but we have to remember that that the negative bias is rather modest in the beginning and it seems to increase through the years when adding more satellites (clearly illustrated in Figure 6.12). Since we only had data from afternoon-night satellites initially but instead have some dominance of data from morning-evening satellites during the last 9 years, we suspect that performance differences are largest for satellites observing mainly under twilight conditions. However, since correlation is higher for the latest period it appears as the difference then is confined to a static bias rather than a more complex difference pattern. We also cannot rule out the possibility of compensating CFC bias differences between morning and afternoon satellite overpasses, and this will be discussed further in subsequent sections.

Table 6.7 Globally integrated CFC differences compared to PATMOS-x over the entire period 1982-2008 calculated from Level 2b product representation. In addition, correlation is given as well as results over three specific periods. The latter corresponds to the initial period with exclusively afternoon-night satellites, the inter-mediate period with one afternoon-night and one morning-evening satellite and the final period with more than two satellites.

Period	Mean Deviation (%)	Correlation (r)
1982-2008	-3.9	0.54
1982-1991	-1.8	0.56
1992-1999	-4.5	0.31
2000-2008	-5.8	0.71

Figure 6.14 summarizes results regarding the geographical CFC distribution during the month of January. Results are shown for the two extremes during day (fully illuminated with lowest possible solar zenith angles – upper panel) and night (complete darkness – lower panel).

The geographic coherency of results indicates CMSAF's ability of capturing major features of global cloud occurrence. Global cloud fractions for the day observation node (upper panel in Figure 6.14) are quantitatively similar for CM SAF (65.7 %) and PATMOS-x (65.4 %). Distinct differences are observed over the poles, where CM SAF has significantly lower cloud fractions relative to PATMOS-x. However, it should be noted that PATMOS-x cloud fractions over much of the Arctic appear to be biased too high considering that these are means for January. Comparison to land based stations around the Arctic countries indicates that January Arctic cloud fractions are slightly less than 70 % (Shupe et al. 2011), although CM SAF still appears lower than that average. Significant global biases emerge when examining the cloud fraction difference figures to the right in Figure 6.14. During the day (upper panel), CMSAF shows much higher cloud fractions than PATMOS-x over the Sahel

and southern African landscapes, western portions of the Americas, the high altitude and snow-covered regions of Asia, dry regions of the Middle East and much of Australia.

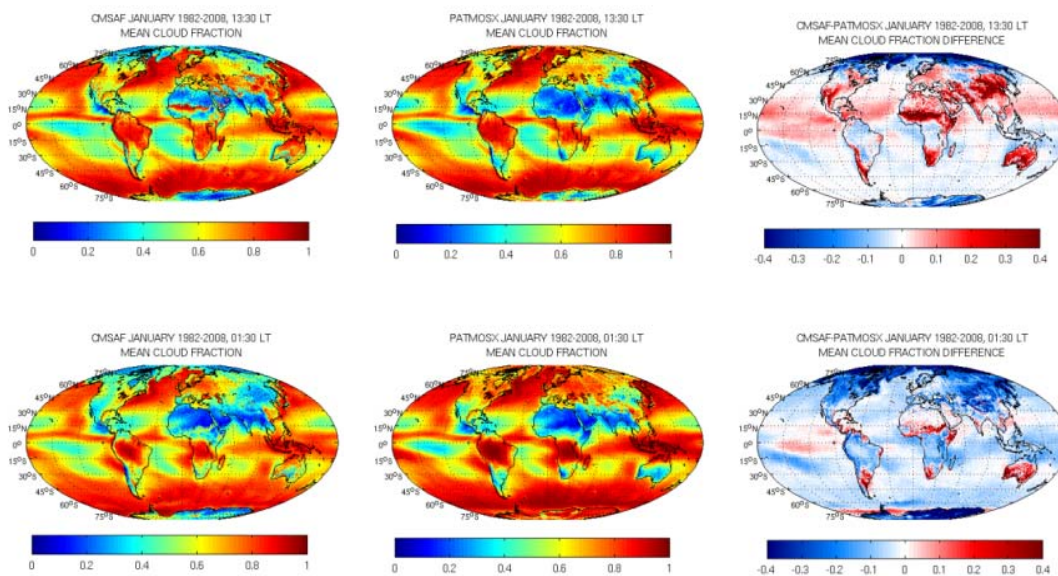


Figure 6.14 Mean cloud fraction for January 1982-2008 for CMSAF (left) and PATMOS-x (middle) and the difference in cloud fraction (CMSAF – PATMOS-x, right). Top panels are for all ascending, afternoon overpasses from NOAA7, NOAA9, NOAA11, NOAA14, NOAA16 and NOAA18 for years 1982-2008; Lower panels are the descending, overnight overpasses for the same satellites for the same years.

Global cloud fractions for the night observation node (lower panel in Figure 6.14) are quantitatively quite different for CM SAF (64.1 %) and PATMOS-x (70.9 %). Overnight, the general trend for CM SAF is globally lower cloud fractions relative to PATMOS-x, especially over the poles, over northern North America and over much of Asia and Siberia, although cloud fractions over the global oceans are slightly higher than PATMOS-x in some tropical and subtropical parts. Most of the positive biases observed for the afternoon orbit node are missing, indicating that these are likely problematic issues linked with cloud masking based on the visible AVHRR channels. However, positive deviations are still found over Australia and over some parts of Africa.

We now turn to the question whether the distribution of clouds differ vertically between the two datasets. To evaluate this we apply the following distinction by utilizing the corresponding cloud top pressure (CTP) information (approximately the same separation as defined in the ISCCP dataset):

Low-level clouds:		CTP \geq 675 hPa
Mid-level clouds:	450 hPa \leq	CTP < 675 hPa
High-level clouds:	450 hPa $>$	CTP

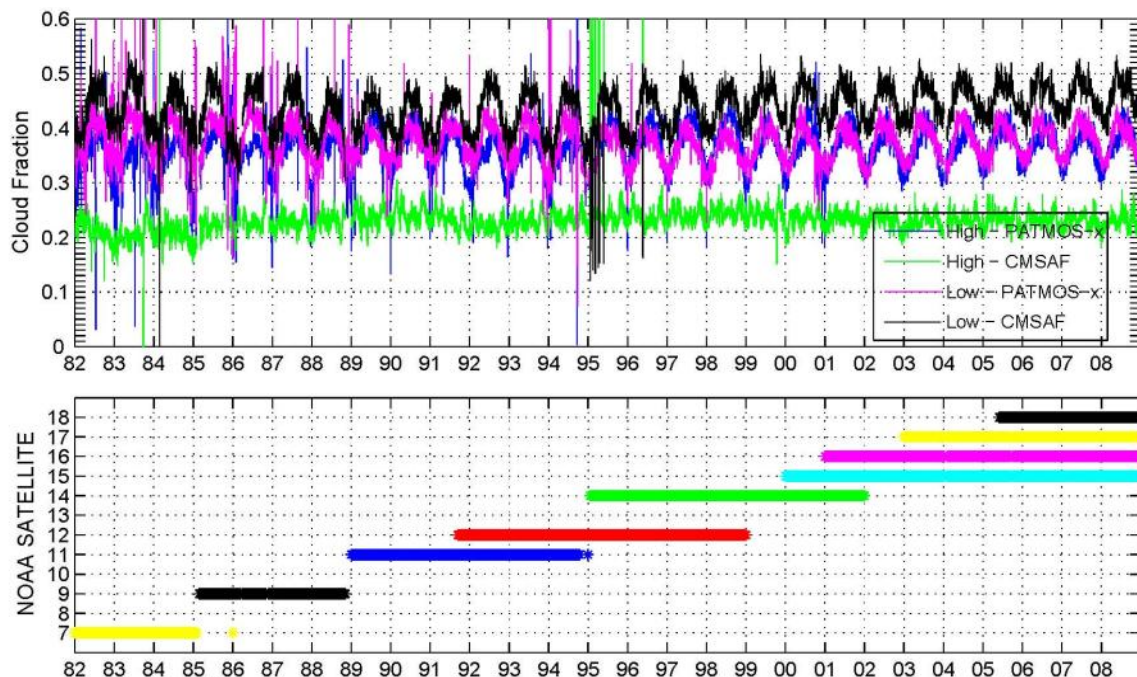


Figure 6.15 Daily mean Low-level and High-level cloud fraction for PATMOS-x and CM SAF. Fractions are relative to the total number of cloudy pixels with valid cloud top pressure estimations. Daily averages are computed from all (ascending/descending) overpasses from all NOAA satellites. The lower panel shows the satellite platform(s) from CM SAF Level2b cloud fractions used to make daily averages.

Figure 6.15 shows the corresponding relative fractions of Low- and High-level clouds for the two datasets for the entire period 1982-2008. We notice a remarkably lower relative fraction of High-level clouds for CM SAF compared to PATMOS-x. This is largely compensated by a higher fraction of Low-level clouds for CM SAF.

Figure 6.16 below illustrates the relative geographical distribution for July 1993-2008 of Low-level and High-level clouds for CM SAF and PATMOS-x separated into the different observation nodes (defining roughly the diurnal cycle). Figure 6.16 can be seen as a poor man's representation of High-level and Low-level cloud fraction diurnal cycles for July 1993-2008. These cloud fractions are normalized by the total cloud fraction at each 0.1x0.1 degree pixels resolution. Therefore, for example, a pixel with a High-cloud fraction of 1 indicates that the total cloud fraction at that pixel is entirely a result of high clouds.

Morning (descending) and evening (ascending) orbits from satellites NOAA12 and NOAA15 give the 07:30 and 19:30 cloud fractions in Figure 6.16, respectively. Afternoon (ascending) and overnight (descending) orbits from NOAA11, NOAA14, NOAA16 and NOAA18 give the 13:30 and 01:30 cloud fractions, respectively. High-cloud fractions are shown on the left and low-cloud fractions are shown on the right.

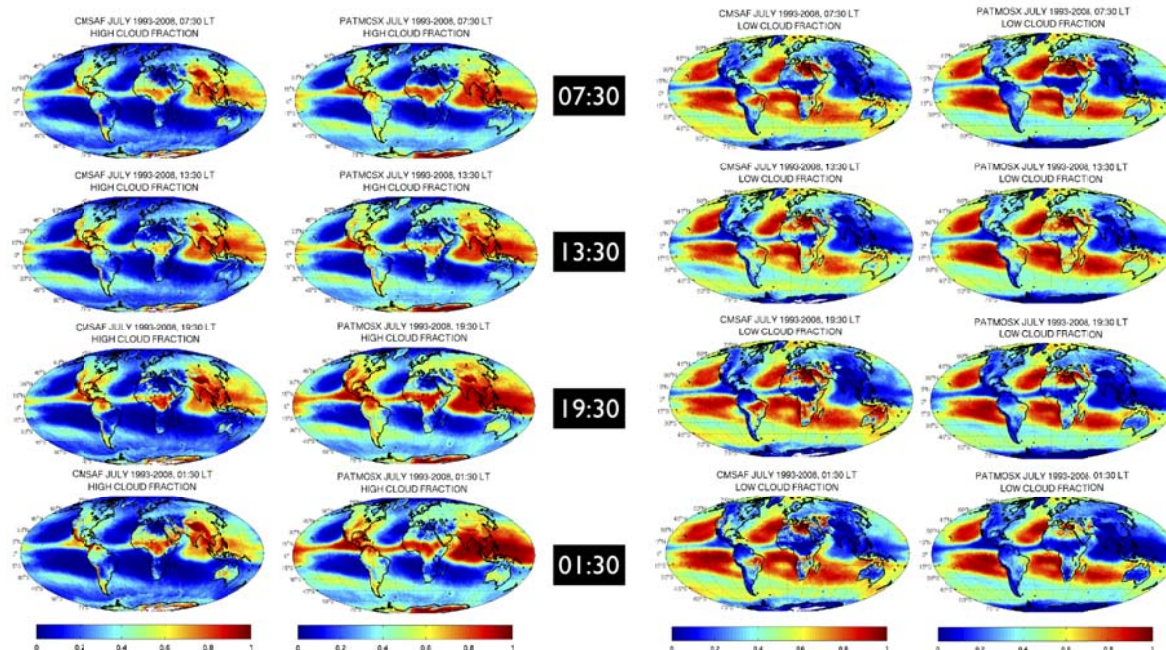


Figure 6.16 Relative Global fractions of High-level (two leftmost plots) and Low-level (two rightmost plots) clouds for CM SAF and PATMOS-x for July in the period 1993-2008 and separated into four observation times (local solar time). See text for further description.

Both high- and low-cloud fractions show similarities in the spatial coherency between CMSAF and PATMOS-x. High clouds are shown to be a prominent feature associated with the ITCZ, Indian Ocean and Western Pacific Ocean regions. It is clear that CMSAF has a lower occurrence of high-cloud fraction in the evening and overnight over the Indian and western Pacific Oceans relative to PATMOS-x. Further examination of mid-level cloud fraction (not shown) indicates that CMSAF has a higher frequency of mid-levels clouds in these regions, indicating a lower displacement of cloud-top heights relative to PATMOS-x. Additionally, CMSAF high-cloud fractions are lower over the Southern Ocean, a region where both data sets indicate climatologically high cloud fraction (see Figure 6.14). Both data sets are in strong agreement on the location of low-cloud fractions, although the absolute magnitudes are slightly different between CMSAF and PATMOS-x. An example of low-cloud differences is the general minimum in low-cloud fraction found in the CMSAF climatology but missing in PATMOS-x in the stratocumulus region off the west coast of Africa, south of the Equator. The Southern Ocean low-cloud fraction in CM SAF is also increased relative to PATMOS-x and seems to be enhanced during the evening and overnight – further suggesting differences in cloud-top location between the two cloud climatologies.

To further illustrate the diurnal variation, Table 6.8 below shows the overall mean deviation for CFC for all afternoon and morning satellites for the months of January and July.

Best agreement is found for the Ascending node for local solar time 13:30. The increased deviation for results of the morning-evening satellites (i.e., observation times 07:30 and 19:30) supports the view that the minor overrepresentation of observations from morning-evening satellites in the period 2000-2008 in Figure 6.12 and might explain the increased bias in this period.

Table 6.8 Globally integrated CFC differences compared to PATMOS-x separated into observation nodes (i.e., local solar times).

Local solar time (observation node)	Mean Deviation (%)	Mean Deviation (%)
	January	July
01:30 (Descending)	-12.3	-7.0
07:30 (Descending)	-12.5	-4.5
13:30 (Ascending)	-5.5	-1.1
19:30 (Ascending)	-8.4	-3.1

A way to investigate how the two datasets agree regarding the variability of cloudiness is to compute the Mean Bias Anomaly (MBA). It is calculated using the following formula:

$$MBA(i, j) = \frac{\sum_{k=1}^n (y_k(i, j) - \overline{y(i, j)})^2}{n_{i,j} - 1} \quad (1)$$

where i, j are the latitude and longitude grid box indices, k is the month index and n is the total number of months with valid data for each grid box, y is the monthly cloud fraction and \overline{y} is the average grid box cloud fraction over the total number of months. The MBA gives an estimate of the amount of deviation in monthly cloud fraction relative to the grid-box mean value. The cloud fraction bias anomaly (BA) timeseries for each grid box (i.e., defining one specific component of the sum in the numerator of Eq. 1) is calculated using the following formula:

$$BA(i, j, k) = (y(i, j, k) - \overline{y(i, j)})^2 \quad (2)$$

Using the time series from (2), a linear regression is fit to BA estimates at each grid box. Then the regression fit of the BA at each grid box for CM SAF is compared with the same grid box BA regression fit for PATMOS-x. A correlation coefficient is calculated, giving a representation of whether the two data sets have similar, positive covariability, no determinable covariability, or opposite, negative covariability. We know that the two data sets have geographic and magnitude differences in absolute cloud fraction (see figures above). However the correlation comparison of BAs is a better test on how much or how little the cloud fraction variability is captured relative to each other.

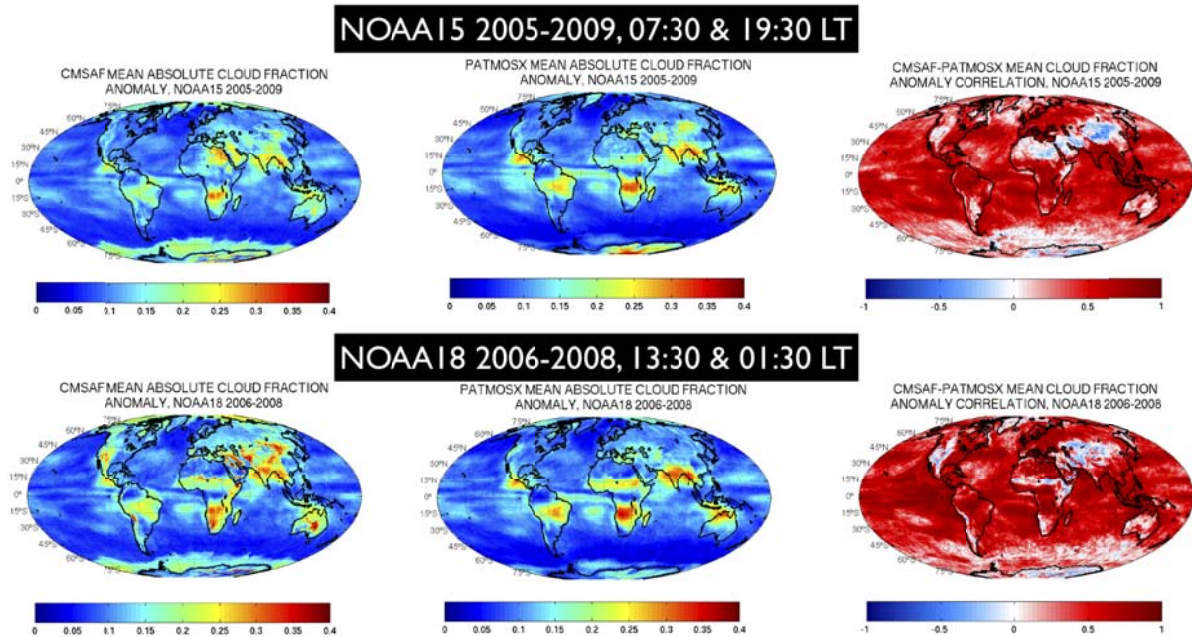


Figure 6.17 Mean bias anomaly (MBA) for CM SAF (left panels) and PATMOS-x (middle panels). The top panels are calculated for the GEWEX-style inter-comparison (described in section 6.1.1.6) of NOAA-15 for 2005-2009, while the lower panels for NOAA-18 for 2006-2008. The right panels are the linearly regressed BA correlations between CMSAF and PATMOS-x for the NOAA-15 (top) and NOAA-18 (bottom). A correlation of 1 indicates the BA is positively correlated between CM SAF and PATMOS-x, while -1 indicates an anti-correlation in BA.

There is a good agreement in Figure 6.17 between MBA for CM SAF and PATMOS-x for most of the globe. The oceans for both data sets generally show the lowest MBA and thus cloud fraction is generally least variable over the oceans relative to over land. Larger MBAs are found over specific land regions, but there are still commonalities in such large MBAs between CM SAF and PATMOS-x.

Interestingly, the MBAs are similar, not only between CM SAF and PATMOS-x for one particular satellite, but they are also similar in geographic location and magnitude across the two satellite platforms. Distinct discrepancies emerge in regions of the Sahel and Northern Africa, the Western Americas, Southern Asia, Australia and the Southern Ocean. These are the same regions where we have previously identified errors emerging from anomalous cloud fractions in CM SAF. The BA correlation distributions are also similar across satellites, and positive correlations are seen to dominate.

These correlations suggest that, although absolute magnitude in cloud fraction may differ, there is a general consistency for CM SAF to exhibit a variability that is comparable to PATMOS-x. Areas of no correlation or anti-correlation are observed, mainly in the same regions where CM SAF has been shown to have consistent, anomalously high cloud fraction relative to PATMOS-x.

Finally, we have examined in more detail the effect of calculating Level 3 products based on Level 2b products (sub-sampled products) versus original Level 2 products (i.e., all products). Table 6.9 lists the mean deviation and bias-corrected RMSE for cloud fraction for the period 1982-2008. These statistics are relative to Level3 estimates computed from the full Level2b PATMOS-x (NOAA satellites only) dataset (Figure 6.12 and Figure 6.13). Statistics for CM SAF are given for the official CM SAF Level3 product, as well as for a semi-Level3 product computed from the full Level2b dataset (NOAA satellites only).

Table 6.9 Mean deviation and bias-corrected RMS results with respect to PATMOS-x computed for the entire dataset 1982-2008. Results are sub-divided in two versions: 1. Based on the official CM SAF GAC product (computed from Level 2 products – column 1), 2. Calculated in the same way as PATMOS-x (i.e., computed from Level 2b products – column 2).

Quantity	CM SAF Official Level 3 1982-2008	CM SAF Level 3 from Level 2b 1982-2008
Mean Deviation [%]	-4.13	-3.89
Bias-corrected RMS [%]	2.56	2.66

We conclude that the difference caused by the different ways of calculating the Level 3 products is small. Thus, the detailed results presented earlier should be largely valid also for the official CM SAF Level 3 products. This is also clearly illustrated in Figure 6.18 plotting the official CM SAF Level 3 product together with corresponding daily mean values based on the Level 2b representation.

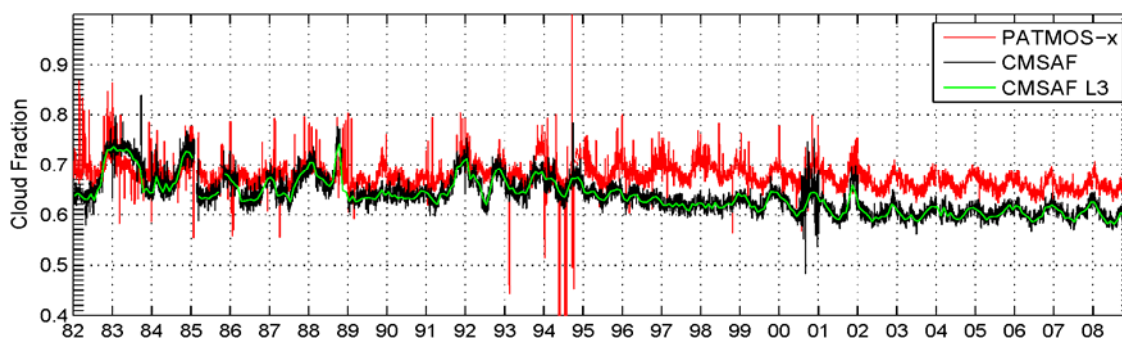


Figure 6.18 Same as Figure 6.12 but with CM SAF Level 3 values plotted as well (green line).

A very final check was also made of the quality of daily mean products. However, in this case we have based them entirely on Level 2b results meaning that daily means were compiled

	EUMETSAT SAF on CLIMATE MONITORING Validation Report Cloud product GAC Edition 1	Doc.No.:SAF/CM/SMHI/VAL/GAC/CLD Issue: 1.1 Date: 30.04.2012
---	---	---

using only the Level 2b products (thus, slightly different compared to the official CM SAF product) for CM SAF and PATMOS-x. We picked results for two months (January and July) and limited the period to 1992-2008 in order to have access to results from both morning-evening satellites and afternoon-night satellites. Results are shown in Table 6.10 and reflect well the seasonal variation seen in e.g. Figure 6.18 (higher differences in Northern Hemisphere winter).

Table 6.10 Mean deviations and bias-corrected RMS for daily mean Level 3 products composed from Level 2b products compared to PATMOS-x.

	Level 3 (daily mean) CFC Mean deviation[%]	Level 3 (daily mean) CFC BC-RMS [%]
January 1992-2008	-10.3	16.9
July 1992-2008	-4.6	14.2

Summary of results

- Compliances with requirements are summarized in Table 6.11
- Good agreement in general (in terms of anomaly correlation and overall global cloud patterns) but CM SAF CFC values are generally lower (2-10 %)
- CFC deviations change with time as explained by a changing availability of satellite observations (increasing over the years)
- Deviations are small between 1982-1995 (when observations are dominated by afternoon-night observations) but increase between 1996-2008 to 5-10 %.
- Best correlation and smallest bias-correct RMS is found for the period 2002-2008 when the number of available satellites is high (3-4 satellites).
- Largest geographical positive deviations (+10-20 %) are found over semi-arid areas during daytime (afternoon observation)
- Largest geographical negative deviations (-10 to -30 %) are found over the Polar Regions and over the Southern Oceans
- Night-time observations indicate that CM SAF misses some of the thinnest Cirrus clouds over ocean surfaces
- CM SAF and PATMOS-x differ in the vertical distribution of clouds – CM SAF has a larger fraction of Low-level clouds but less High-level clouds
- Available uncertainty information for the PATMOS-x dataset (see section 5.4) indicates problems with cloud detection, especially over the Polar Regions. This means that the information of the large deviations found here between CM SAF and PATMOS-x should be used with some caution.




 	<p align="center">EUMETSAT SAF on CLIMATE MONITORING Validation Report Cloud product GAC Edition 1</p>	<p>Doc.No.:SAF/CM/SMHI/VAL/GAC/CLD Issue: 1.1 Date: 30.04.2012</p>
---	--	--

Table 6.11 *Compliance matrix of found global CFC monthly mean product characteristics with respect to the defined product requirements for accuracy and precision. Comparisons were made against PATMOS-x observations.*

	CFC product requirements Level 3 (MM)			PATMOS-x Level 3 (1982-2008)	PATMOS-x Level 2 (1982-2009)
	Threshold	Target	Optimal		
Bias	20%	10%	10%	-4.1 %	-3.9 %
bc-RMS	40%	20%	15%	2.6 %	2.7

 	EUMETSAT SAF on CLIMATE MONITORING Validation Report Cloud product GAC Edition 1	Doc.No.:SAF/CM/SMHI/VAL/GAC/CLD Issue: 1.1 Date: 30.04.2012
---	---	---

6.1.1.4 Evaluation against MODIS

In this section CFC Level 3 (monthly means) of CM SAF GAC is compared to MODIS (MOD08_M3) equivalents. In detail, two exemplary months were chosen (January and July 2007 – see Figure 6.19 and Figure 6.20) to visualize and discuss both products. To minimize differences in the products caused by local equator crossing times of the different satellites, AVHRR/Noaa-17 is compared to MODIS/Terra, and AVHRR/Noaa-18 is compared to MODIS/Aqua.

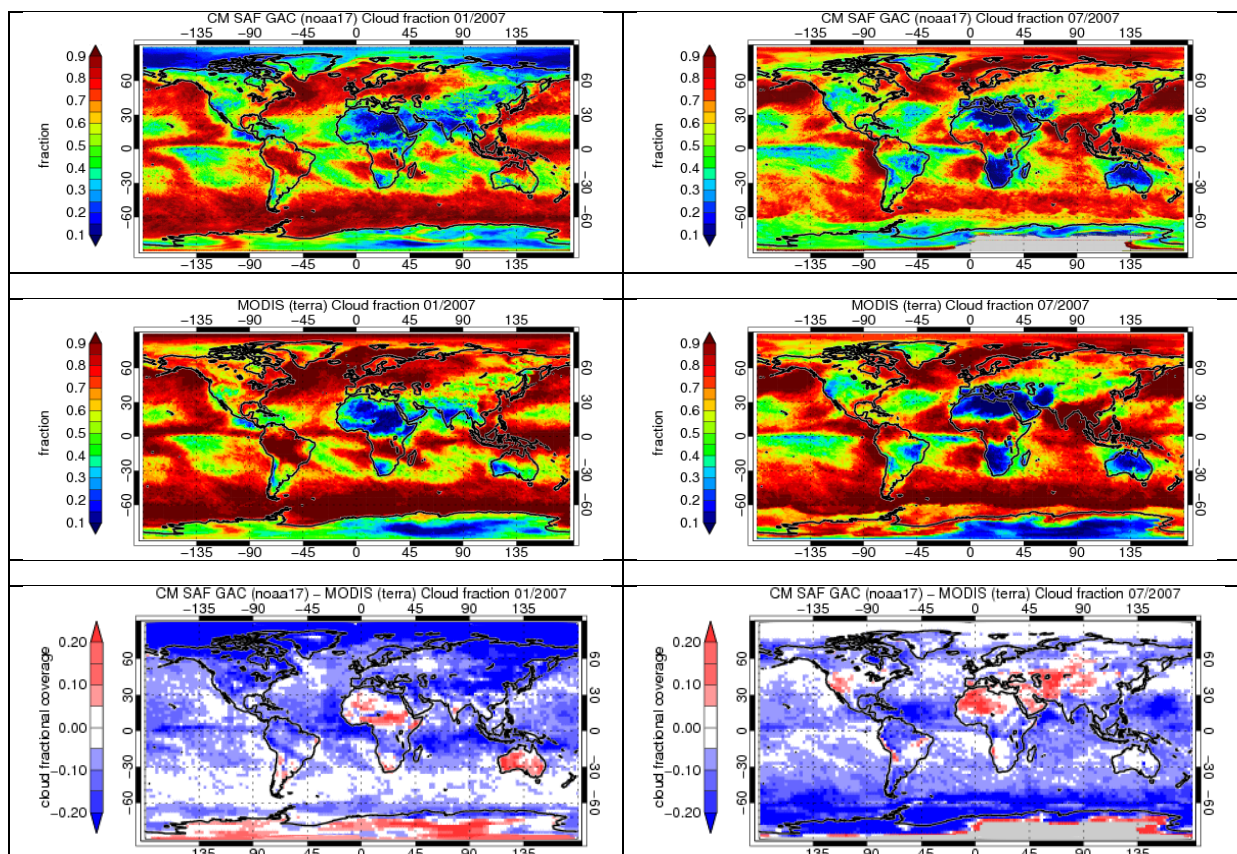



Figure 6.19 Global map of monthly mean cloud fractional coverage for CM SAF (NOAA-17 only, top row), MODIS (Terra only, middle row) and their differences (bottom row). Shown are January 2007 (left) and July 2007 (July). Regions without values are grey-shaded.

In general, the comparison shown in both figures reveals a consistent global structure of global CFC in CM SAF GAC compared to MODIS, with the following general features found in both products.

For both months, high CFC values are visible in the ITCZ, in the Southern Mid-Latitudes and in the oceanic regions of the Northern Mid-Latitudes. Low CFC values are found in the subtropical subsidence regions, over Australia and desert regions of Sahara and Kalahari. Low cloud amounts can also be seen for Southeast Asia for January, while this region shows high cloud amounts in July.

 	EUMETSAT SAF on CLIMATE MONITORING Validation Report Cloud product GAC Edition 1	Doc.No.:SAF/CM/SMHI/VAL/GAC/CLD Issue: 1.1 Date: 30.04.2012
---	---	---

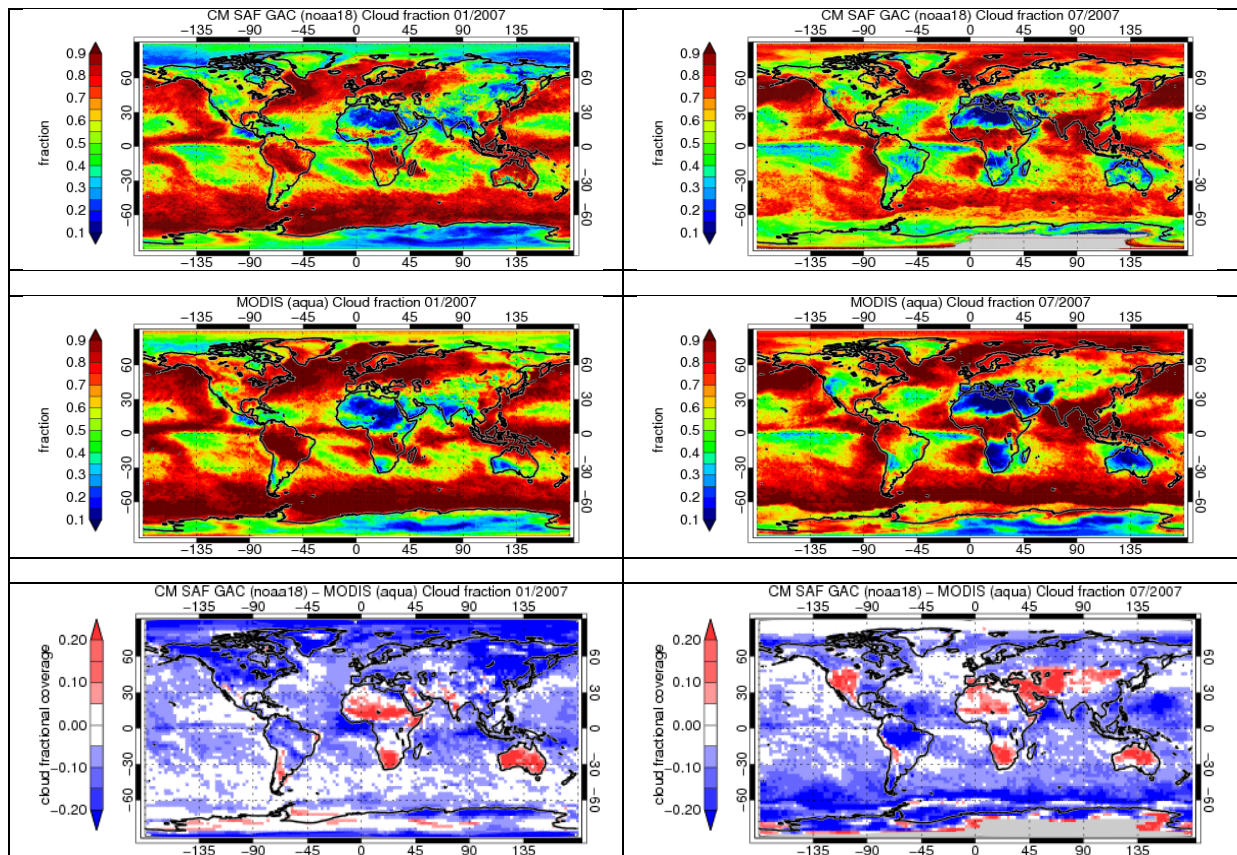


Figure 6.20 Global map of monthly mean cloud fractional coverage for CM SAF (NOAA-18 only, top row), MODIS (Aqua only, middle row) and their differences (bottom row). Shown are January 2007 (left) and July 2007 (July). Regions without values are grey-shaded.

Despite these common patterns, some significant differences are found between CM SAF and MODIS. As visible in the difference plots of Figure 6.19 and Figure 6.20, the CM SAF cloud fraction seems to be lower for most parts of the globe with smaller (near-zero) values in the Southern mid-latitudes in January and the oceanic regions of the Northern mid-latitudes in July. Largest negative differences are found for the entire Arctic region in January and for the Antarctic region in July. Over land some positive differences compared with MODIS are found, particularly over northern Africa and partly over South Africa, Central Asia and Australia. These are more pronounced for the comparisons of CM SAF NOAA-18 against MODIS Aqua.

Some further results (Figure 6.22 and Figure 6.23) based on global and latitude-band dependent averages for CFC monitored over the entire GAC period will be discussed in the next section (section 6.1.1.5).

 	<p align="center">EUMETSAT SAF on CLIMATE MONITORING Validation Report Cloud product GAC Edition 1</p>	<p>Doc.No.:SAF/CM/SMHI/VAL/GAC/CLD Issue: 1.1 Date: 30.04.2012</p>
---	---	--

Summary of results

- Compliances with requirements are summarized in Table 6.12
- Good agreement in general cloud pattern descriptions but overall lower CFC values for CM SAF (about -10 %)
- Largest negative deviations are seen in the Polar regions during the Polar winter season
- Noticeable negative deviations are also seen over oceanic areas, especially in the Southern oceans close to Antarctica, and in the ITCZ region.
- CM SAF show higher CFC (+10-20 %) over semi-arid regions
- As for PATMOS-x, uncertainties in the MODIS-derived results are largest over the Polar Regions, which call for some carefulness in the interpretation here.

Table 6.12 Compliance matrix of found global CFC monthly mean product characteristics with respect to the defined product requirements for accuracy and precision. Comparisons were made against MODIS observations (consistency check).

	CFC product requirements L3 (MM)			MODIS/Aqua (2005-2009)	MODIS/Terra (2002-2009)
	Threshold	Target	Optimal		
Bias	20 %	10 %	10 %	-10 %	-20 % to -10 %
bc-rms	40 %	20 %	15 %	~20 %	20% to 27%

6.1.1.5 Evaluation against ISCCP

In this section CFC Level 3 (monthly means) of CM SAF GAC is compared to ISCCP equivalents. In detail, two exemplary months were chosen (January and July 2007) to visualize and discuss both products.

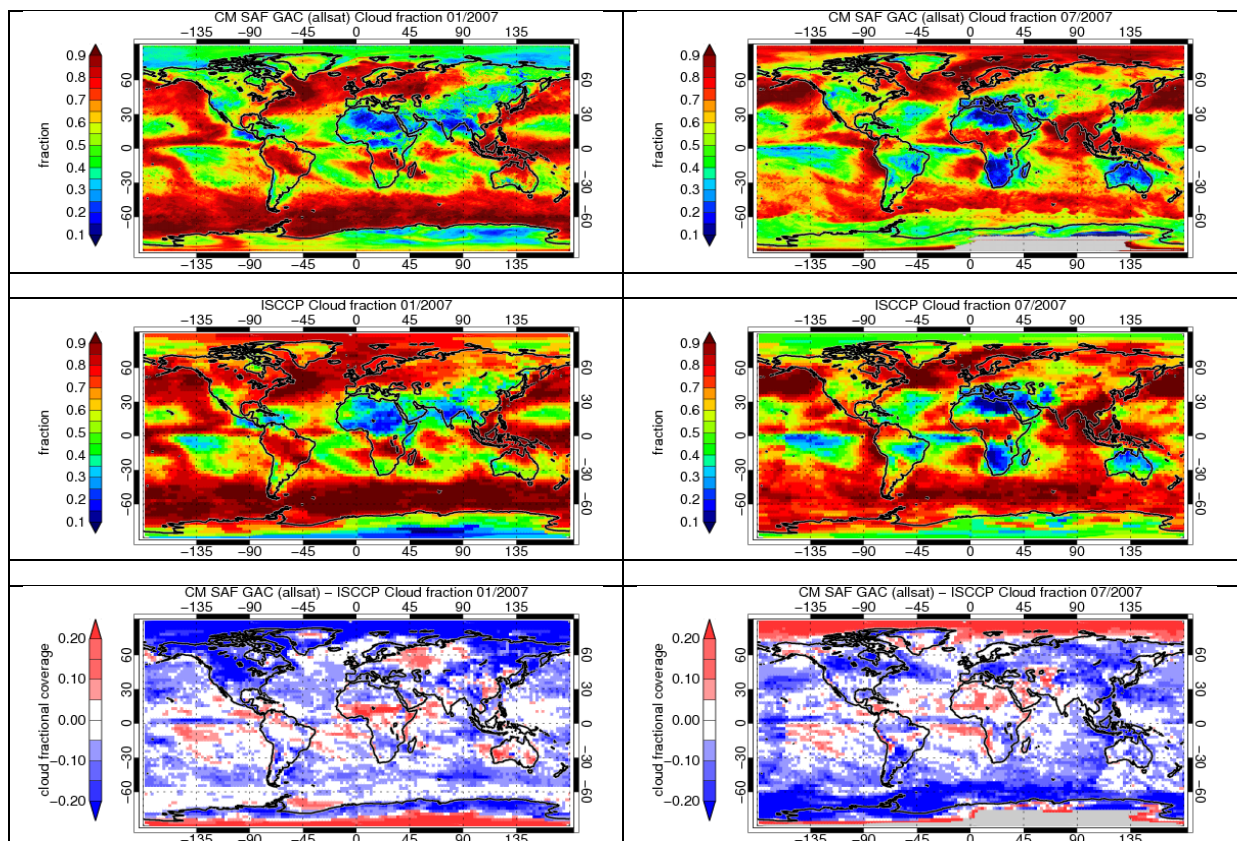


Figure 6.21 Global map of monthly mean cloud fractional coverage for CM SAF (all satellites, top row), ISCCP (middle row) and their differences (bottom row). Shown are January 2007 (left) and July 2007 (right). Regions without values are grey-shaded.

Figure 6.21 presents the comparisons of CM SAF GAC cloud fractional coverage against ISCCP. Here, the CM SAF monthly means over all available NOAA satellites is considered. For both months considered CM SAF and ISCCP provide similar values for most parts of the globe. The spatial patterns of CFC are nearly identical to what is shown earlier in Figure 6.19 and Figure 6.20. Most striking differences appear in the Polar Regions, where CM SAF shows much smaller CFC values compared to ISCCP over the Arctic during January and over Antarctica during July. On the other hand, significantly higher CFC values are found in CM SAF products over central Antarctica in January and the Arctic in July. Compared to these extremes, northern and Southern Mid-Latitudes, and the Tropics are characterized by smaller differences in CFC between CM SAF and ISCCP. Here, some land areas, e.g. Sahel zone during January, are found to exhibit higher values in CM SAF than in ISCCP. This feature is

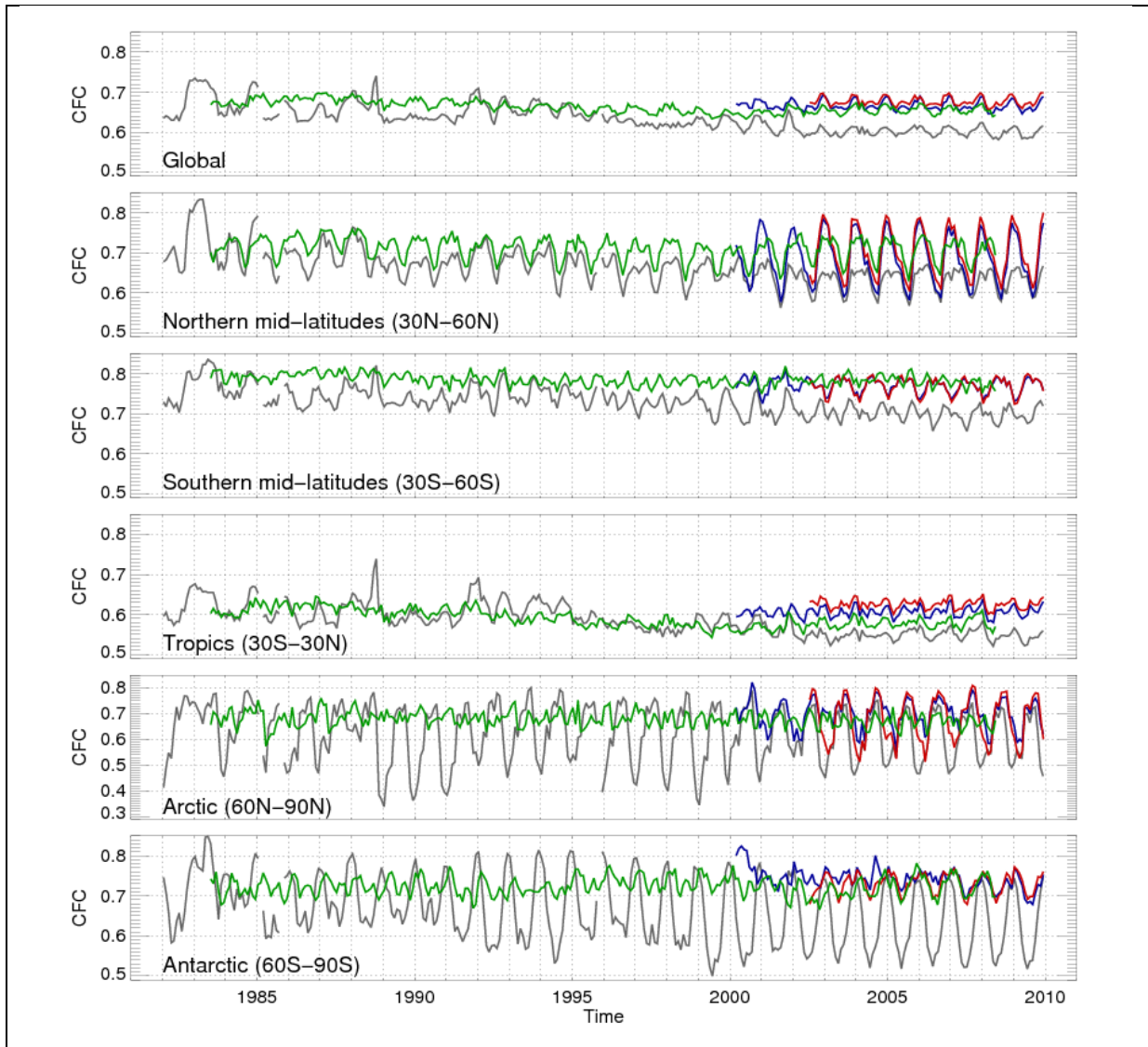


Figure 6.22 Time series of mean cloud fractional coverage of CM SAF (grey), ISCCP (green), MODIS/Terra (blue) and MODIS/Aqua (red). Shown are the global values (upper panel) and the separation into various latitude-bands.

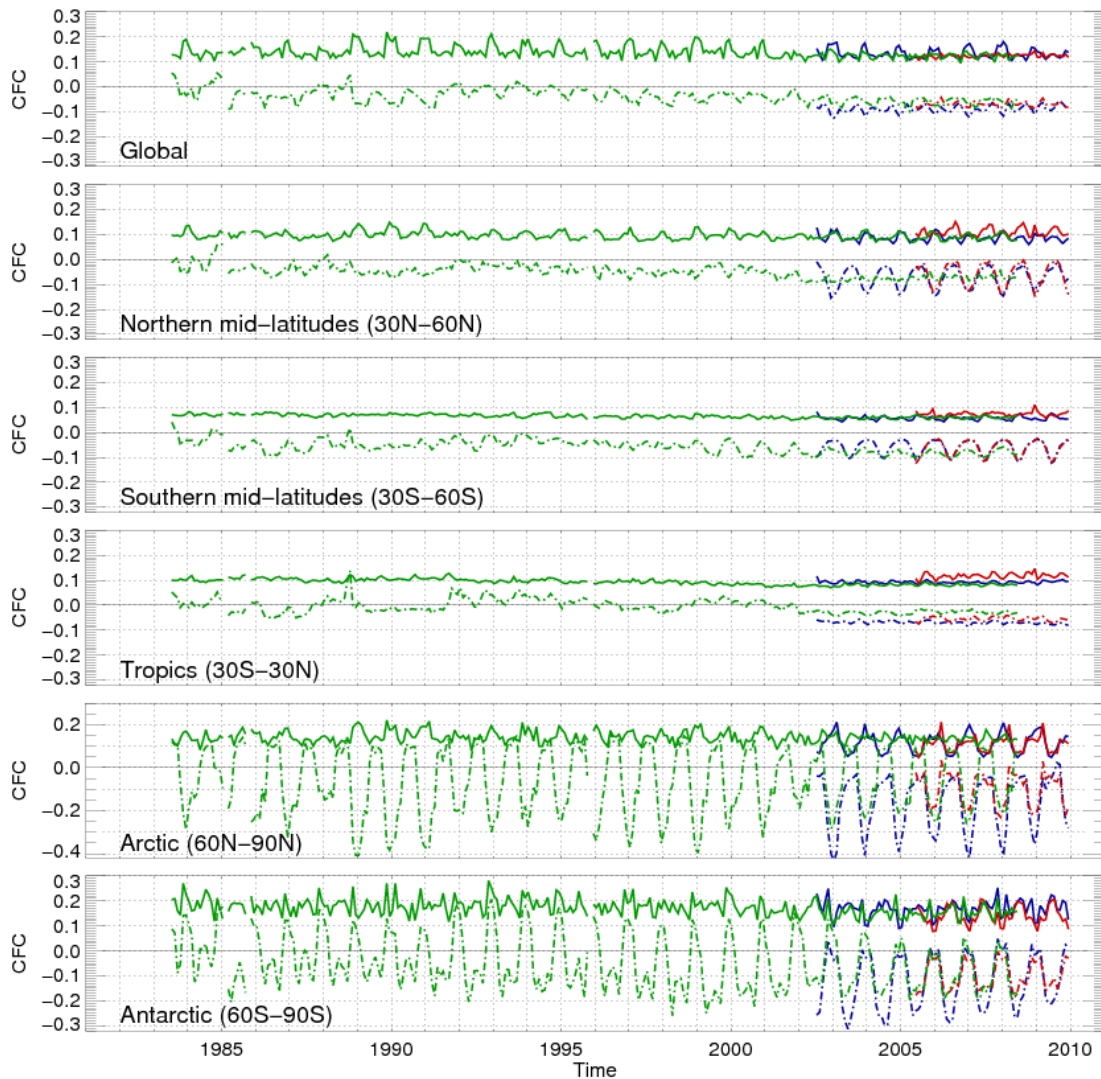



Figure 6.23 Time series of relative mean (dashed lines) and standard deviation (solid lines) of CFC of CM SAF compared to ISCCP (green), MODIS/Terra (blue) and MODIS/Aqua (red). Shown are the global values (upper panel) and the separation into various latitude-bands.

similar to what is visible in Figure 6.19 and Figure 6.20 for the comparisons to MODIS for January.

Figure 6.22 presents time series of mean CFC for CM SAF, ISCCP, MODIS/Terra and MODIS/Aqua. The averages are reported for the entire globe and for specific latitude bands. For the global values ISCCP and both MODIS instruments seem to agree quite well in the overlapping period. For this period, the CM SAF seems to have a negative bias of about 0.07. On the other hand, the CMSAF seasonal cycle compares well to ISCCP and MODIS. Considering the entire GAC period, the global mean values reveal some unstable behavior in the first ten years, while ISCCP shows only small variations.

The latitude-band dependent values in Figure 6.22 show similar results for the Tropics, where in all datasets the lowest mean values are found, and in the Northern and Southern Mid-

	EUMETSAT SAF on CLIMATE MONITORING Validation Report Cloud product GAC Edition 1	Doc.No.:SAF/CM/SMHI/VAL/GAC/CLD Issue: 1.1 Date: 30.04.2012
---	---	---

Latitudes, where in particular in the Northern Mid-Latitudes show an significant seasonal cycle in all datasets. In the polar region, this investigation exhibits a very strong seasonal cycle in the CM SAF dataset. This cannot be seen with the same amplitude in MODIS or ISCCP. The deviation reaches partly up to 20% during polar winter. This behavior is likely to be explained by problems for cloud detection during polar winter in CM SAF and also in twilight conditions. This is supported by comparisons with MODIS results in Figure 6.20 (bottom panel), having a documented improved performance over the Polar Regions (see Karlsson and Dybbroe, 2010). Further, the time series of CM SAF global average CFC shows a slight negative trend over the full period with all latitude-bands being affected. This trend seems to disappear in last 8-years of the GAC period when more AVHRR instruments become available. A similar trend is also visible in ISCCP but less pronounced. MODIS cannot serve as reference here, since it is not available before 2000.

Figure 6.23 summarizes the standard and mean deviations of the CM SAF L3 product collocated to ISCCP and both MODIS instrument products. Considering mean deviations, a negative deviation is visible for the global mean CM SAF CFC compared to ISCCP for the entire period with maximum value around -0.1 at the end of the period. This deviation is very similar for the MODIS (Terra and Aqua) comparisons against CM SAF (NOAA-17 and NOAA-18 only) products. As mentioned above, largest mean deviations are found for the Arctic and Antarctic regions with a very significant seasonal cycle -0.4 and 0.15 against MODIS and ISCCP. The standard deviation against ISCCP remains nearly constant on global scale over the full period with a slight seasonal cycle revealing higher values up to 0.2. Again, the Polar Regions are characterized by the highest standard deviations (of all latitude bands) between the CM SAF GAC with respect to ISCCP and with respect to both MODIS respectively. The Southern Mid-Latitude and the Tropics is the latitude region showing the best agreement between CM SAF CFC and the reference products.

Summary of results

- [Compliances with requirements are summarized in Table 6.13](#)
- [Good agreement in the description of general global cloud features compared to ISCCP](#)
- [Overall lower CM SAF values \(0 % to -20 %\) with largest negative deviations \(down to -40 %\) seen for Arctic and Antarctic regions](#)
- [ISCCP and CM SAF agrees on a downward trend in CFC 1982-2000 but not for the last years where CM SAF is almost 10 % lower than both ISCCP and MODIS](#)
- [Positive deviations against ISCCP is seen over semi-arid regions and over the Polar regions in the Polar summer](#)
- [Global values for mean deviation and bias-corrected RMS are generally fulfilling target requirements but exceptions are seen for some regions \(e.g. Southern Mid-Latitudes\)](#)
- [The assumed ISCCP uncertainty figure of +/- 10 % for CFC probably means that the main features of the results given here are relatively robust \(in terms of showing either general negative or positive biases\) but that the exact numbers still could be questioned \(e.g., ISCCP should also exhibit large uncertainties over the Polar Regions\).](#)

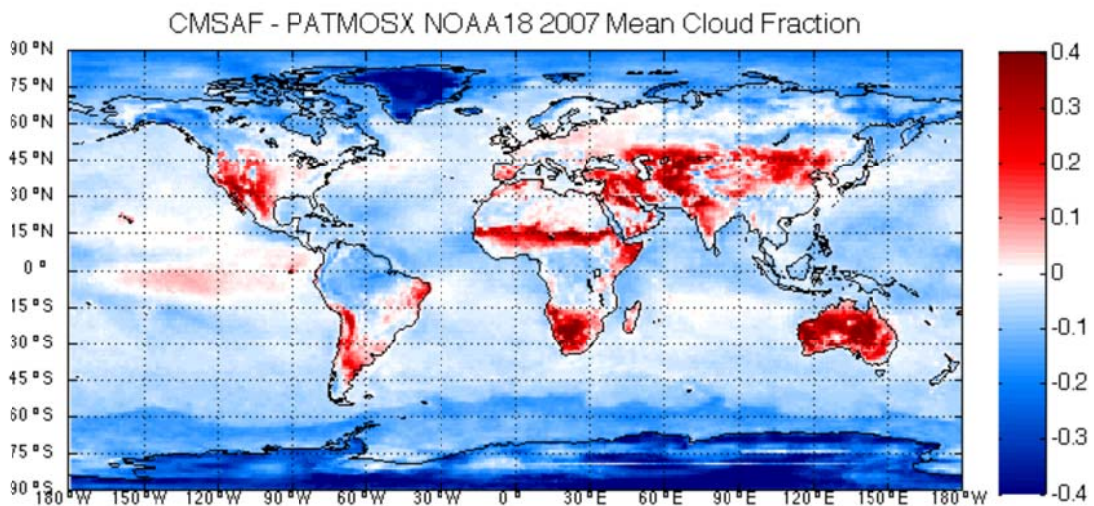
Table 6.13 Compliance matrix of found global CFC monthly mean product characteristics with respect to the defined product requirements for accuracy and precision. Comparisons were made against ISCCP observations (consistency check).

	CFC product requirements L3 (MM)			ISCCP (1982-2008)
	Threshold	Target	Optimal	
Bias	20 %	10 %	10 %	0% to -12 %
bc-RMS	40 %	20 %	15 %	10 % to 20 %

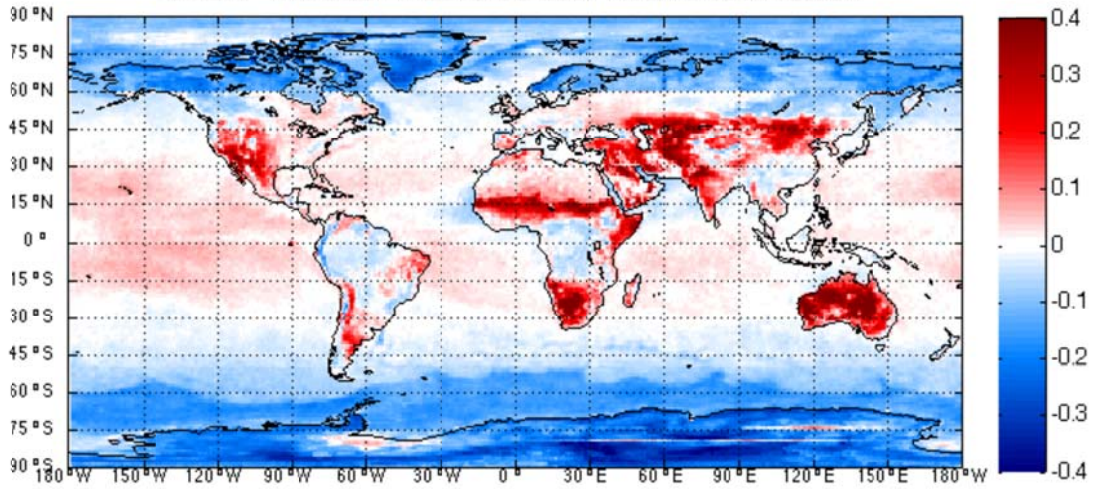
6.1.1.6 GEWEX inter-comparisons

GEWEX-style inter-comparisons, allowing simultaneous inter-comparisons with several other cloud datasets on the global scale, are presented in this section. CM SAF CFC products were prepared for a few different time periods and satellite orbits where also several other datasets were accessible. To make legitimate comparisons to the other data sets, contributing to the GEWEX inter-comparison efforts, the 0.1x0.1 degree CM SAF Level2b products were first converted to a 1x1 degree latitude-longitude grid resolution, then monthly cloud fraction was computed from the daily estimates. The results of these comparisons are shown and described below. First, we will show results for one year (2007) and one afternoon-night satellite (NOAA18). We complement these results with further GEWEX-style inter-comparisons between CM SAF and PATMOS-x CFC for different time periods and platforms.

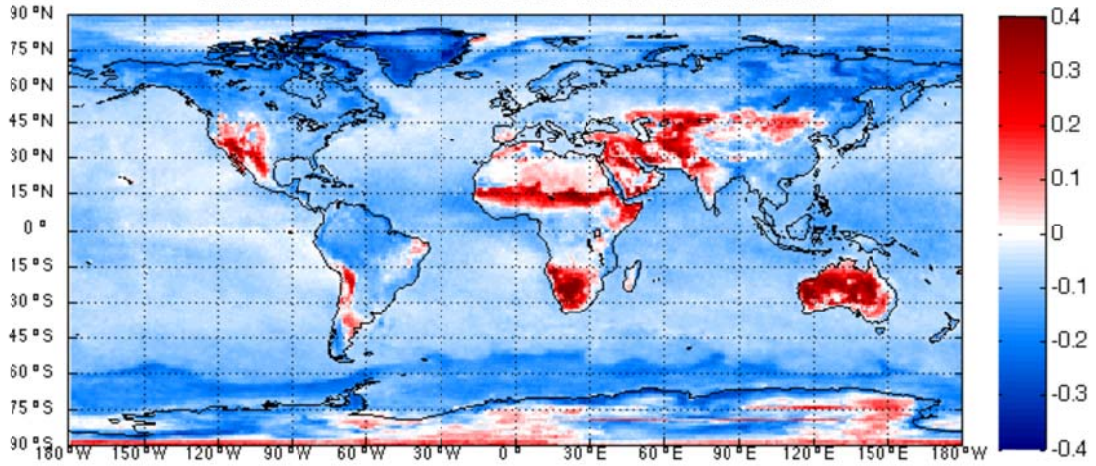
2007 - NOAA18 ASC(13:30) and DES(01:30) orbits



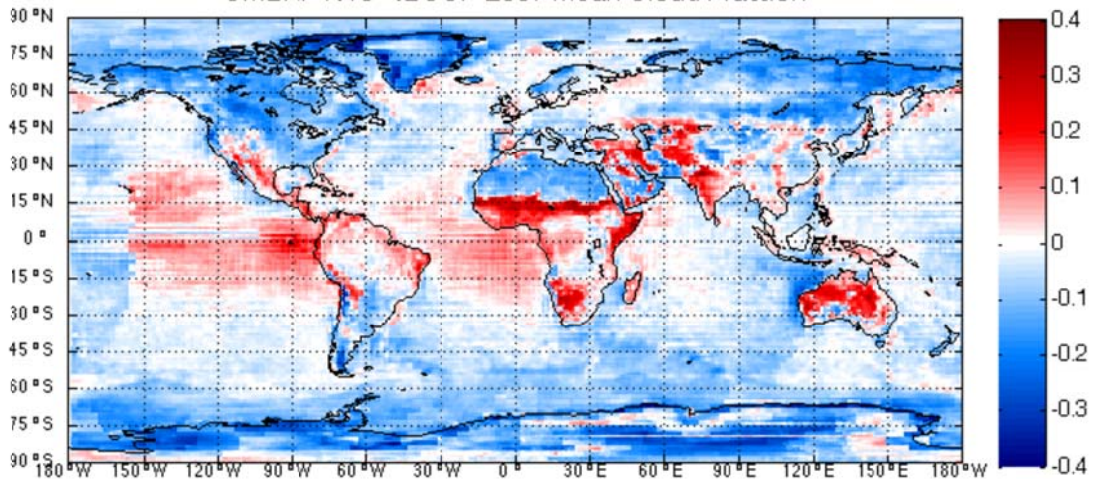
CMSAF N18 DES - MODIS-CE 2007 Mean Cloud Fraction



CMSAF N18 - MODIS-ST 2007 Mean Cloud Fraction



CMSAF N18 - ISCCP 2007 Mean Cloud Fraction



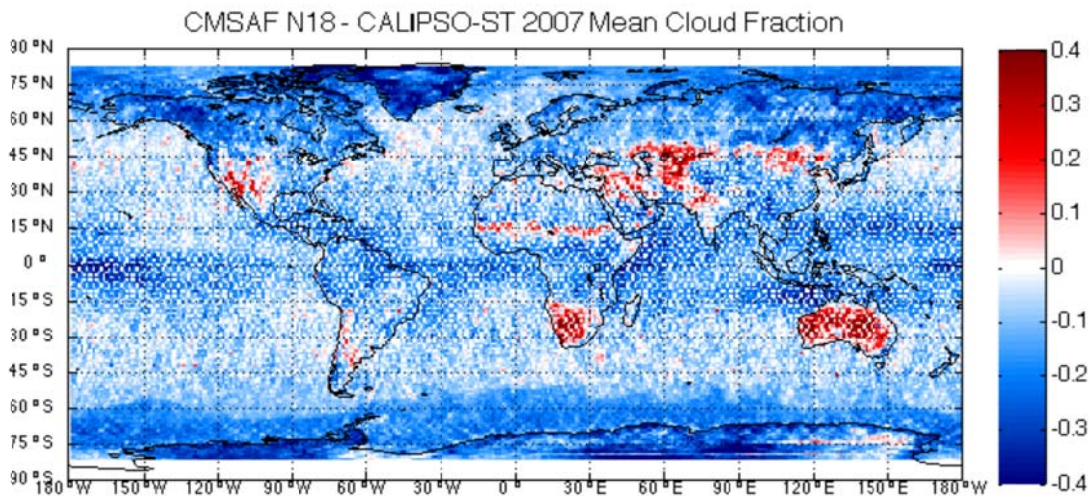




Figure 6.24 CMSAF cloud fraction differences for NOAA-18 ASC+DES overpasses for 2007 for five global cloud datasets. These are (from top to bottom): PATMOS-x, MODIS CERES Team (CE), MODIS Science Team (ST), ISCCP and CALIPSO Science Team (ST). (Ignore title of CMSAFMODIS-CE, it includes both ASC and DES overpasses.)

The different panels of Figure 6.24 show both positive and negative deviations for the global ocean cloud fractions for the different data sets, although the absolute magnitudes of these differences are small. Most alarming is the large positive deviation of cloud fraction over semi-arid and high-altitude land surfaces of the Americas, Africa, Southern Asia and Australia.

The anomaly over semi-arid and high-altitude land surfaces is seen in all plots, indicating that the CM SAF results are really significantly deviating from all other datasets. The magnitude of the overestimation in these regions is lowest when compared to ISCCP, suggesting some preference of ISCCP to also identify clouds over semi-arid landscapes. In addition, distinct lower cloud fraction is seen in all plots poleward of 70°S and 70°N, and CM SAF persistently gives lower cloud occurrences over the Southern Ocean. A more general underestimation (except over semi-arid and high-altitude surfaces) is seen in the plot for CALIPSO-ST but this is clearly a result of a much higher cloud detection sensitivity for the CALIPSO-CALIOP sensor (i.e., no filtering of the very thinnest clouds are made here).

Figure 6.25 summarizes results as zonal averages and here we recognize many of the differences we noticed in Figure 6.24. From approximately 40°S to 40°N, the zonal cloud fraction distributions indicate a rather good agreement between CM SAF and the other passive sensor climatologies, generally within +/- 5% (except for CALIPSO, explained by the much higher cloud detection sensitivity). The zonal cloud fraction structures are also captured well, with the equatorial maxima, subtropical minima and increasing mid-latitude cloud fraction. However CM SAF is clearly the outlier in the Southern Ocean, in terms of absolute magnitude as well as spatial location for the peak cloud fraction (slight further north displacement compared with the other data sets). Poleward of 60°S and 60°N, CM SAF is also clearly an outlier, severely underestimating cloud fraction on the order of 20%, and in some cases even larger. Considering the biases seen earlier in Figure 6.14 and Figure 6.16, we

 	EUMETSAT SAF on CLIMATE MONITORING Validation Report Cloud product GAC Edition 1	Doc.No.:SAF/CM/SMHI/VAL/GAC/CLD Issue: 1.1 Date: 30.04.2012
---	---	---

now examine the zonal mean cloud fraction distribution in terms of afternoon and overnight NOAA-18 overpasses.

Figure 6.26 illustrates again the generally lower CM SAF cloud fraction across much of the globe relative to the other datasets. This amounts to approximately 10% during the overnight overpass (left panels). The Southern Ocean maximum has a negative deviation of 10-20% occurring during the night. The general agreement for CM SAF to the other data sets during the afternoon orbit (right panels) is quite good for much of the globe. However, we see that the reason for this is due to the anomalously high values of cloud fraction over the semi-arid regions seen in Figure 6.14 and Figure 6.16 and easily identifiable in the zonal mean cloud fraction in latitude bands of -30 to -10 degrees and 25 to 45 degrees. Thus, the CM SAF zonal mean cloud fraction for the ascending (afternoon-night) orbit in Figure 6.26 (right) is in general in good agreement with the other data sets, but for the wrong reasons.

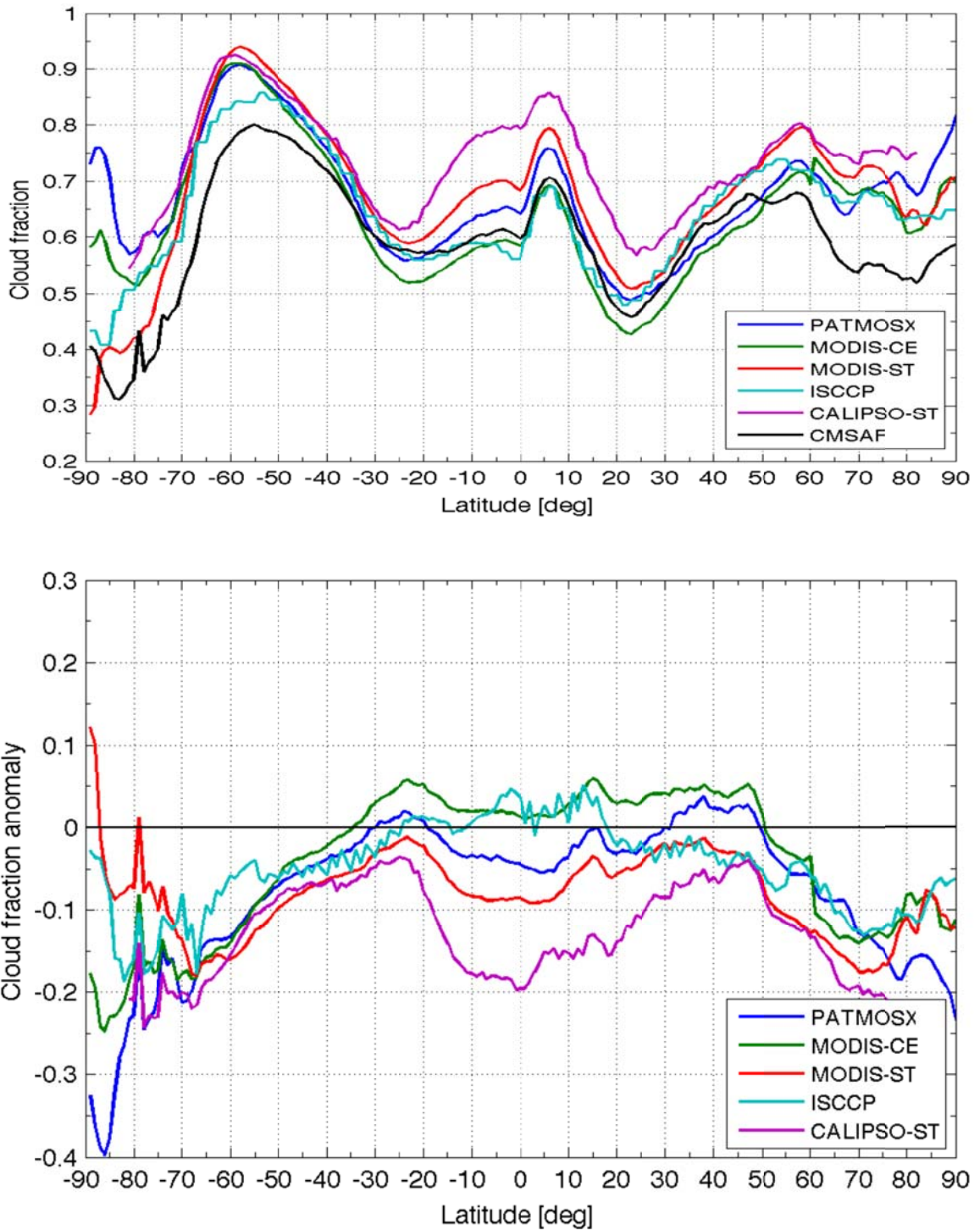


Figure 6.25 Zonal mean cloud fraction and zonal mean cloud fraction anomaly relative to CM SAF for the same datasets as in Figure 6.24. Northern Hemisphere latitudes are positive.

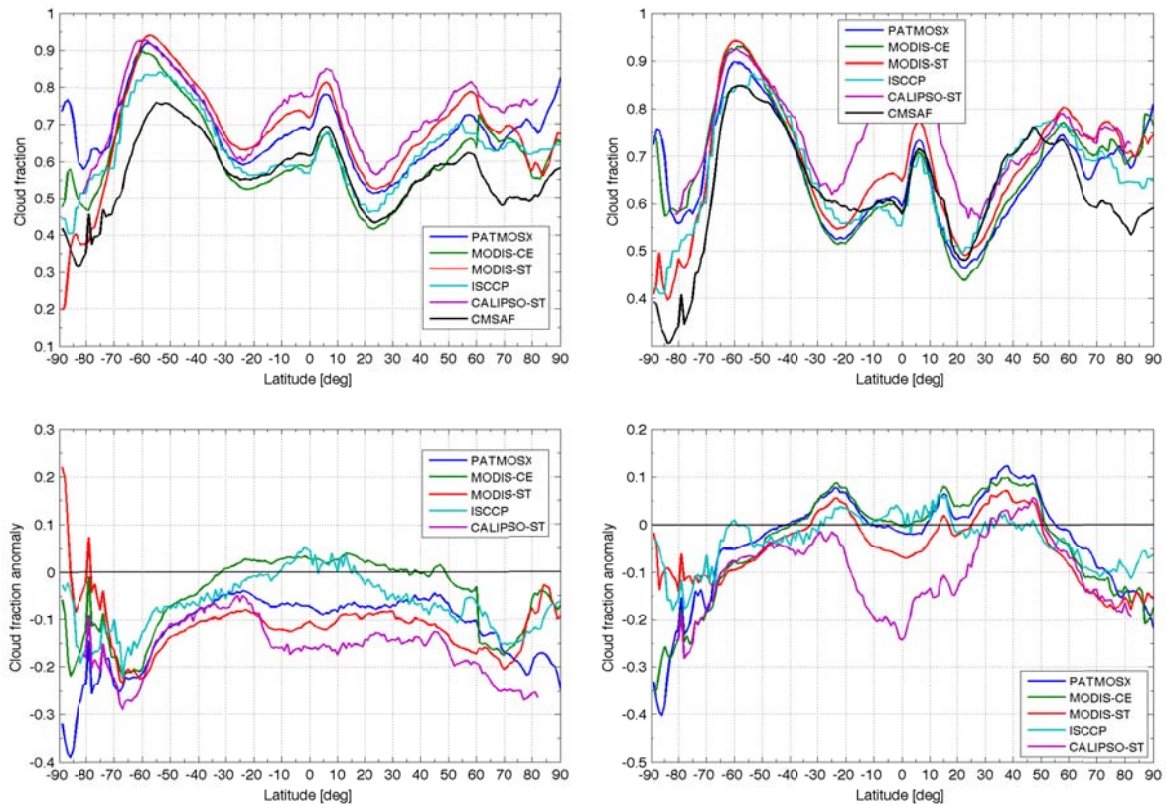


Figure 6.26 Zonal mean cloud fraction (top panels) and zonal mean cloud fraction anomalies (bottom panels) for NOAA-18 descending orbit (01:30, left panels) and ascending orbit (13:30, right panels) for CM SAF and five other global cloud datasets in 2007.

Finally, we compare zonal means of CFC and CFC anomalies with PATMOS-x results for the morning-evening satellite NOAA-15 for the period 2005-2009 (Figure 6.27) and the afternoon-overnight satellite NOAA-18 for 2006-2008 (Figure 6.28). As in Figure 6.26, the results are separated. Figure 6.27 show similar geographical differences in cloud fraction as we have seen earlier (e.g., in Figure 6.14) and primarily the large negative deviations over the poles and over the Southern Oceans. We also note an overall negative deviation of 5-10 % at low- and mid-latitudes. Both morning and evening orbits contribute similarly to the zonal mean cloud fraction distribution in the southern hemisphere, although the PATMOS-x morning cloud fraction is larger than the evening cloud fraction in the latitude band -30°S to the equator (see thin and dashed lines); these differences are not as large in the CM SAF zonal means. The situation is different for the northern hemisphere. PATMOS-x cloud distributions suggest that the morning cloudiness is larger than the evening for all latitudes in the northern hemisphere. The CM SAF distribution is opposite, indicating an increased cloud fraction during the evening. This causes the large anomaly differences between the ASC (thin solid) and DES (thin dashed) in the zonal mean anomaly plot, but overall these large differences average out for a total cloud fraction anomaly generally on the order of only -5 to -7% - again another case of decent results for the wrong, or opposing, reasons.

Figure 6.28 shows some similar results but we notice a better agreement over low- and mid-latitude regions. However, clearly the generally good zonal agreement between ASC+DES

	<p align="center">EUMETSAT SAF on CLIMATE MONITORING Validation Report Cloud product GAC Edition 1</p>	<p>Doc.No.:SAF/CM/SMHI/VAL/GAC/CLD Issue: 1.1 Date: 30.04.2012</p>
---	---	--

cloud fraction is a result of CM SAF overestimation of clouds in the subtropics and mid-latitudes from the afternoon orbits and an underestimation from the overnight orbits. Interestingly, the Southern Ocean cloud fraction maxima for CM SAF is within 5% of PATMOS-x cloud fraction and the geographic peak is broadly at the same latitude for the afternoon orbits, while this peaks shifts equator-ward due to contribution from the overnight orbits. The South Pole cloud fraction is strongly biased negative in NOAA-18 for these years.

Summary of results

- Compliances with requirements are summarized in Table 6.14
- Fair agreement in the description of general global cloud features in latitude bands
- Better agreement in tropics than outside tropics (poleward of 50°S and 50°N)
- Generally lower values (-5 % to -40 %) outside of tropics
- Largest deviations at Southern oceans and over the poles

Table 6.14 Compliance matrix of found global CFC monthly mean product characteristics with respect to the defined product requirements for accuracy and precision. Comparisons were made against PATMOS-x, MODIS (Science Team and CERES team), ISCCP and CALIPSO observations in the time period 2005-2009. Only results from CALIPSO represent independent observations and the remaining results should be considered as consistency checks.

	CFC product requirements L3 (MM)			PATMOS-x	MODIS/ Terra/Aqua	ISCCP	CALIPSO
	Thres.	Targ.	Opt.				
Bias	20%	10%	10%	+/- 5 % <i>(Tropics)</i> -10 % to -40 % elsewhere <i>(poleward of 50 degrees)</i>	ST: -10 % CE: + 4 % <i>(tropics)</i> -10 % to -20 % elsewhere <i>(poleward of 50 degrees)</i>	-5 % to +5 % <i>(tropics)</i> -5 % to -20 % elsewhere <i>(poleward of 50 degrees)</i>	-5 % to -20 % <i>(best agreement at -30°S and 30°N)</i>

2005-2009 - NOAA15 ASC(19:30) and DES(07:30) orbits
 ZONAL MEAN CLOUD FRACTION, NOAA15 2005-2009

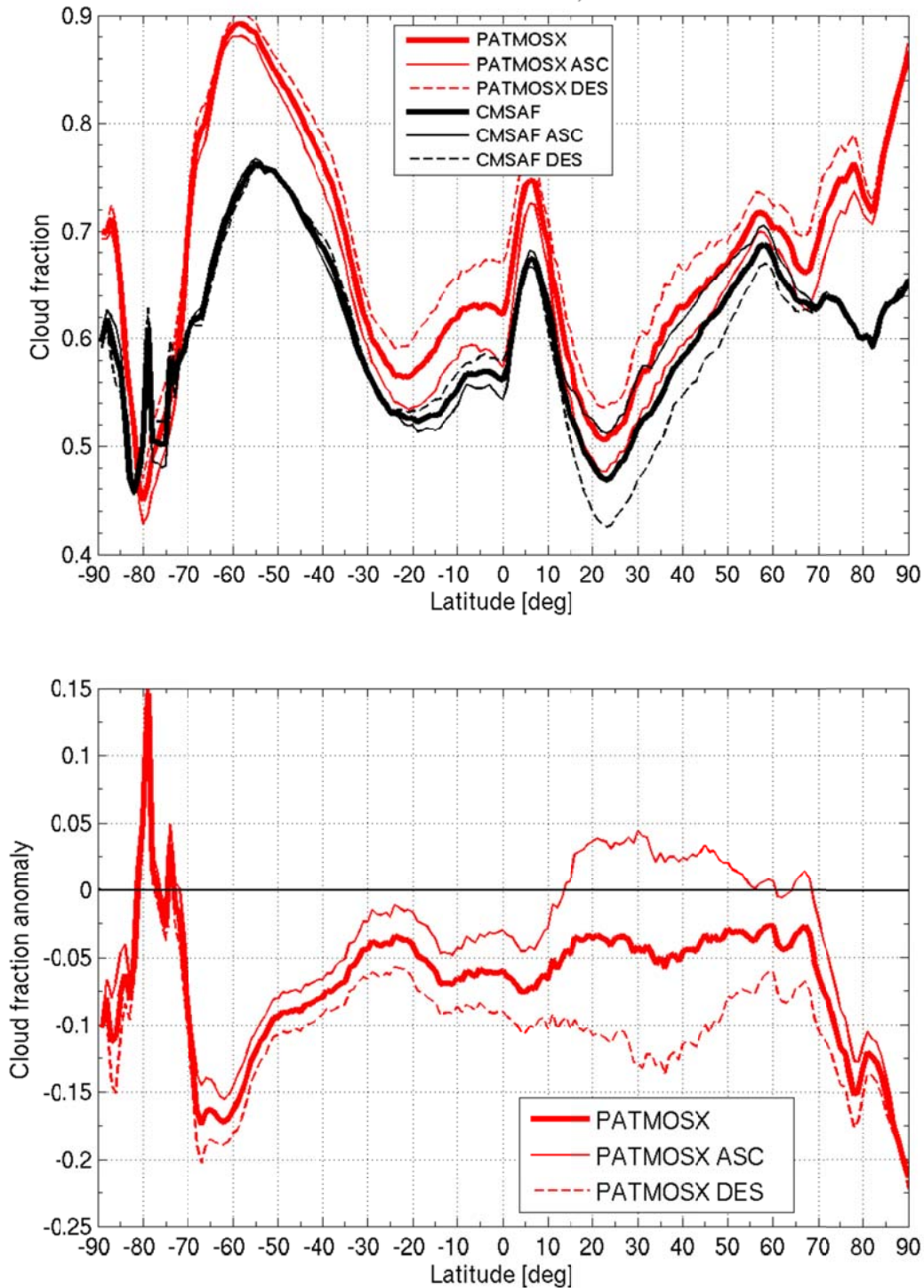


Figure 6.27 Zonal mean cloud fraction (top panel) for NOAA-15 2005-2009 ASC+DES orbits (thick) for PATMOS-x (red) and CM SAF (black). Thin solid line is the zonal mean cloud fraction for the ASC (19:30) orbit and thin dashed is for the DES (07:30) orbit. Lower panel: Zonal mean cloud fraction anomaly for PATMOS-x relative to CM SAF, thick line for ASC+DES, thin and dashed for ASC (19:30) and DES (07:30) orbits, respectively.

2006-2008 - NOAA18 ASC(13:30) and DES(01:30) orbits

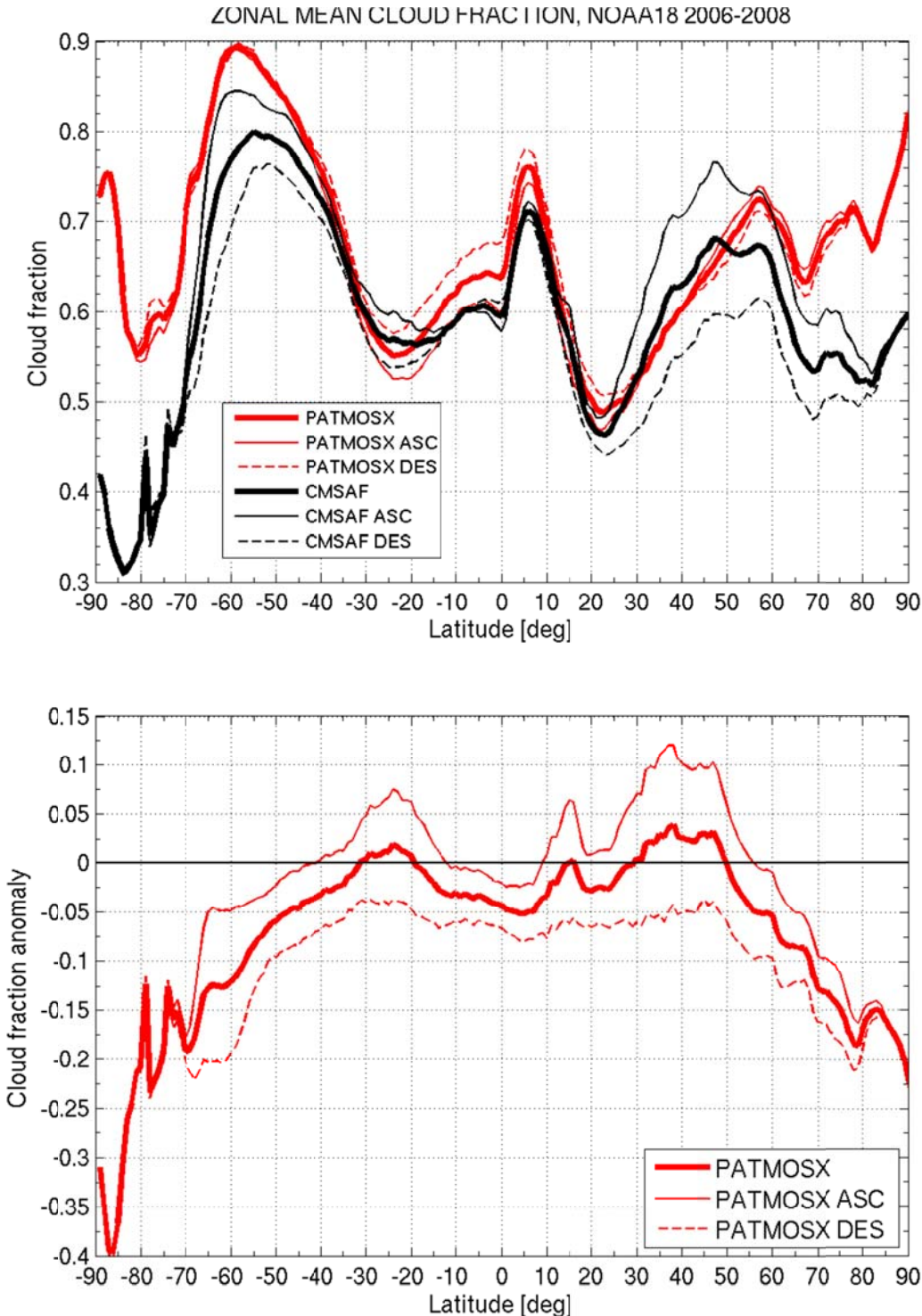



Figure 6.28 Same as in, Figure 6.27 but for NOAA-18 for 2006-2008.

 	<p align="center">EUMETSAT SAF on CLIMATE MONITORING Validation Report Cloud product GAC Edition 1</p>	<p>Doc.No.:SAF/CM/SMHI/VAL/GAC/CLD Issue: 1.1 Date: 30.04.2012</p>
---	---	--

6.1.1.7 Summary of overall results


Based on the previously described individual studies of the performance of the CM SAF GAC CFC product, we summarize results in the following two tables (one for the Mean Error and one for the bias-corrected RMS error). Here, compliance with requirements is indicated by simple YES or NO statements.

Table 6.15 Overall requirement compliance of the CM SAF GAC CFC product with respect to the Mean Error. Consistency checks marked in blue.

Reference	Bias	Fulfilling Threshold requirements (20 %)	Fulfilling Target requirements (10 %)	Fulfilling Optimal requirements (10 %)
SYNOP	3.6 %	YES	YES	YES
CALIPSO <i>(all COTs)</i> <i>(COT > 0.3)</i>	-10 % 5 %	YES YES	YES YES	YES YES
PATMOS-x	-4.1 %	YES	YES	YES
MODIS	-(10-20) %	YES	NO	NO
ISCCP	-12 % - 0 %	YES	YES (?)	NO

Table 6.16 Overall requirement compliance of the CM SAF GAC CFC product with respect to the bias-corrected RMS error. Consistency checks marked in blue.

Reference	bc-RMS	Fulfilling Threshold requirements (40 %)	Fulfilling Target requirements (20 %)	Fulfilling Optimal requirements (15 %)
SYNOP	11 %	YES	YES	YES
CALIPSO	n/a	-	-	-
PATMOS-x	2.6 %	YES	YES	YES
MODIS	20-30 %	YES	NO	NO
ISCCP	10-20 %	YES	YES	YES (?)

	<p align="center">EUMETSAT SAF on CLIMATE MONITORING Validation Report Cloud product GAC Edition 1</p>	<p>Doc.No.:SAF/CM/SMHI/VAL/GAC/CLD Issue: 1.1 Date: 30.04.2012</p>
---	--	--

We conclude that the CM SAF GAC CFC product fulfils the Threshold requirement when compared with all references. The product also fulfils the Target requirement in most cases. The only exception is when comparing with MODIS results. Optimal requirements are fulfilled when comparing with SYNOP results, with CALIPSO results and with PATMOS-x results.

When considering available information about uncertainties in the reference dataset, results do not change significantly. However, it is interesting to notice that CALIPSO results, after filtering out the thinnest clouds ($COT < 0.3$) and adding 1-2 % of the presumed missing clouds (i.e., leading to a reduction of the bias with the same amount), agrees well with SYNOP results. Also, since CALIPSO results appear to have the highest credibility of all observations over the Polar Regions, it seems very likely that the large negative deviations seen for CM SAF results with respect to many of the references is indeed a genuine feature.

Finally, it is interesting to contemplate further the results from the most trustworthy reference - CALIPSO (with detailed results presented in Section 6.1.1.2) – and put it in relation to the results from the other sources of information. Again, we repeat that CALIPSO and SYNOP results agree quite well if applying a filtering of the optically thinnest clouds in the CALIPSO dataset. In that sense, the CM SAF results could still be quite useful if taking this kind of cloud optical thickness limit into account and also if apparent deficiencies (like the overestimation of cloudiness over semi-arid areas and the lack of clouds over very cold areas in the polar winter) are taken care of. Secondly, all of the other satellite-based datasets indicate in Table 6.15 that CM SAF has a considerable underestimation of global cloudiness. Partly, the suggestion is that the underestimation is equal (ISCCP) or even larger (MODIS) than what the comparison with the unfiltered CALIPSO observation shows. But this could actually be questioned since none of these other references could reasonably have the same sensitivity to cloud detection as the CALIPSO-CALIOP sensor. This suggests that some overestimation of global cloud cover could also be present, at least over some regions and in some situations, for the MODIS and ISCCP datasets which leads to unrealistically large differences compared to CMSAF results. On the other hand, it is very clear from all the previously presented results that CM SAF GAC cloud detection has specific problems over semi-arid land areas in the sub-tropical region where land surfaces are systematically misinterpreted as clouds. In addition, failing cloud detection in the polar areas remains as a substantial challenge for the CM SAF GAC method. Both these aspects have to be addressed and improved in future reprocessing activities.

	EUMETSAT SAF on CLIMATE MONITORING Validation Report Cloud product GAC Edition 1	Doc.No.:SAF/CM/SMHI/VAL/GAC/CLD Issue: 1.1 Date: 30.04.2012
---	---	---

6.1.2 Cloud Top level (CTO)

6.1.2.1 Evaluation against A-Train (CALIPSO-CALIOP)

We have here used exactly the same dataset of 107 matched global orbits as was described previously in Section 6.1.1.2. Comparisons have been made for all points where both CM SAF and CALIPSO have valid cloud top level estimations. Also here we have tried to take into account the fact that the very thinnest CALIPSO-observed clouds should not theoretically be detected by passive imagery. Thus, single-level situations where cloud optical thicknesses below a certain threshold have been discarded. More important, in multi-layer situations, we have discarded the uppermost layers if their total COT does not exceed the same threshold. For remaining layers we have then used the mid-layer height of the uppermost layer as the cloud top height to compare with. In the case of optically thick clouds (i.e., when CALIPSO-CALIOP cannot see through the entire cloud layer), the reported mid-layer height will be more representative of the cloud top than the true mid-layer height which is beneficial for this approach.

We first look at the total statistics (Table 6.17). These results are also subdivided into two additional categories where CALIPSO observations of clouds with total vertically integrated optical thickness less than 0.5 and 0.3, respectively, are given. Results clearly indicate that cloud tops are underestimated, even in the case when only retaining clouds with optical thicknesses exceeding 0.5.

Table 6.17 *Total CTH statistics for 106 matched orbits in the period October 2006 – December 2009, including reduced CALIOP datasets after applying cloud optical thickness filtering.*

	CTHresults Total dataset	CTH results COT threshold 0.3	CTH results COT threshold 0.5
Samples	288731	262044	253583
Bias (m)	-2661	-433	-124
RMS (m)	4734	2437	2141

Results can be further detailed (Table 6.18) if separating clouds using the associated vertical feature mask information in the CALIPSO dataset (building upon the ISCCP definition separating layers using the 440 hPa and 640 hPa pressure levels). We notice that the findings of Karlsson and Dybbroe (2010), pointing at a considerable overestimation of cloud tops for low-level clouds and the opposite for high-level clouds, appears to be valid also outside the Arctic region. Especially, we notice a considerable underestimation of high-level cloud tops and an overestimation of low-level cloud tops. Evidence of both these effects are actually visible in the example plot shown earlier in Figure 6.10. For example, in this figure we notice a systematic underestimation of CM SAF cloud tops for the highest clouds and a systematic overestimation of low-level cloud tops at positions 7000-8000.

 	<p align="center">EUMETSAT SAF on CLIMATE MONITORING Validation Report Cloud product GAC Edition 1</p>	<p>Doc.No.:SAF/CM/SMHI/VAL/GAC/CLD Issue: 1.1 Date: 30.04.2012</p>
---	---	--

Table 6.18 Total CTH statistics for 106 matched orbits in the period October 2006 – December 2009 – separated according to three vertical levels.

	CTHresults Low-level clouds	CTH results Medium-level clouds	CTH results High-level clouds
Samples	92204	42852	153675
Bias (m)	620	-688	-5179
RMS (m)	1281	1605	6356

Summary of results

- Compliances with requirements are summarized in Table 6.19
- Total global results indicate a large underestimation of globally estimated CTH (-2661 m)
- However, if excluding (i.e., interpreting as cloud-free) cases when vertically integrated optical thicknesses are less than 0.3 the global agreement is improved (-433 m)
- If setting the optical thickness limit to 0.5 results improve even further (-124 m)
- However, total unfiltered results are misleading since CTH is overestimated for Low-level clouds (+620 m) and greatly underestimated for High-level clouds (-5179 m)
- We have no reason to question the quality of CTH estimations from CALIOP (i.e., lidar ranging well proven technically). The effects of which cloud particles that were detected and at which particle density of the cloud layer are probably much more important than potential errors in the actual height assignment of the reflected lidar pulse.

Table 6.19 Compliance matrix of found global CTH monthly mean product characteristics with respect to the defined product requirements for accuracy and precision. Comparisons were made against CALIPSO observations. Observe that the Level 3 to Level 2 comparison made here is only theoretically valid for the Bias error and not for RMS errors.

	CTH product requirements Level 3 (MM)			CALIPSO Level 2 (Oct 2006-2009)	CALIPSO Level 2 (Oct 2006-2009) COT > 0.3
	Threshold	Target	Optimal		
Bias	1800 m	1200 m	1000 m	-2661 m	-433 m
bc-RMS	4000 m	2000 m	1500 m	-	-

6.1.2.2 Evaluation against PATMOS-x

The evaluation of the CTO products has basically been made based on inter-comparisons of individual Level 2b products (i.e., after conversion of CM SAF products to Level 2b representation). Accumulated statistics have been produced and compared to target requirements (where applicable).

Figure 6.29 shows global plots of averaged cloud top pressure values in January for CM SAF and PATMOS-x over the entire period 1982-2008 for afternoon-night satellites. Notice that here we have calculated the arithmetic mean for both datasets from individual Level 2b products.

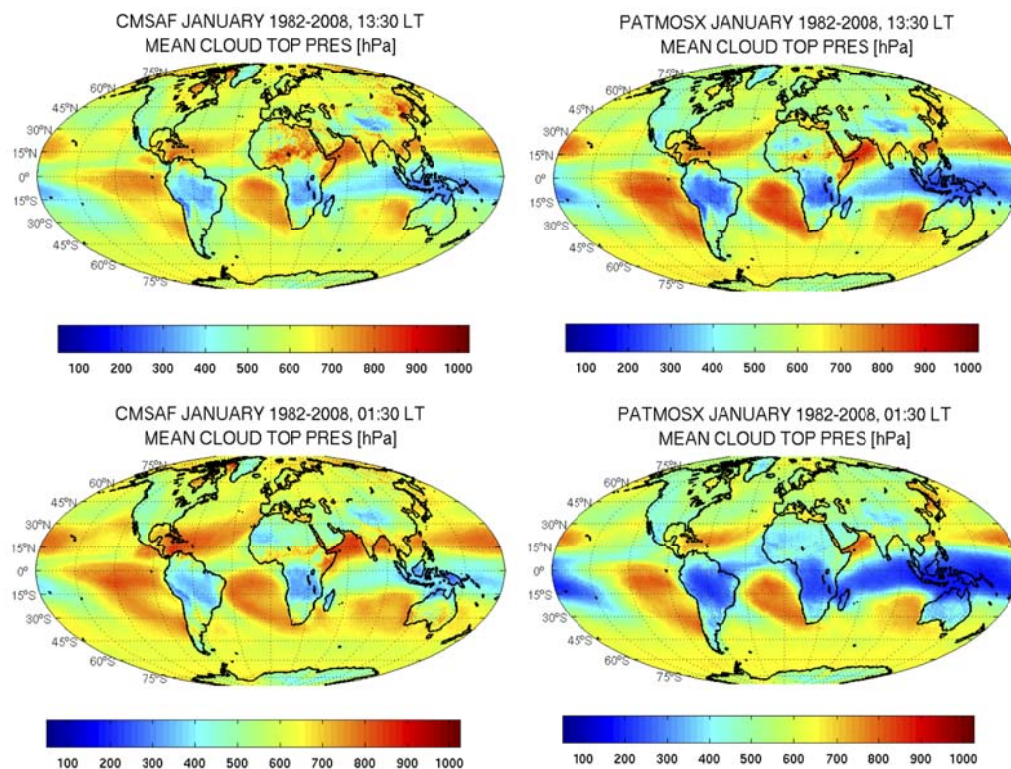


Figure 6.29 Mean cloud top pressure (arithmetic means, hPa) for afternoon satellites at 13:30 LT (top panels) and overnight satellites at 01:30 LT for January from 1982-2008. The left panels are CM SAF mean cloud top pressures and the right panels are PATMOS-x means.

Figure 6.29 shows that during the afternoon (upper panels), the marine stratocumulus regions in the sub-tropics tend to have lower cloud top pressures (i.e., higher geometrical heights) for CM SAF than for PATMOS-x. The situation is reversed overnight, where CM SAF stratocumulus regions tend to show higher cloud top pressures. Outside of the marine stratocumulus regions in the tropics and sub-tropics, PATMOS-x shows significantly lower

cloud top pressures, especially for the overnight overpasses. The same trend also holds over many of the land masses. The agreement is better over high-latitude and Polar Regions.

Figure 6.30 shows corresponding scatterplots of cloud top pressure for CM SAF and PATMOS-x for the afternoon orbits but for both January and July. The majority of cloud tops are found along the 1:1 line. There is also a tendency for CM SAF to place these low- and mid-level clouds geometrically higher (lower CTP) than PATMOS-x. These results suggest that many of the stratocumulus regions will have higher cloud tops in CM SAF than in PATMOS-x, and this discrepancy may impact the interpreted greenhouse effect of these low- and mid-level clouds. Additionally, there is an opposite situation for CM SAF when examining the high clouds. CM SAF tends to place the highest clouds lower than PATMOS-x. The histogram peak of PATMOS-x cloud top pressure near 150 hPa is likely a result of the 1st test of the naïve-Bayesian classifier used to produce a cloud mask and resulting cloud top pressure (e.g., Heidinger et al, 2012). If, through Bayesian probability testing, the PATMOS-x algorithm is confident of a cloud-filled pixel, but the tests cannot place the cloud top below the observed tropopause level, then PATMOS-x defaults the cloud top to be at the presumed tropopause height.

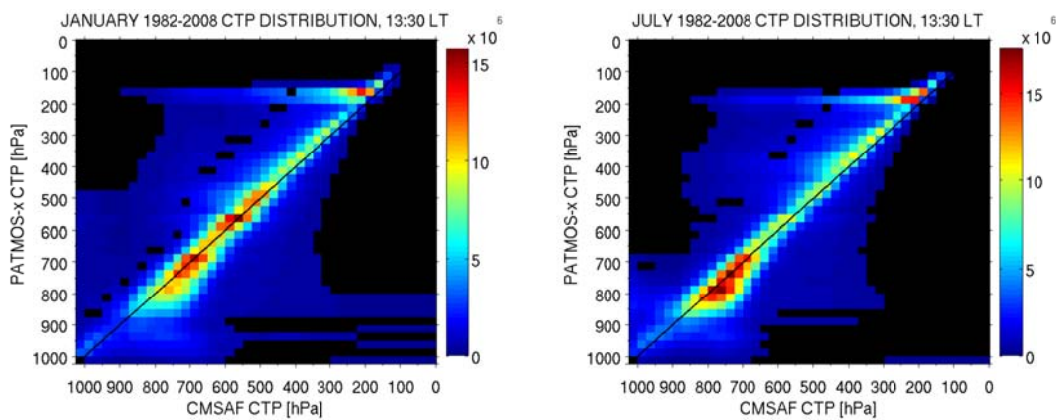


Figure 6.30 Histograms (colors) of PATMOS-x cloud top pressure (hPa) against CM SAF cloud top pressure for afternoon 13:30 LT overpasses from 1982-2008 for January (left) and July (right). Only scenes where both PATMOS-x and CM SAF agree on cloud presence are included.

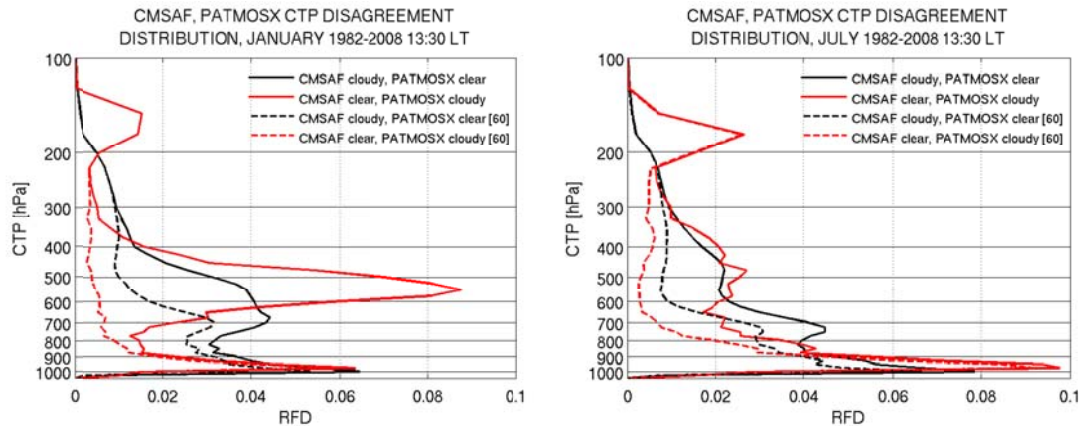


Figure 6.31 Cloud top pressure disagreement distribution for CM SAF and PATMOS-x in January (left) and July (right) for the period 1982-2008. See text for further explanation.

Figure 6.31 shows cloud top statistics for the cases when CM SAF pixels are cloudy while PATMOS-x pixels are clear (black) and vice versa (red) for afternoon satellites during 1982-2008 for January (left) and July (right). Full lines are for the full globe and dashed lines are cloud top pressure distributions within the 60°S to 60°N latitude bands. Both the full globe and the 60°S-60°N region are normalized by the respective total global number of CTP observations. Thus, the difference between the full lines and the dashed lines are the polar contribution to cloud top pressure/cloud mask differences.

We notice that the very lowest clouds (i.e., CTP higher than 900 hPa) are the ones that most often are observed by one data set but not by the other. Another very clear feature is that the CM SAF method is missing a significant portion of high clouds (with CTP lower than 200 hPa). There are also significant differences between the global distributions and the distributions from 60°S-60°N, where often polar mid-level clouds are seen by one data set and missed in the other. This suggests errors in the thermodynamic profiles as well as the potential influence of ice covered surfaces, especially in January. The peak in January for clouds between 500 and 600 hPa observed by PATMOS-x and not by CM SAF is a remarkable feature. This feature is also pronounced in the Joint Cloud property histograms (JCH) as seen later in section 6.3.1.1.

Table 6.20 summarizes the mean deviation for CTP for all satellite observation nodes. Notice here that values are given as the arithmetic mean for which we have defined our target accuracy of 110 hPa in the PRD document (see Table 4.1).

	<p align="center">EUMETSAT SAF on CLIMATE MONITORING Validation Report Cloud product GAC Edition 1</p>	<p>Doc.No.:SAF/CM/SMHI/VAL/GAC/CLD Issue: 1.1 Date: 30.04.2012</p>
---	---	--

Table 6.20 Mean errors (bias) for CM SAF CTP compared to PATMOS-x for all observation nodes in the period 1982-2008.


Local solar time <i>(observation node)</i>	Mean deviation (hPa)	Mean deviation (hPa)
	January	July
01:30 <i>(Descending)</i>	61.9	62.9
07:30 <i>(Descending)</i>	27.0	29.5
13:30 <i>(Ascending)</i>	17.7	11.6
19:30 <i>(Ascending)</i>	58.9	51.3

We conclude that CM SAF results are well within target requirements if having PATMOS-x as the reference. Interesting is to see that deviations are largest for the descending node at 01:30 and the ascending node at 19:30 regardless of the chosen month. It could mean that the lower relative frequency of high-level clouds and opposite higher relative frequency of low-level clouds for CM SAF, as illustrated in Figure 6.15 and Figure 6.16, is more pronounced at these two observation nodes than in the morning and in the afternoon.

A very final check was also made of the quality of daily mean products. However, in this case we have based them entirely on Level 2b results meaning that semi-Level 3 CTPs were compiled using only the Level 2b products (thus, slightly different compared to the official CM SAF product) for CM SAF and PATMOS-x. We picked results for two months (January and July) and limited the period to 1992-2008 in order to have access to results from both morning-evening satellites and afternoon-night satellites. Results are shown in Table 6.21.

Table 6.21 Mean deviations and bias-corrected RMS for daily mean Level 3 CTP products composed from Level 2b products compared to PATMOS-x.

	Level 3 (from daily Level 2b) CTP mean deviation [hPa]	Level 3 (from daily Level 2b) CTP BC-RMS [hPa]
January 1992-2008	43.6	71.8
July 1992-2008	40.5	66.2

	<p align="center">EUMETSAT SAF on CLIMATE MONITORING Validation Report Cloud product GAC Edition 1</p>	<p>Doc.No.:SAF/CM/SMHI/VAL/GAC/CLD Issue: 1.1 Date: 30.04.2012</p>
---	---	--

Summary of results

- Compliances with requirements are summarized in [Table 6.22](#)
- Good agreement in overall global cloud patterns but CM SAF CFC values are generally higher (approximately +40 hPa)
- Largest deviations are seen in the tropical region where PATMOS-x values are sometimes 200-300 hPa lower
- Best agreement is found for the afternoon ascending node (13:30) while largest deviations are found for the evening ascending node (19:30) and the night descending node (01:30)
- PATMOS-x is picking up very high and mid-level clouds that are not observed at all by CM SAF
- Both CM SAF and PATMOS-x appear to pick up near-surface clouds that the other dataset does not observe
- Interesting is that the presumed uncertainties of PATMOS-x results (i.e., overestimation of high-level clouds and underestimation of low-level clouds) act in the opposite way as CM SAF error characteristics (i.e., as deduced from CALIPSO studies – see previous section). Despite this, total results still indicate good agreement with target requirements.


Table 6.22 Compliance matrix of found global CTP monthly mean product characteristics with respect to the defined product requirements for accuracy and precision. Comparisons were made against PATMOS-x observations (consistency check).

	CFC product requirements Level 3 (MM)			PATMOS-x Level 3 (1992-2008)	PATMOS-x Level 2 (1982-2009)
	Threshold	Target	Optimal		
Bias	150 hPa	110 hPa	80 hPa	42 hPa	10-60 hPa
bc-RMS	160 hPa	130 hPa	100 hPa	40 hPa	-

6.1.2.3 Evaluation against MODIS

In this section CTP Level 3 (monthly means) of CM SAF GAC is compared to MODIS (MOD08_M3) equivalents. In detail, two exemplary months were chosen (January and July 2007) to visualize and discuss both products. Further, to minimize differences in the products caused by local equator crossing times of the different satellites, AVHRR/NOAA-17 is compared to MODIS/Terra, and AVHRR/NOAA-18 is compared to MODIS/Aqua.

Figure 6.32 and Figure 6.33 show the monthly mean values for cloud top pressure for the CM SAF L3 product (NOAA-17 only) and MODIS/Terra, and CM SAF (NOAA-18 only) and MODIS/Aqua, respectively for January and July 2007. It can be seen that the general patterns for CM SAF and MODIS products are similar: areas with low cloud tops can be identified in the subsidence regions of the subtropics on the Northern and Southern Hemisphere. On the other hand, regions of high mean cloud tops can be found in both products e.g. in the ITCZ. In the difference plots it can be seen that the CM SAF CTP on average includes smaller values for CTP than MODIS. This underestimation is more pronounced in the subtropics for

 	EUMETSAT SAF on CLIMATE MONITORING Validation Report Cloud product GAC Edition 1	Doc.No.:SAF/CM/SMHI/VAL/GAC/CLD Issue: 1.1 Date: 30.04.2012
---	---	---

both months. CTP overestimations in CM SAF are found in Africa, over Australia (in January) and over the Arctic (less pronounced for MODIS/Aqua comparisons).

Time series of mean CTP for all products, and for mean and standard deviations of CM SAF compared to other similar datasets (for consistency checks) are reported in Figure 6.35 and Figure 6.36 and discussed in the next subsection.

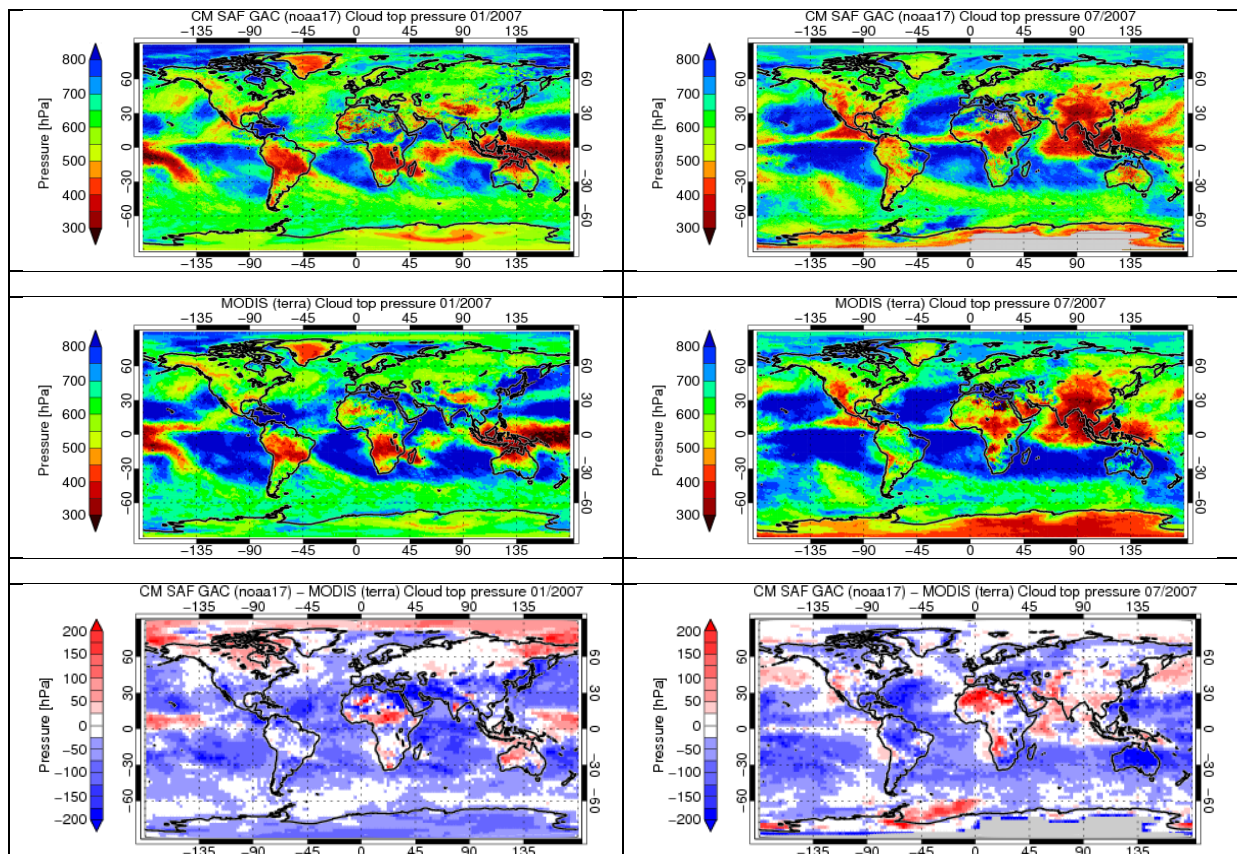


Figure 6.32 Global map of monthly mean cloud top pressure for CM SAF (NOAA-17 only, top row), MODIS (Terra only, middle row) and their differences (bottom row). Shown are January 2007 (left) and July 2007 (July). Regions without values are grey-shaded.

	EUMETSAT SAF on CLIMATE MONITORING Validation Report Cloud product GAC Edition 1	Doc.No.:SAF/CM/SMHI/VAL/GAC/CLD Issue: 1.1 Date: 30.04.2012
---	---	---

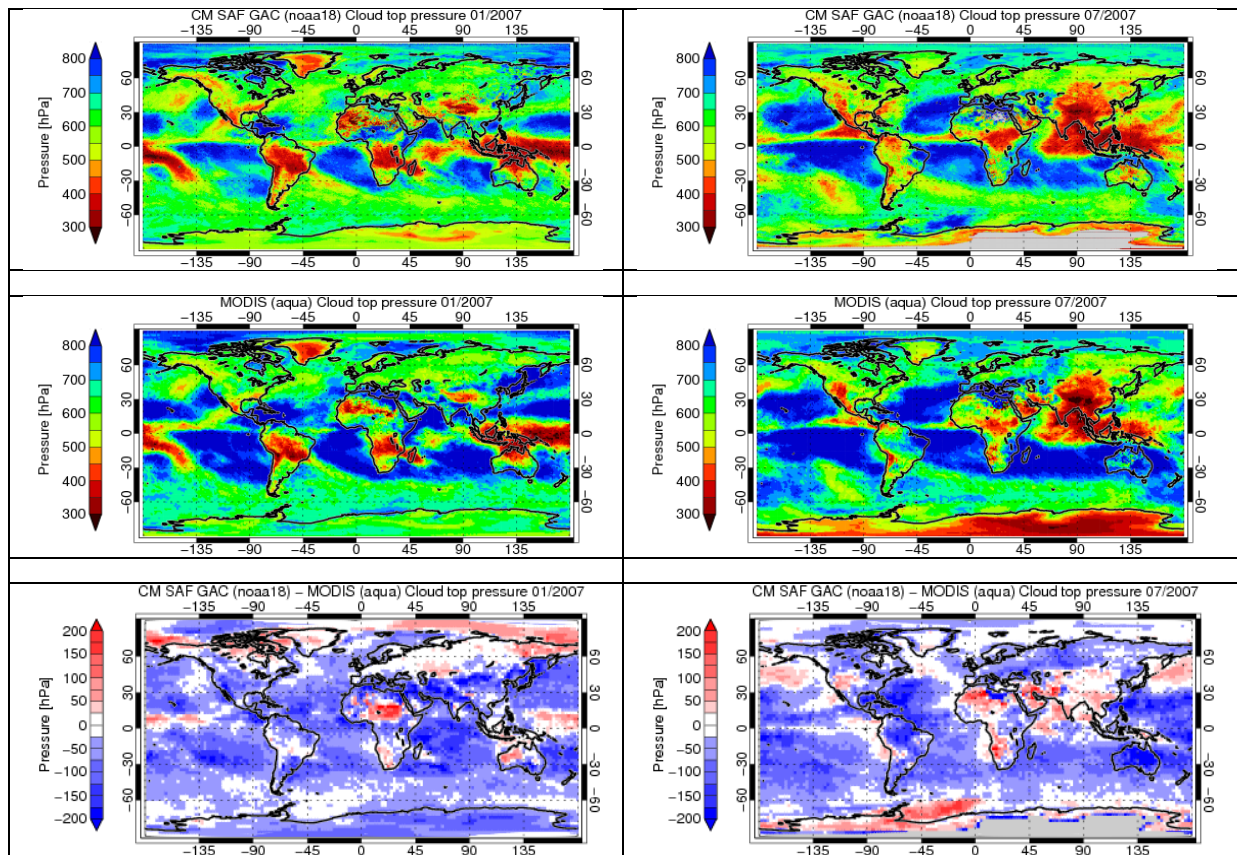


Figure 6.33 Global map of monthly mean cloud top pressure for CM SAF (NOAA-18 only, top row), MODIS (Aqua only, middle row) and their differences (bottom row). Shown are January 2007 (left) and July 2007 (July). Regions without values are grey-shaded.

Summary of results

- Compliances with requirements are summarized in Table 6.23
- Good agreement in overall vertical distribution of clouds and their geographical distribution
- CM SAF CTP values are generally lower (almost -50 hPa), especially over ocean.
- Some positive deviations are found over the poles in the Polar winter and over semi-arid tropical regions
- Uncertainties of MODIS retrievals (as described in section 5.6) appear very similar to the CM SAF error characteristics if relying on results from CALIPSO in section 6.1.2.1. This might explain the very good agreement with requirements (even with Optimal requirements) in Table 6.23.


	EUMETSAT SAF on CLIMATE MONITORING Validation Report Cloud product GAC Edition 1	Doc.No.:SAF/CM/SMHI/VAL/GAC/CLD Issue: 1.1 Date: 30.04.2012
---	---	---

Table 6.23 Compliance matrix of found global CTP monthly mean product characteristics with respect to the defined product requirements for accuracy and precision. Comparisons were made against MODIS results (consistency check).

	CFC product requirements L3 (MM)			MODIS/Aqua (2005-2009)	MODIS/Terra (2002-2009)
	Threshold	Target	Optimal		
bias	150 hPa	110 hPa	80 hPa	-50 to - 40 hPa	-50 to -30 hPa
bc-rms	160 hPa	130 hPa	100 hPa	<80 hPa	<80 hPa

6.1.2.4 Evaluation against ISCCP

In this section CTP Level 3 (monthly means) of CM SAF GAC is compared to ISCCP equivalents. In detail, two exemplary months were chosen (January and July 2007) to visualize and discuss both products.

The comparisons of CM SAF CTP against ISCCP in Figure 6.34 reveal many similarities. The large scale patterns of e.g. high CTPs in maritime stratocumulus regions and low CTPs in the ITCZ (in particular over land) are comparable to what was found and discussed in the comparisons to MODIS in the previous subsection.

Greatest differences between CM SAF and ISCCP are in general visible over land, with higher values for CM SAF e.g. over Australia, the Sahel zone, South America, some parts of Asia and the Arctic regions. Artificially introduced features found in the difference plots are most likely due to some satellite instrument borders in ISCCP.

Figure 6.35 and Figure 6.36 report the long-term values for global and latitude-band dependent mean values of CTP and the standard and mean deviations of CM SAF CTP L3 compared to ISCCP and both MODIS products. The global mean of the CM SAF CTP product is found to be fairly stable around 600hPa over the entire period. Compared to these, ISCCP reveals permanently smaller mean values also characterized by a slight negative trend. The global mean values of the MODIS products are approximately 50 hPa higher than CM SAF around 650 hPa with MODIS/Aqua being slightly higher than MODIS/Terra. All products do not exhibit a strong seasonal cycle in on global scale.

Similar results are found for the comparison for the separation into latitude bands. These comparisons give a similar picture for Northern and Southern Mid-Latitudes. An exception is the Polar Regions, where much stronger seasonal cycles are found for all products. These seasonal cycles are in general in phase with each other among the different products, with minima in polar winter and maxima in polar summer. It needs to be mentioned that some jumps in the ISCCP time series are clearly visible as for example for the Tropics in 2001.

It also needs to be noted that in these comparison the mean over all available satellites is considered, which could lead to some sampling errors in the comparisons against MODIS due to different satellite over-passing times. The monitoring of mean and standard deviations in Figure 6.36 does on the other hand emphasize the CM SAF/NOAA-17 and CM SAF/NOAA-18 matchups with MODIS/Terra and MODIS/Aqua, respectively.

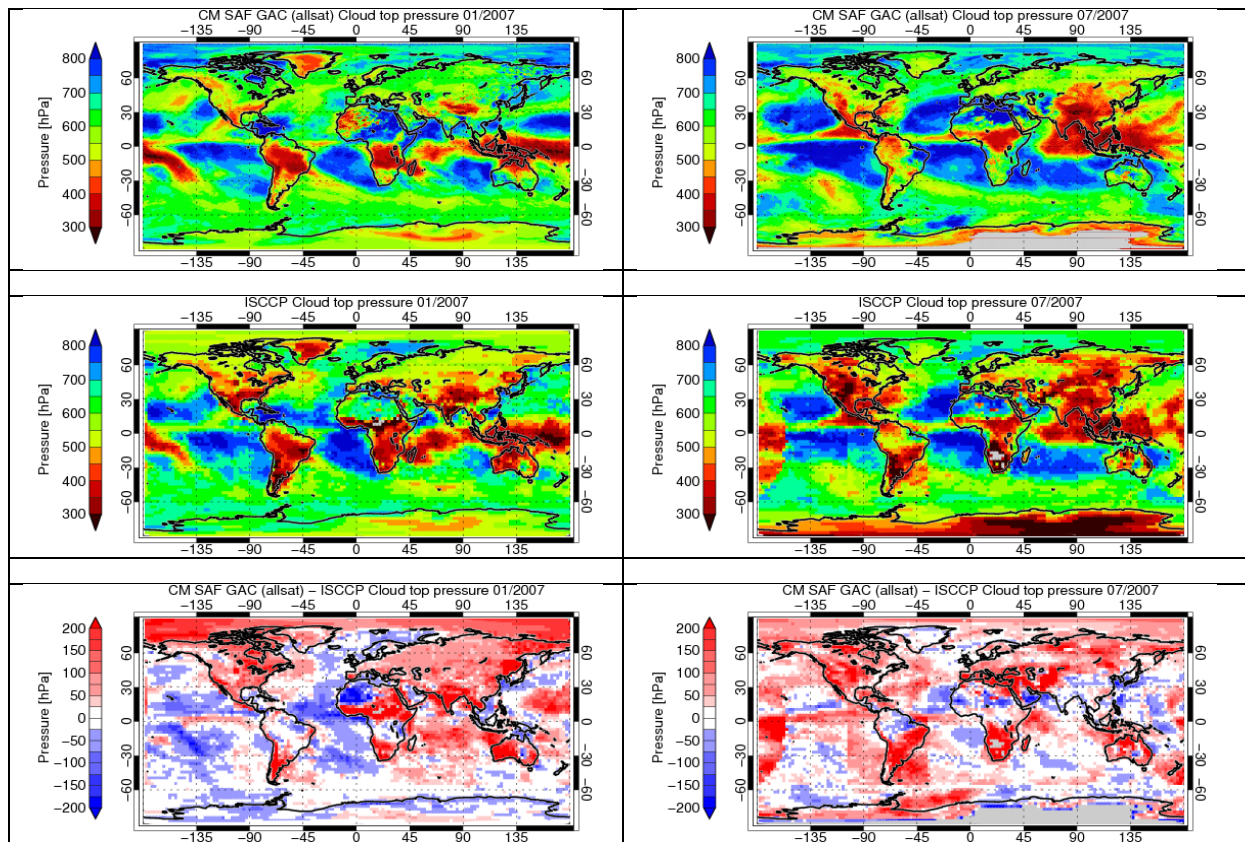


Figure 6.34 Global map of monthly mean cloud top pressure for CM SAF (all satellites, top row), ISCCP (middle row) and their differences (bottom row). Shown are January 2007 (left) and July 2007 (July). Regions without values are grey-shaded.

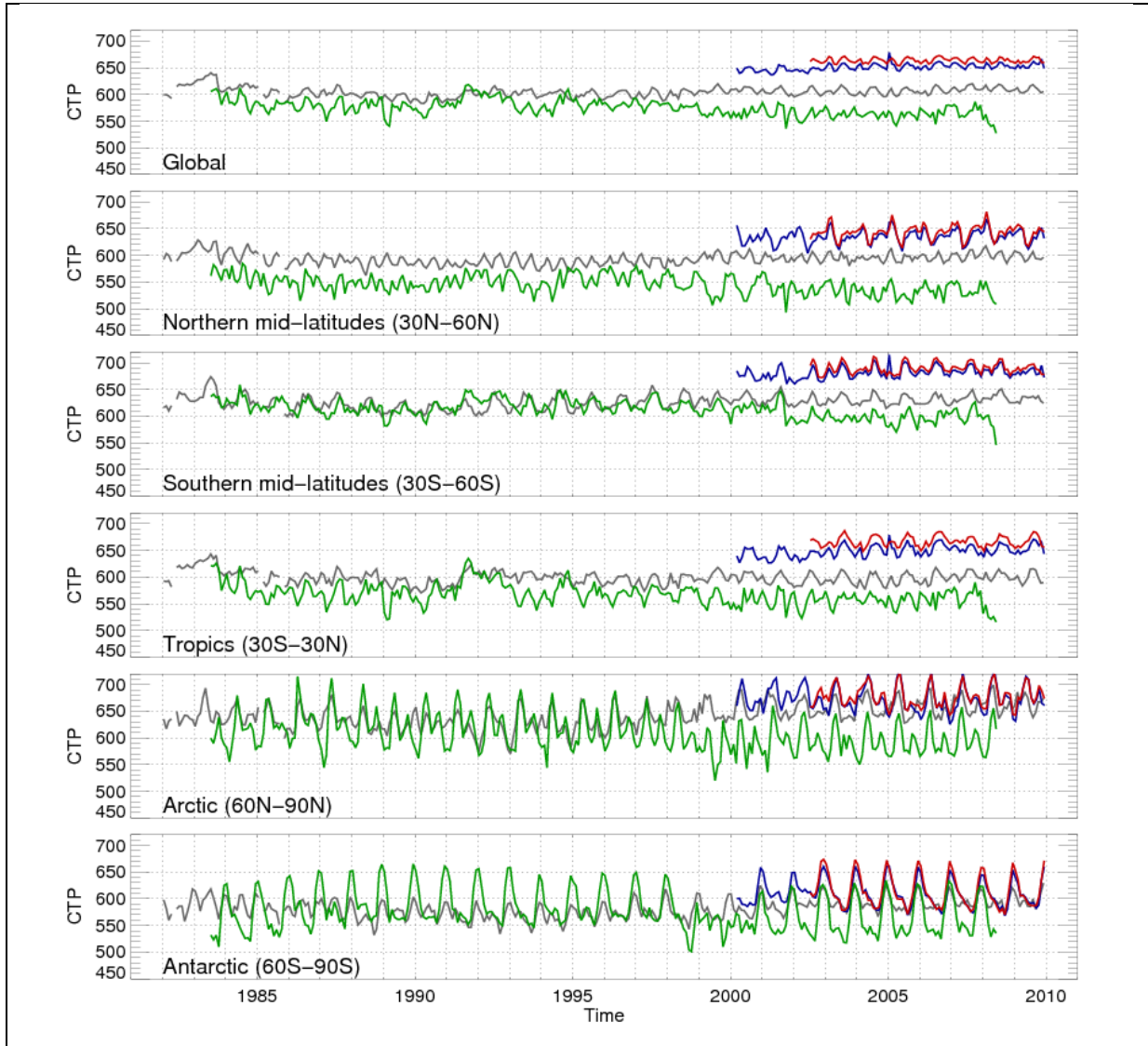


Figure 6.35 Time series of mean cloud top pressure of CM SAF (grey), ISCCP (green), MODIS/Terra (blue) and MODIS/Aqua (red). Shown are the global values (upper panel) and the separation into various latitude-bands.

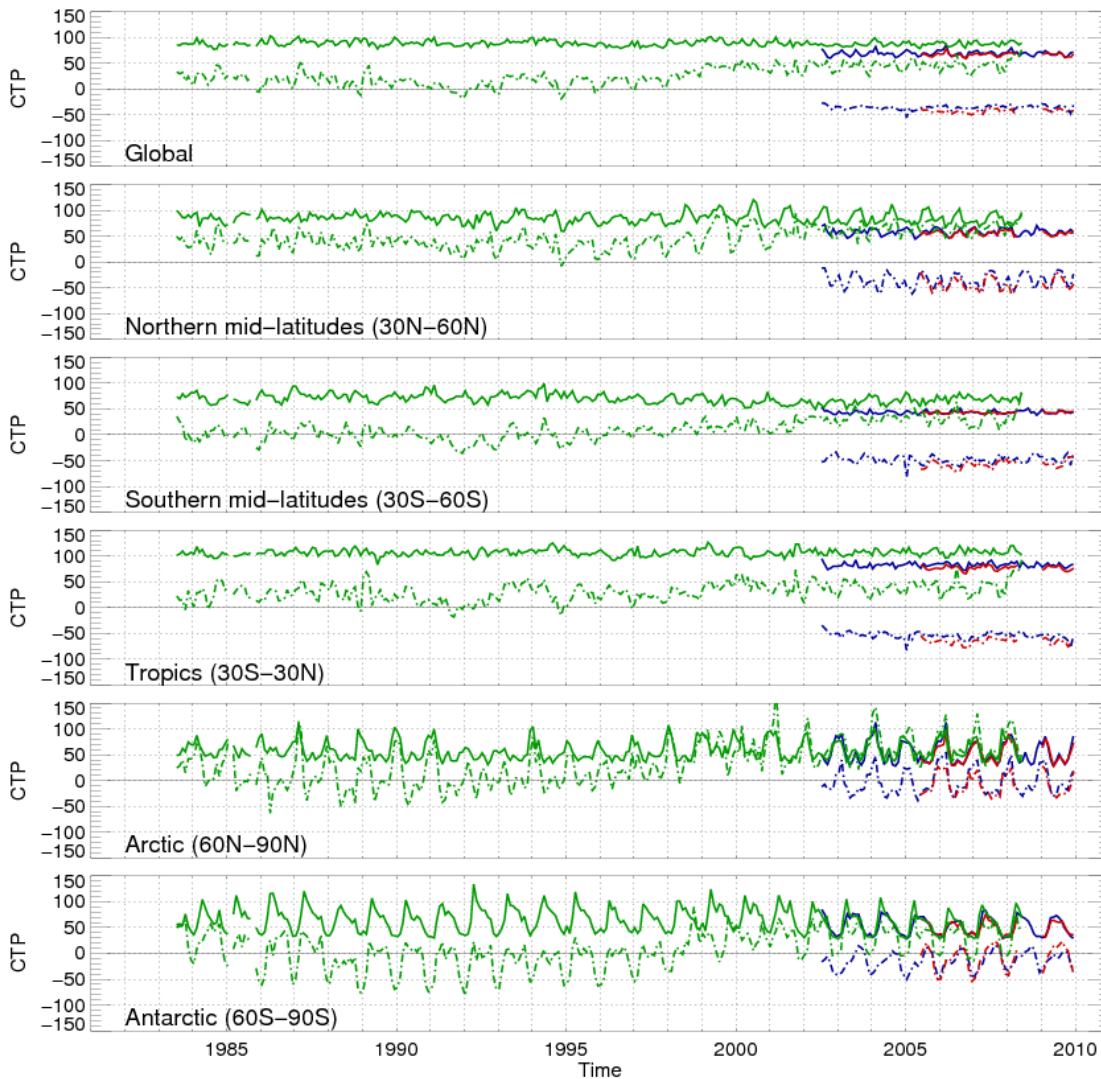


Figure 6.36 Time series of mean (dashed lines) and standard (solid lines) deviation of CTP of CM SAF compared to ISCCP (green), MODIS/Terra (blue) and MODIS/Aqua (red). Shown are the global values (upper panel) and the separation into various latitude-bands.

Summary of results

- Compliances with requirements are summarized in Table 6.24
- Good agreement in overall vertical distribution of clouds and their geographical distribution
- CM SAF and ISCCP CTP values do not show as large differences as against other studied datasets (i.e., differences are not large and they have both positive and negative signs)
- However, for the last 10 years ISCCP values are generally about 50 hPa lower than CM SAF

	<p align="center">EUMETSAT SAF on CLIMATE MONITORING Validation Report Cloud product GAC Edition 1</p>	<p>Doc.No.:SAF/CM/SMHI/VAL/GAC/CLD Issue: 1.1 Date: 30.04.2012</p>
---	---	--

- Target requirements are generally fulfilled, also after considering the uncertainty in the ISCCP estimation (being of the same order as the CM SAF Target requirement)

Table 6.24 Compliance matrix of found global CTP monthly mean product characteristics with respect to the defined product requirements for accuracy and precision. Comparisons were made against ISCCP results (consistency check).

	CFC product requirements L3 (MM)			ISCCP (1982-2008)
	Threshold	Target	Optimal	
bias	150 hPa	110 hPa	80 hPa	-20 to 60 hPa
bc-rms	160 hPa	130 hPa	100 hPa	90hPa

6.1.2.5 Summary of all results

Based on the previously described individual studies of the performance of the CM SAF GAC CTP product, we summarize results in the following two tables (one for the Mean Error and one for the bias-corrected RMS error). Here, compliance with requirements is indicated by simple YES or NO statements.

Table 6.25 Overall requirement compliance of the CM SAF GAC CTP product with respect to the Mean Error. Consistency checks marked in blue.

Reference	Mean Error	Fulfilling Threshold requirements (CTP:150 hPa) (CTH:1800 m)	Fulfilling Target requirements (CTP:110 hPa) (CTH:1200 m)	Fulfilling Optimal requirements (CTP:80 hPa) (CTH:1000 m)
CALIPSO (all COTs) (COT > 0.3)	-2661 m -433 m	NO YES	NO YES	NO YES
PATMOS-x	-20 hPa to 60 hPa	YES	YES	YES
MODIS	-(40-50) hPa	YES	YES	YES
ISCCP	-20 hPa to 60 hPa	YES	YES	YES



	<p align="center">EUMETSAT SAF on CLIMATE MONITORING Validation Report Cloud product GAC Edition 1</p>	<p>Doc.No.:SAF/CM/SMHI/VAL/GAC/CLD Issue: 1.1 Date: 30.04.2012</p>
---	---	--

Table 6.26 Overall requirement compliance of the CM SAF GAC CTP product with respect to the bias-corrected RMS error. Consistency checks marked in blue.

Reference	bc-RMS	Fulfilling Threshold requirements (CTP:160 hPa) (CTH:4000 m)	Fulfilling Target requirements (CTP:130 hPa) (CTH:2000 m)	Fulfilling Optimal requirements (CTP:100 hPa) (CTH:1500 m)
CALIPSO	n/a	-	-	-
PATMOS-x	< 100 hPa	YES	YES	YES
MODIS	< 80 hPa	YES	YES	YES
ISCCP	< 100 hPa	YES	YES	YES

We conclude that the CM SAF GAC CTO product fulfils all levels of requirements except in the case when comparing with unfiltered CALIPSO results when none of the requirements is fulfilled. The latter result is explained by the fact that for the thinnest detected clouds (with COT < 0.3), corrections for the semi-transparency effect is still a major issue.

Comparisons with similar datasets (consistency checks) show all rather good agreement, even after considering available information on uncertainties in individual datasets.

 	<p align="center">EUMETSAT SAF on CLIMATE MONITORING Validation Report Cloud product GAC Edition 1</p>	<p>Doc.No.:SAF/CM/SMHI/VAL/GAC/CLD Issue: 1.1 Date: 30.04.2012</p>
---	---	--

6.2 Microphysical cloud products

The evaluation of this specific group of products, formally denoted Cloud Physical Products (CPP) and consisting of products COT, CPH, LWP and IWP, has been performed with a common methodology. Consequently, we describe this approach already in the following for avoiding the need to repeat this description in each individual product sub-section.

Since the official Level 3 CPP products were not yet fully available at the time the analysis started, the evaluation of CPP products was based on gridded Level 2 (termed Level2b) products generated by SMHI on $0.1^\circ \times 0.1^\circ$ resolution (as introduced in Section 5.4). The Level 2b generation mimicked the procedures followed for the PATMOS-x dataset. The daily Level 2b fields were aggregated to monthly Level 3 fields at $1^\circ \times 1^\circ$ using pixel-weighted averaging, similar to the methodology used by the MODIS Science Team. Meanwhile, the official Level 3 products were generated, and it was confirmed that those do not differ significantly from the products generated earlier from Level 2b. For the CPP products, all comparisons are based on all-sky averages, i.e. the cloudy sky averages of all datasets were multiplied by the respective cloud fractions for the specific month. For those products that were divided into liquid (ice), the all-sky averages were computed using the liquid (ice) cloud fractions. Because the CPP retrieval algorithm is restricted to solar zenith angles within 72° , results obtained by the twilight satellites (NOAA-12 and NOAA-15, with local overpass times between 5 AM/PM and 7:30 AM/PM) were not included. To limit the amount of Level 2b data to be downloaded from the ECMWF computer system, only four months (Jan, Apr, Jul, Oct) per year were analysed. These months should give a reasonable representation of the four seasons.

The CPP Level 3 products are compared with three datasets: PATMOS-x, MODIS and ISCCP (as introduced in sections 5.4, 5.5 and 5.6). In addition, liquid water path (LWP) was validated with the O'Dell et al. (2008) climatology based on passive microwave observations (denoted UWisc, see Section 5.3).

Table 6.27 *Datasets, their version and instruments that were used for the evaluation of the CPP products.*

Dataset	version	Instruments
PATMOS-x	V05r02	NOAA-xx AVHRR
MODIS	Collection 5.1	Terra, Aqua
ISCCP	D1	Various GEO+LEO
UWisc	V3	SSM/I, TMI, AMSR-E

Evaluation of the CPP datasets was done in terms of the bias and root mean square error (RMS) compared to the other datasets. Since high latitudes are characterized by (i) lack of data during the winter season (too low solar elevation) and (ii) troublesome retrievals due to snow- and ice-covered surfaces, those are excluded from the calculation of bias and RMS values. In practice, the bias and RMS for a specific month have been calculated as the mean and root-mean-square difference between two datasets, respectively, over all pixels from 50°S to 50°N .

The CPP product evaluation is often split into morning and afternoon satellites. For the former only NOAA-17 is considered; for the latter NOAA-7, -9, -11, -14, -16, and -18 are considered. It is very important to note that the CPP retrievals are based on different channel combinations for the different satellites. The non-absorbing channel used is always channel 1

(at 0.6 μm). The absorbing channel active during daytime on most AVHRR instruments is channel 3b (at 3.7 μm). However, NOAA-17 as well as NOAA16 for the years 2001-2003 had channel 3a (at 1.6- μm) active. Thus, NOAA-17 is both the only morning satellite and the only satellite carrying an AVHRR with a 1.6- μm channel (except three years of NOAA-16). As a result, differences between CM SAF products for morning and afternoon may rather be related to the channel combination than to the time of day.

6.2.1 Cloud Thermodynamic Phase (CPH)

6.2.1.1 Evaluation against PATMOS-x, MODIS, and ISCCP

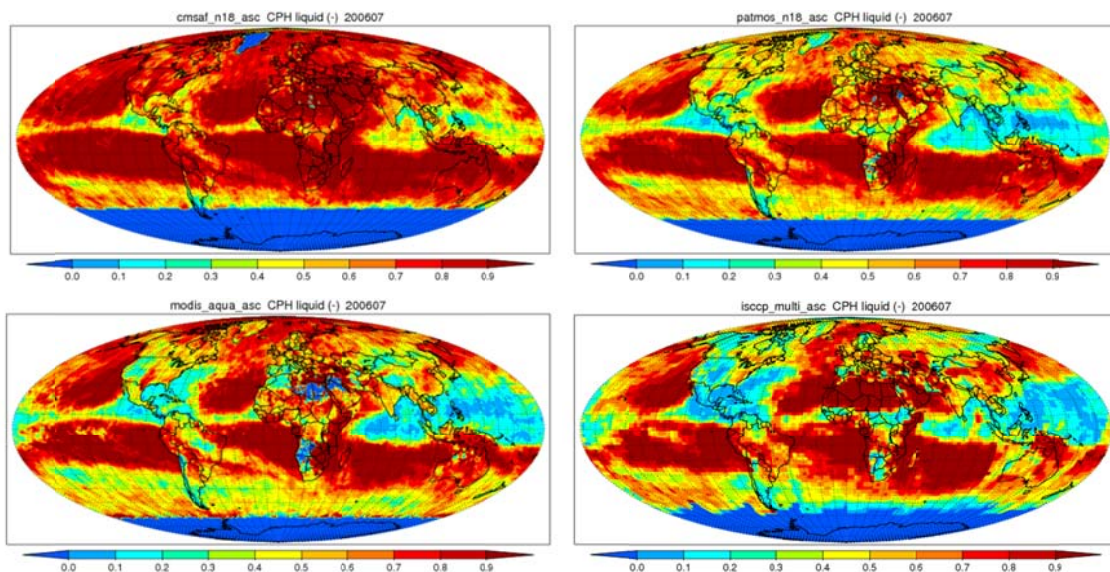


Figure 6.37 CPH for July 2006 expressed as the fraction liquid water clouds (of the total cloud amount) for CM SAF(upper left), PATMOS-x(upper right), MODIS Aqua(lower left), and ISCCP(lower right). For MODIS the optical properties cloud phase is shown.

Figure 6.37 shows the global distribution of CPH, expressed as the amount of liquid water clouds as a fraction of the total cloud amount, for July 2006. The plots were obtained using NOAA-18 data for CM SAF and PATMOS-x, Aqua data for MODIS (the ‘optical properties’ retrieval product, termed MODIS_OPT hereafter), and additional geostationary satellite data for ISCCP. It can be seen that the large patterns are resolved by the CM SAF dataset. However, it also follows that the fraction of water clouds is generally overestimated by CM SAF relative to PATMOS-x, MODIS_OPT, and ISCCP.

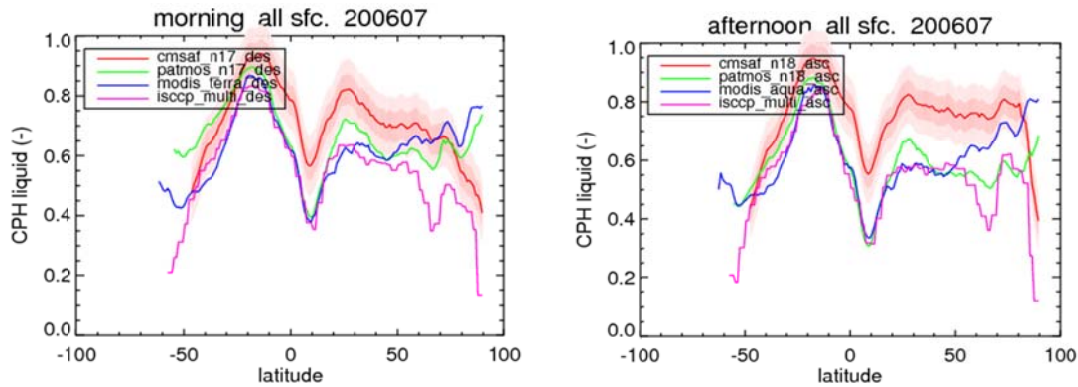


Figure 6.38 Zonal mean liquid water cloud fraction for CM SAF, PATMOS-x, MODIS, and ISCCP for morning (left) and afternoon satellites (right) for July 2006. The lighter and darker shaded areas around the CMSAF curve denote the threshold and target accuracy, respectively. For MODIS the optical properties cloud phase is shown.

Figure 6.38 shows the zonal mean distribution of the liquid water cloud fraction. All datasets clearly show a peak at about 20°N and 20°S, which represents the subtropical stratocumulus fields and a minimum around 5°N, which indicates the location of the Inter Tropical Convergence Zone (ITCZ). For both the morning and afternoon satellites, there is an overestimation of the water cloud fraction by CM SAF. Other datasets are just outside the threshold accuracy edges for the morning satellites, while differences are somewhat larger for the afternoon satellites.

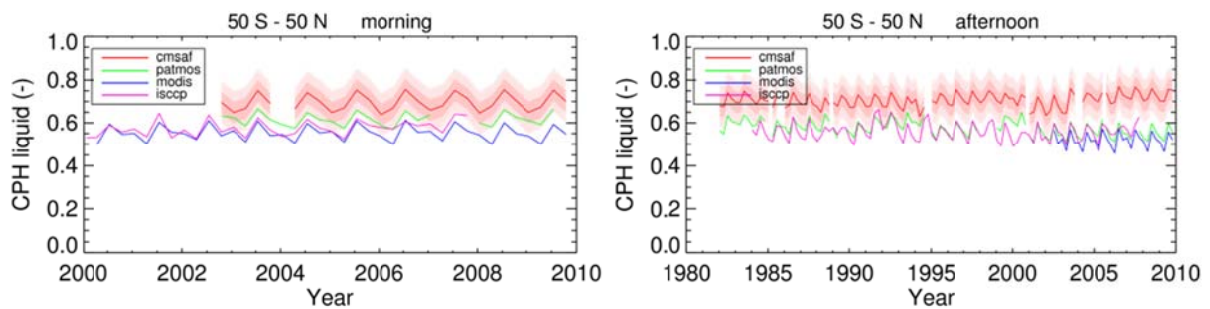


Figure 6.39 Time series of the liquid water cloud fraction averaged between 50°S and 50°N for CM SAF, PATMOS-x, MODIS, and ISCCP for the morning satellites (left, 2000 - 2009) and the afternoon satellites (right, 1982 – 2009). The lighter and darker shaded areas around the CM SAF curve denote the threshold and target accuracy, respectively. For MODIS the optical properties cloud phase is shown.

Figure 6.39 presents the time series for the morning (2000 – 2009) and afternoon (1982 – 2009) satellites, which were obtained between 50°S and 50°N. The annual cycle of cloudiness is fairly consistent between all datasets. There is especially good agreement between MODIS_OPT-Terra and ISCCP. On the other hand, PATMOS-x is slightly higher than MODIS_OPT-Terra and ISCCP, while CM SAF is even about 10% higher than PATMOS-x.

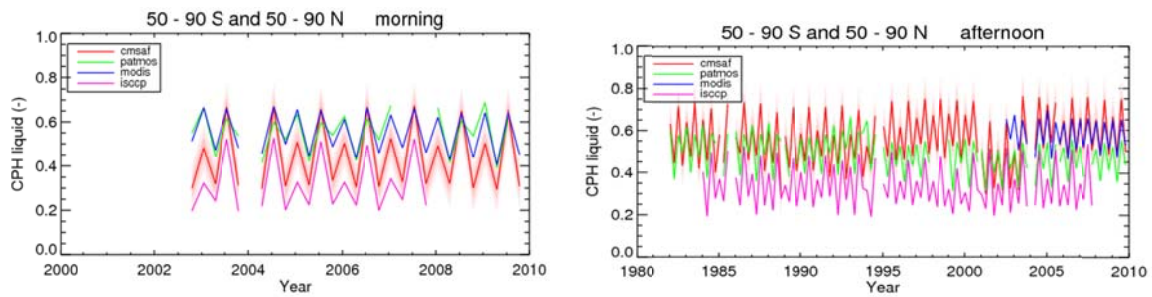


Figure 6.40 As Figure 6.39 but for the area between 50-90°S plus 50-90°N. Averages for each individual dataset were calculated based on those grid cells for which the CM SAF datasets had valid data available.

South of 50°S and north of 50°N retrievals are unavailable during part of the year as a consequence of too high solar zenith angles. Therefore, time series for this part of the globe have been compiled separately, using only those grid cells for which the CM SAF dataset had valid retrievals. The result for CPH is shown in Figure 6.40. While the annual cycles in these plots are generally consistent between the datasets, there are significant offsets. Interpretation of these differences is difficult, because towards the poles several complications arise: (1) the presence of snow and ice at the land/sea surface gives rise to large retrieval errors, especially if the snow and ice cover is not represented in the ancillary data; (2) solar zenith angles are large in winter giving rise to larger retrieval errors; (3) different choices can be made for aggregation of the data because there are multiple satellite overpasses over a given grid cell.

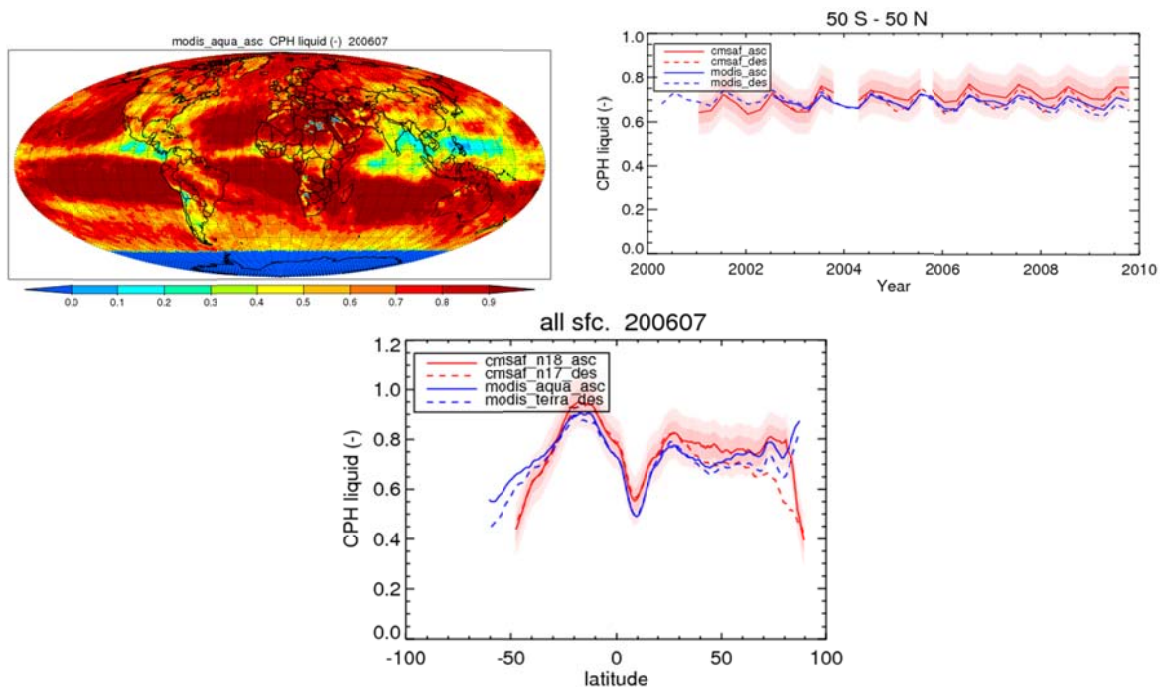


Figure 6.41 Upper left: MODIS Aqua IR-derived liquid water cloud fraction for July 2006. Bottom: Mean liquid water cloud fraction. Upper right: Time series of liquid water cloud fraction between 50°S and 50°N from 2000 to 2009. The bottom and upper right panels show CM SAF (red) and MODIS IR-derived (blue) CPH for morning (dashed) and afternoon (solid) satellites.

Figure 6.41 shows the behaviour of the CM SAF CPH product against the MODIS IR-derived cloud phase, termed MODIS_IR hereafter. The upper panel shows the global patterns of MODIS_IR cloud phase, which are very similar to that of CM SAF. This is further confirmed by the zonal means and time series. During both the morning and afternoon, the CM SAF zonal mean liquid water cloud fraction is slightly larger than that obtained by MODIS_IR, except for $> 60^{\circ}\text{N}$. This difference is close to the target accuracy. The time series of CM SAF and MODIS_IR CPH are very similar, both for the morning and afternoon satellites. The CM SAF CPH retrieval is a combined optical properties and IR based method. It is unclear why the CM SAF CPH agrees considerably better with the MODIS_IR than the MODIS_OPT product. Further research will be needed to explain this.

Summary of results

- Figure 6.42 summarizes the evaluation of CM SAF liquid water cloud fraction in terms of the bias and RMSE of CM SAF with respect to PATMOS-x, MODIS, and ISCCP
- Both the bias and RMSE are shown for the separate satellites relative to PATMOS-x, whereas they are divided between the morning and afternoon satellites relative to MODIS and ISCCP.
- Compared to PATMOS-x, the bias in liquid water cloud fraction is close to or below the threshold accuracy for NOAA-7, -9, and -17, while for NOAA-14, -16, and -18, as well as compared to the MODIS_OPT and ISCCP CPH dataset the threshold accuracy is exceeded.
- The RMSE values against PATMOS-x are on average within the threshold, while they are exceeding the threshold somewhat with respect to ISCCP and the MODIS_OPT CPH product.
- By contrast, the CM SAF CPH performance relative to MODIS_IR is much better, with bias values within the target accuracy and RMSE being just above the target.

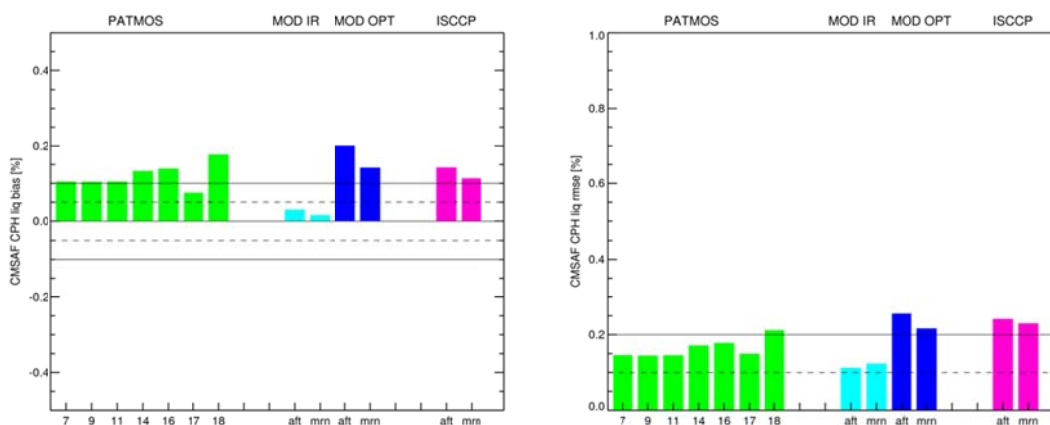



Figure 6.42 CM SAF bias (left) and RMSE (right) for liquid cloud fraction relative to PATMOS-x, MODIS, and ISCCP calculated between 50°S and 50°N . Bar colours correspond to the colours used in the time series plot. The numbers on the x-axis refer to the respective NOAA satellites, while ‘aft’ and ‘mnn’ refer to afternoon and morning, respectively. For MODIS both the IR-based (‘MOD IR’, pale blue) and optical properties (‘MOD OPT’, dark blue) cloud phase are presented. The solid and dashed horizontal lines indicate the threshold and target values from the PRT, respectively.

 	EUMETSAT SAF on CLIMATE MONITORING Validation Report Cloud product GAC Edition 1	Doc.No.:SAF/CM/SMHI/VAL/GAC/CLD Issue: 1.1 Date: 30.04.2012
---	---	---

6.2.1.2 Summary of overall results

Based on the previously described individual studies of the performance of the CM SAF GAC CPH product, we summarize results in the following two tables (one for the Mean Error and one for the RMS error). Here, compliance with requirements is indicated by simple YES or NO statements.

Table 6.28 Overall requirement compliance of the CM SAF GAC CPH product with respect to the Mean Error. Observe that results refer to the success of estimating the frequency of water clouds. Consistency checks marked in blue.

Reference	Mean Error	Fulfilling Threshold requirements 10 %	Fulfilling Target requirements 5 %	Fulfilling Optimal requirements 3 %
PATMOS-x	7-15 %	YES (?)	NO	NO
MODIS	3 % (IR) 14-20 % (Opt)	YES NO	YES NO	YES NO
ISCCP	12-15 %	NO	NO	NO

Table 6.29 Overall requirement compliance of the CM SAF GAC CPH product with respect to the RMS error. Consistency checks marked in blue.

Reference	RMS	Fulfilling Threshold requirements 20 %	Fulfilling Target requirements 10 %	Fulfilling Optimal requirements 5 %
PATMOS-x	15-20 %	YES	NO	NO
MODIS	12 % (IR) 15-20 % (Opt)	YES YES	NO NO	NO NO
ISCCP	24 %	NO	NO	NO

We conclude that the CM SAF GAC CPH product fulfils threshold requirements against most references except ISCCP. Target or Optimal requirements are generally not fulfilled (except if comparing against MODIS IR method).

Observe that we were here forced to rely exclusively on consistency checks since no independent validation source was available. Also, no information about uncertainties in the CPH retrievals from the references was available.

6.2.2 Cloud Optical Thickness (COT)

6.2.2.1 Evaluation against PATMOS-x, MODIS, and ISCCP

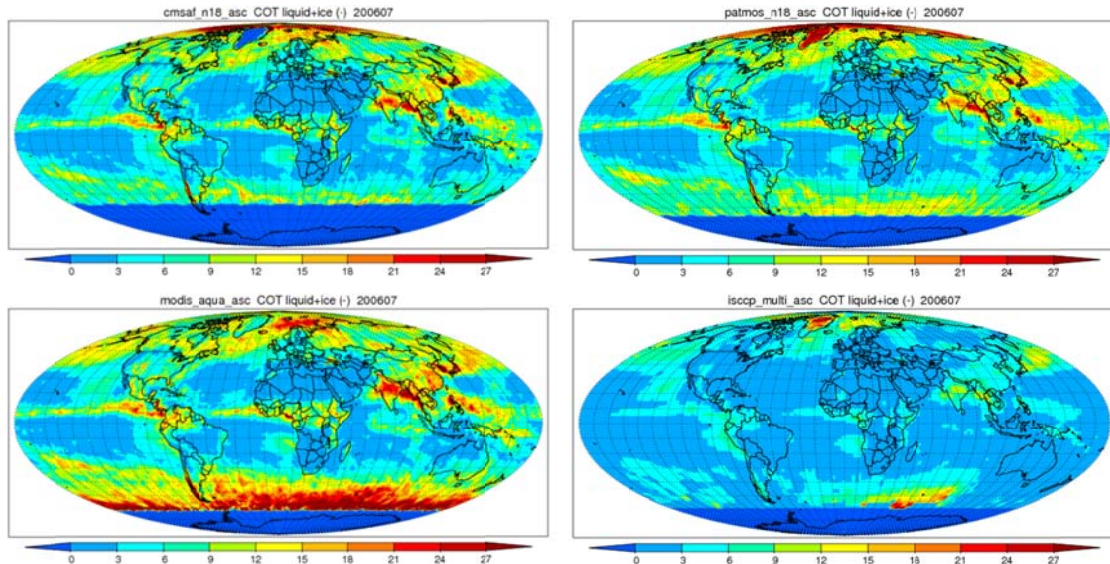


Figure 6.43 All-cloud COT for July 2006 for CM SAF (upper left), PATMOS-x (upper right), MODIS Aqua (lower left), and ISCCP (lower right).

Figure 6.43 shows the global distribution of all-sky average COT for all clouds (liquid+ice) for CM SAF, PATMOS-x, MODIS, and ISCCP. The general well-known cloud features show clearly up in the former three datasets; areas with thick clouds in the ITCZ and SPCZ, as well as the mid-latitude storm tracks are detected. MODIS exhibits a large area of high COT values south of 40°S, which does not show up in CM SAF and PATMOS-x. The ISCCP dataset clearly is an outlier in comparison to the other three datasets, because the areas with high COT are not that prominent. In addition, the range of COT values of ISCCP is much lower than of CM SAF, MODIS, and PATMOS-x.

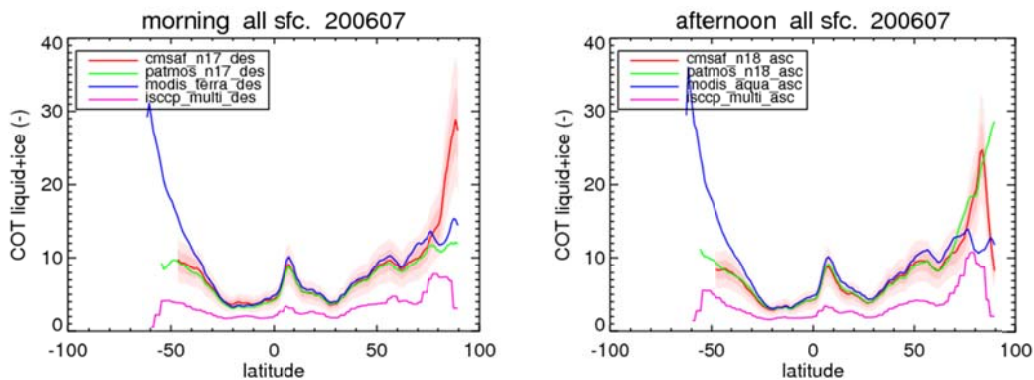


Figure 6.44 Zonal mean all-cloud COT for CM SAF, PATMOS-x, MODIS, and ISCCP for July 2006 for morning (left) and afternoon (right) satellites. The lighter and darker shaded areas around the CM SAF curve denote the threshold and target accuracy, respectively.

The zonal mean plots for the morning and afternoon satellites in Figure 6.44 show close agreement between CM SAF, PATMOS-x, and MODIS between 40°S and 70°N. South of 40°S, MODIS-Terra and –Aqua diverge from CM SAF and PATMOS-x, while north of ~70°N all datasets tend to diverge. These features are probably related to the low solar elevations in combination with ice- and snow-covered surfaces.

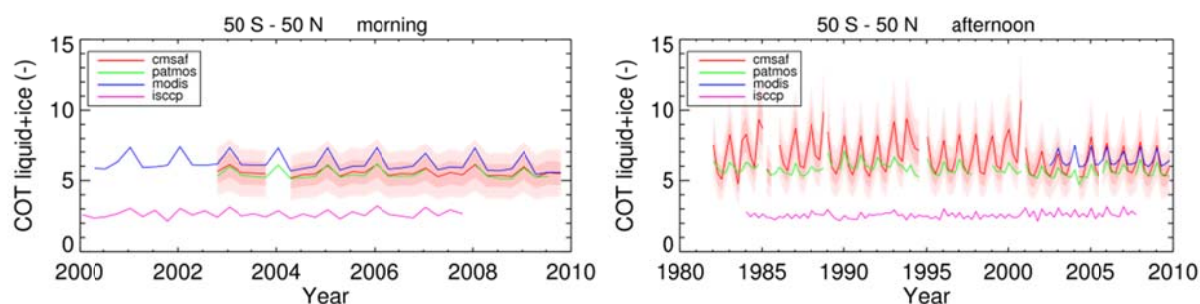


Figure 6.45 Time series of liquid+ice COT averaged between 50°S and 50°N for CM SAF, PATMOS-x, MODIS, and ISCCP for the morning satellites (left, 2000 - 2009) and the afternoon satellites (right, 1982 - 2009). The lighter and darker shaded areas around the CM SAF curve denote the threshold and target accuracy, respectively.

From Figure 6.45, left panel, it follows that the agreement between CM SAF and PATMOS-x is very close for NOAA-17. Further, MODIS-Terra is higher than both CM SAF and PATMOS-x, but still within the threshold accuracy. For the afternoon satellites it is particularly apparent that CM SAF COT has larger amplitude of the annual cycle than the other datasets. Also, there seems to be a significant effect of orbital drift on CM SAF COT, with COT increasing at later overpass times (especially for the satellites with large orbital drift, i.e. NOAA-7, -9, -11, and -14). It is speculated that both these features are related to the solar zenith angle. The CM SAF product based on the 0.6-3.7- μ m combination shows a relatively large number of maximum-COT (set to a value of 100) retrievals at high SZA (not shown). Combined with the annual cycle of SZA and the increase of SZA at later overpass times, this might explain the observed features in mean COT. Further research is needed to elucidate the causes of these possible retrieval artefacts. The time series of the ISCCP COT is – as was also observed for the zonal means and global patterns – considerably lower than that of the other three datasets.

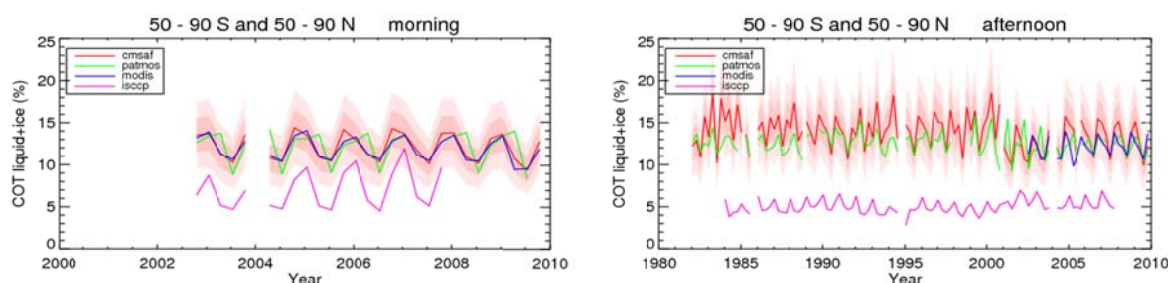


Figure 6.46 As Figure 6.45 but for the area between 50-90°S plus 50-90°N. Averages for each individual dataset were calculated based on those grid cells for which the CM SAF datasets had valid data available.

South of 50 °S and north of 50 °N retrievals are unavailable during part of the year as a consequence of too high solar zenith angles. Therefore, time series for this part of the globe have been compiled separately, using only those grid cells for which the CM SAF dataset had valid retrievals. The result for COT is shown in Figure 6.46. Despite considerable retrieval uncertainties – as discussed in Section 6.2.1 – the agreement between CM SAF, PATMOS-x and MODIS is not worse than at lower latitudes. ISCCP again shows a much lower average COT than the other datasets.

Finally, a separate more detailed study, inter-comparing Level 2b products from CM SAF and PATMOS-x, investigated the cases when the datasets showed disagreement (i.e., when one dataset had clouds and the other no clouds, and vice versa). Figure 6.47 shows results from this inter-comparison.

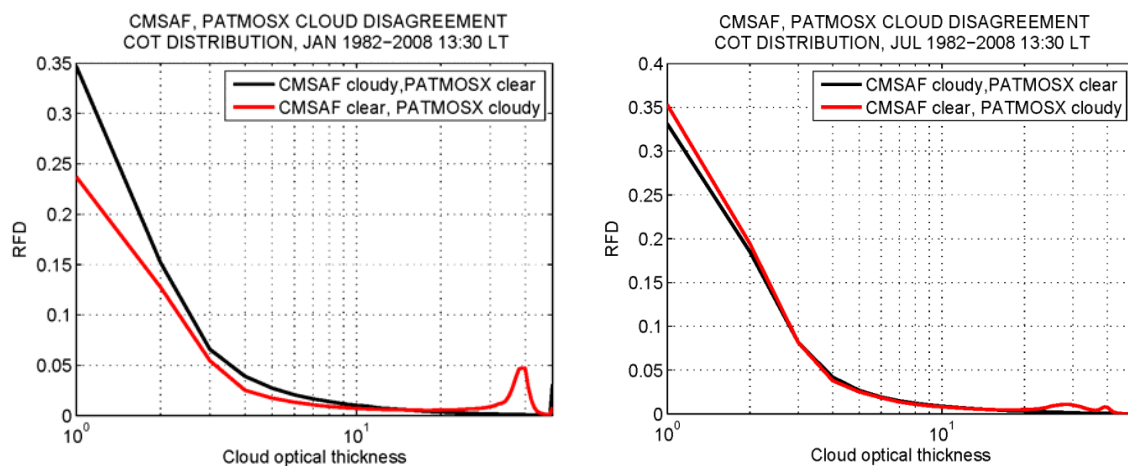


Figure 6.47 *Relative Frequency Distribution (RFD) of cloud optical thickness for cases when CM SAF sees a cloud while PATMOS-x is clear (black) and vice versa (red) for January (left) and July (right) for afternoon satellites during 1982-2008.*

Clearly, the cases, that each data set finds a cloud when the other does not, occur frequently for optically thin clouds. This is most likely explained by that PATMOS-x appears to have a higher sensitivity of detecting thin Cirrus clouds and the unfortunate CM SAF misclassification of land surfaces as clouds (giving pre-dominately thin clouds with low COT) in the semi-arid regions. Furthermore, there is a significant peak in the PATMOS-xRFD for optical thicknesses between 30-40 for January, but there is also a peak near optical thickness of 50 for CM SAF. These peaks suggest contributions from mis-classified ice and snow-covered surfaces (discussed further in Section 6.3.1.1).

Summary of results

- Figure 6.48 summarizes the performance of CM SAF COT for all clouds in relation to PATMOS-x, MODIS, and ISCCP
- The agreement is good to very good, with bias values relative to PATMOS-x and MODIS being largely within the target accuracy

- Compared to ISCCP, CM SAF overestimates > 50%, but given the firm agreement between PATMOS-x, MODIS, and CM SAF this dataset can be considered an outlier
- Compliances with requirements hold generally also after taking into account uncertainties of the references, except for the comparison with the ISCCP dataset. However, again we have to put some doubt in the ISCCP estimation, especially if claiming that uncertainty should be within 10 %.
- The RMS compared to PATMOS-x and MODIS is well below the threshold and even close to the target
- The CM SAF and PATMOS-x datasets show frequent disagreement in the occurrence of thin clouds
- In disagreement plots, PATMOS-x shows a peak of clouds with COT between 30 and 40 where CM SAF report clear conditions

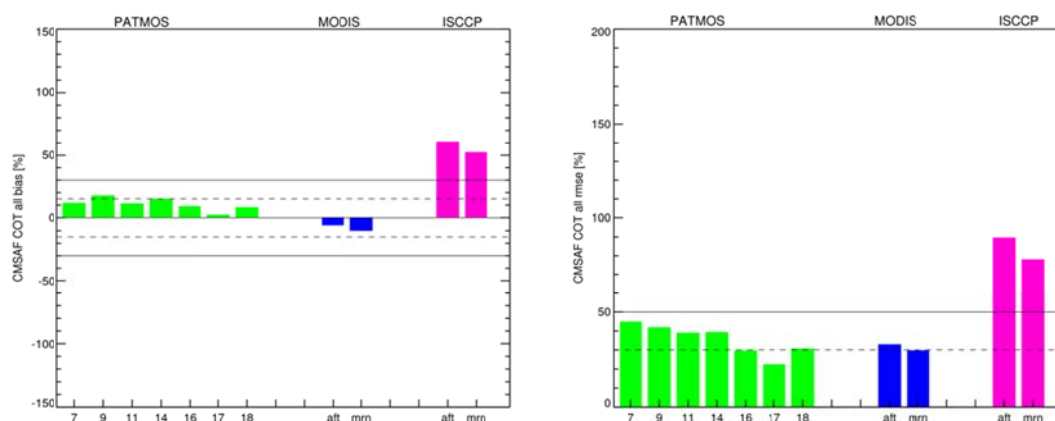


Figure 6.48 CM SAF bias (left panel) and RMS (right panel) for all-cloud COT relative to PATMOS-x, MODIS, and ISCCP, calculated between 50°S and 50°N. Bar colours correspond to the colours used in the time series plot. The numbers on the x-axis refer to the respective NOAA satellites, while ‘aft’ and ‘mrn’ refer to afternoon and morning, respectively. The solid and dashed horizontal lines indicate the threshold and target values from the PRT, respectively.

6.2.2.2 Summary of overall results

Based on the previously described individual studies of the performance of the CM SAF GAC COT product, we summarize results in the following two tables (one for the Mean Error and one for the RMS error). Here, compliance with requirements is indicated by simple YES or NO statements.



 	<p align="center">EUMETSAT SAF on CLIMATE MONITORING Validation Report Cloud product GAC Edition 1</p>	<p>Doc.No.:SAF/CM/SMHI/VAL/GAC/CLD Issue: 1.1 Date: 30.04.2012</p>
---	---	--

Table 6.30 Overall requirement compliance of the CM SAF GAC COT product with respect to the Mean Error. Consistency checks marked in blue.

Reference	Mean Error	Fulfilling Threshold requirements 30 %	Fulfilling Target requirements 15 %	Fulfilling Optimal requirements 5 %
PATMOS-x	3-20 %	YES	YES (?)	NO
MODIS	-(5-10) %	YES	YES	NO (?)
ISCCP	50-60 %	NO	NO	NO

Table 6.31 Overall requirement compliance of the CM SAF GAC COT product with respect to the RMS error. Consistency checks marked in blue.

Reference	RMS	Fulfilling Threshold requirements 50 %	Fulfilling Target requirements 30 %	Fulfilling Optimal requirements 10 %
PATMOS-x	25-45 %	YES	NO (?)	NO
MODIS	30 %	YES	YES	NO
ISCCP	80-90 %	NO	NO	NO

We conclude that the CM SAF GAC COT product fulfils threshold and target requirements when compared to PATMOS-x and to MODIS. However, differences are very large if comparing to ISCCP (not even within threshold requirements).

6.2.3 Liquid Water Path (LWP)

6.2.3.1 Evaluation against PATMOS-x, MODIS, and ISCCP

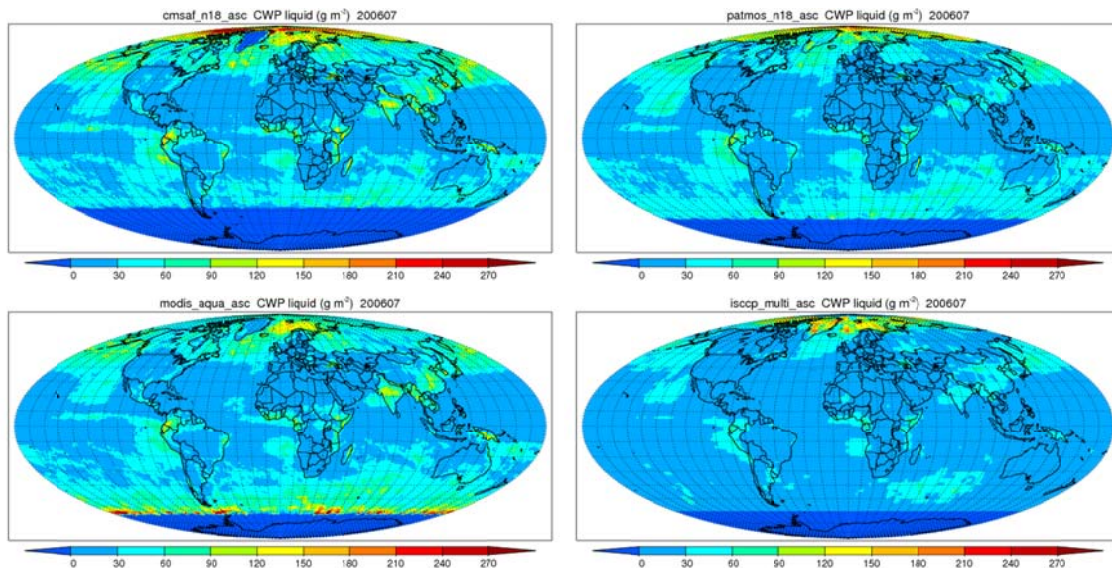


Figure 6.49 LWP for July 2006 for CM SAF (upper left), PATMOS-x (upper right), MODIS Aqua (lower left) and ISCCP (lower right).

Global patterns of LWP (Figure 6.49) look similar for all four datasets; the stratocumulus fields west of the continents are well represented. The main differences occur at the northern- and southernmost latitudes: e.g., MODIS-Aqua has high LWP values between 50°S and 60°S.

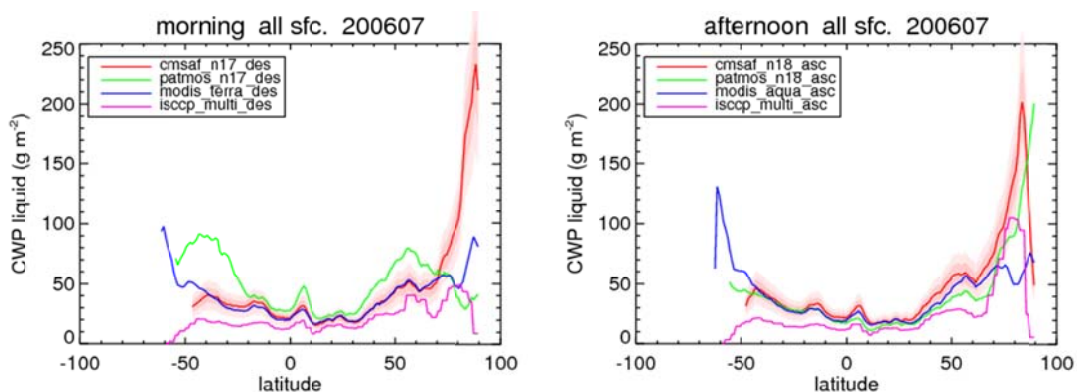



Figure 6.50 Zonal mean LWP for July 2006 for CM SAF, PATMOS-x, MODIS, and ISCCP for morning (left) and afternoon (right) satellites. The lighter and darker shaded areas around the CM SAF curve denote the threshold and target accuracy, respectively.

The zonal mean plots in Figure 6.50 reveal that for the morning satellite (NOAA-17), there is close agreement between MODIS-Terra and CM SAF over almost the entire latitudinal range.

	EUMETSAT SAF on CLIMATE MONITORING Validation Report Cloud product GAC Edition 1	Doc.No.: SAF/CM/SMHI/VAL/GAC/CLD Issue: 1.1 Date: 30.04.2012
---	---	--

The only remarkable feature of CM SAF is the steep increase north of 70°N, which might be related to difficulties the retrieval scheme has over sea ice areas. PATMOS-x closely follows MODIS-Terra and CM SAF within the tropical band (30°S - 30°N), but shows higher values over the southern and northern mid-latitudes. For the afternoon satellites, PATMOS-x, and MODIS-Aqua are within the threshold accuracy boundaries of CM SAF, which confirms the good performance of CM SAF LWP. In both panels ISCCP LWP is significantly lower than all other datasets.

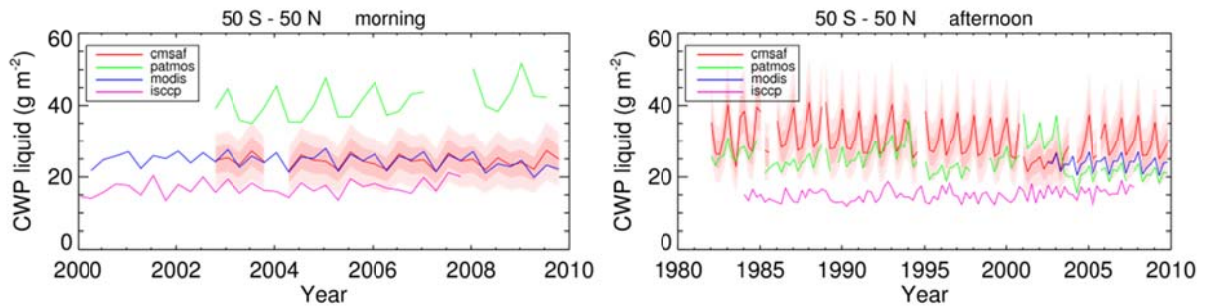


Figure 6.51 Time series of LWP covering 50°S - 50°N for CM SAF, PATMOS-x, MODIS, and ISCCP for the morning satellites (left, 2000 - 2009) and the afternoon satellites (right, 1982 - 2009). The lighter and darker shaded areas around the CM SAF curve denote the threshold and target accuracy, respectively.

The time series of the morning satellite in Figure 6.51 (left panel) reveals that CM SAF and MODIS-Terra agree very well. PATMOS-x LWP is significantly higher, which can largely be attributed to the higher LWP in the mid-latitudes (see Figure 6.50, left panel). ISCCP underestimates relative to CM SAF and MODIS-Terra, but stays close to the lower threshold accuracy.

The afternoon time series show a couple of interesting features. First, the equator overpass time drift to the CM SAF LWP has less impact compared to the COT time series (Figure 6.45, right panel). In contrast, the PATMOS-x time series shows clear upward trends in afternoon LWP, related to the orbital drift of the NOAA-satellites. Another interesting feature is that there is excellent agreement between CM SAF and MODIS-Aqua LWP for the period 2001 - 2003, which is the period that the 1.6 μm channel on NOAA-16 was switched on (see Table 3.2). The PATMOS-x LWP for this period reveals a considerable overestimate compared to CM SAF and MODIS-Aqua. However, after switching on the 3.7 μm after 2003 the behaviour of CM SAF and PATMOS reverses; CM SAF is significantly higher than MODIS-Aqua, while PATMOS-x LWP is slightly lower than MODIS-Aqua. Throughout the entire afternoon time series, ISCCP LWP values are much lower than the other three datasets.

South of 50°S and north of 50°N retrievals are unavailable during part of the year as a consequence of too high solar zenith angles. Therefore, time series for this part of the globe have been compiled separately, using only those grid cells for which the CM SAF dataset had valid retrievals. The result for LWP is shown in Figure 6.52. Similar features as for lower latitudes are observed. PATMOS-x has high LWP values if the 1.6-μm channel is used, whereas CM SAF has rather high values if the 3.7-μm channel is used. ISCCP has the lowest LWP.

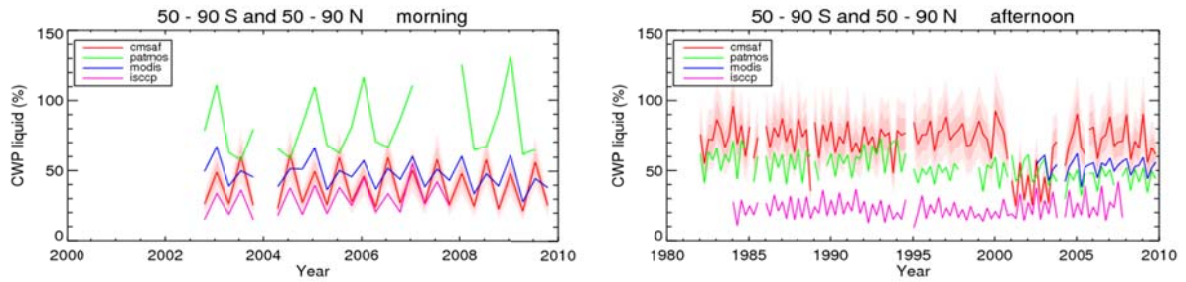


Figure 6.52 As Figure 6.51 but for the area between 50-90°S plus 50-90°N. Averages for each individual dataset were calculated based on those grid cells for which the CM SAF datasets had valid data available.

As discussed in RD-1 and RD-5, an important uncertainty component in LWP concerns the retrieval of effective radius for thin clouds, which is inherently uncertain. Different strategies are taken to deal with this problem: the PATMOS-x optimal estimation r_e retrieval for thin clouds is relaxed to the a priori value; MODIS does not employ prior information but uses a clear-conservative cloud mask, not retrieving optical properties for many thin / broken cloud scenes; in CPP the r_e retrieval for thin clouds is weighted with a climatological value. Although these different strategies yield different results, the contribution of thin clouds to the average LWP will be modest. A specific inter-comparison for thin clouds requires analysis of level-2 rather than level-3 products and is outside the scope of this validation report.

Summary of results

- Figure 6.53 summarizes the evaluation against PATMOS, MODIS, and ISCCP
- For NOAA-17 the CM SAF LWP bias exceeds the threshold, while for the other satellites the bias is within these boundaries
- RMS values are close to the threshold for PATMOS-x, with an exception for NOAA-17, which is evidently beyond this value
- The bias relative to MODIS is well below the threshold and even negligible relative to Terra; the RMSE is between the threshold and target.
- Compared to ISCCP, both the bias and RMSE are above the threshold.

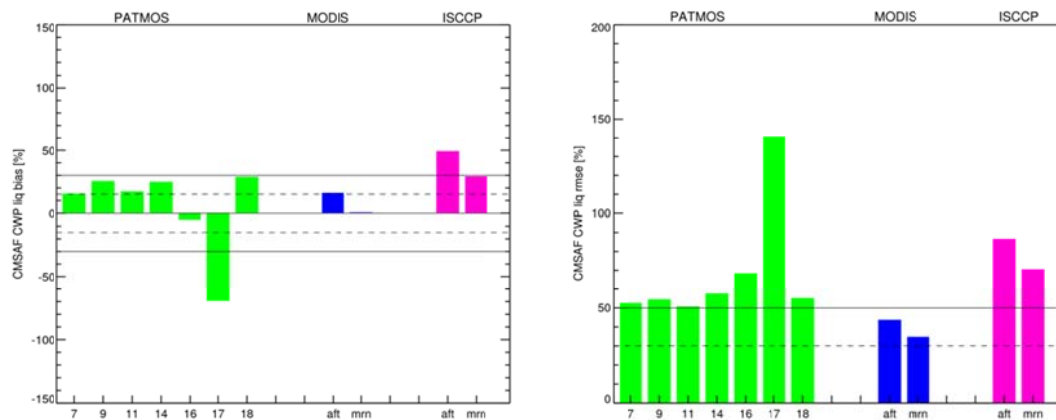



Figure 6.53 CM SAF bias (left panel) and RMSE (right panel) for LWP relative to PATMOS-x, MODIS, and ISCCP, calculated between 50°S - 50°N. The numbers refer to the different NOAA satellites. The abbreviations 'aft' and 'mrn' refer to afternoon and morning, respectively.

	EUMETSAT SAF on CLIMATE MONITORING Validation Report Cloud product GAC Edition 1	Doc.No.:SAF/CM/SMHI/VAL/GAC/CLD Issue: 1.1 Date: 30.04.2012
---	---	---

6.2.3.2 Evaluation against University of Wisconsin (UWisc) MW LWP dataset

The UWisc LWP dataset (see Section 5.3) comprises monthly mean LWP in $1^\circ \times 1^\circ$ grid boxes that is based on all available data for a specific month. In addition, for each month and each grid box over the 1988 – 2008 period the mean diurnal cycle of LWP is available. In order to obtain the monthly mean LWP from UWisc closest to the overpass times of the respective NOAA satellites, we have included the mean diurnal cycle parameters to adjust the monthly mean grid box values:

$$\langle LWP(Y, t) \rangle = \langle LWP(Y) \rangle + A_1 \cos \omega(t - T_1) + A_2 \cos 2\omega(t - T_2)$$

in which $\langle LWP(Y) \rangle$ represents the uncorrected monthly mean LWP for year Y , t the local time (h), ω the radial frequency that corresponds to a 24-h period, and A_1 (T_1) and A_2 (T_2) are the amplitudes (phases) of the first and second harmonics of the diurnal cycle, respectively.

The drift in equator crossing times (see Figure 3.3) was accounted for in the calculations using ephemeris data from <ftp://ftp2.ncdc.noaa.gov/pub/data/orbit/crossing/>. More information on equator crossing time drifting for various satellites can be found in Ignatov et al. (2004).

Because microwave instruments are able to penetrate through deep convective clouds or ice over water clouds and measure the liquid water path at lower altitudes, which is not possible for passive imagers, our evaluation was restricted to regions with very few (<5%) ice clouds. Therefore we selected three well-known areas dominated by stratocumulus clouds: the oceanic area west of South America at $8^\circ - 28^\circ\text{S}$, $70^\circ - 90^\circ\text{W}$, the area west of Africa at $5^\circ - 25^\circ\text{S}$, $10^\circ\text{W} - 15^\circ\text{E}$, and the area west of California at $20^\circ - 30^\circ\text{N}$, $120^\circ - 130^\circ\text{W}$ (see for their locations Figure 6.54). As a result of the CPP algorithm not being able to perform retrievals beyond solar zenith angles larger than 72° , we note again that we refrained from using NOAA-12 and NOAA-15 data. These satellites have typical overpass times around 7:00 and 19:00 LT, which would lead to a very limited number of valid retrievals.

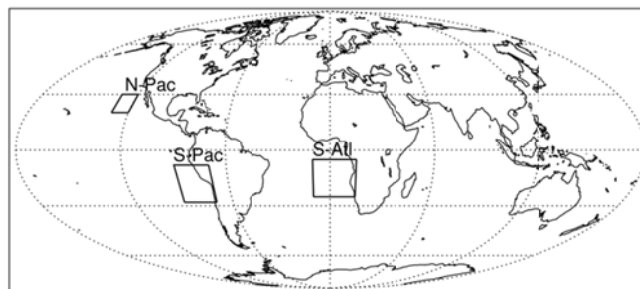


Figure 6.54 The locations of the S-Atl, S-Pac and N-Pac validation areas.

Figure 6.55 shows the results of the comparison for the period 1989 – 2008 (NOAA-11 to NOAA-18). The absolute monthly mean LWP values for UWisc and GAC are shown in the left panels, while the relative biases $(GAC - UWisc) / UWisc$ (in %) are shown in the right panels.

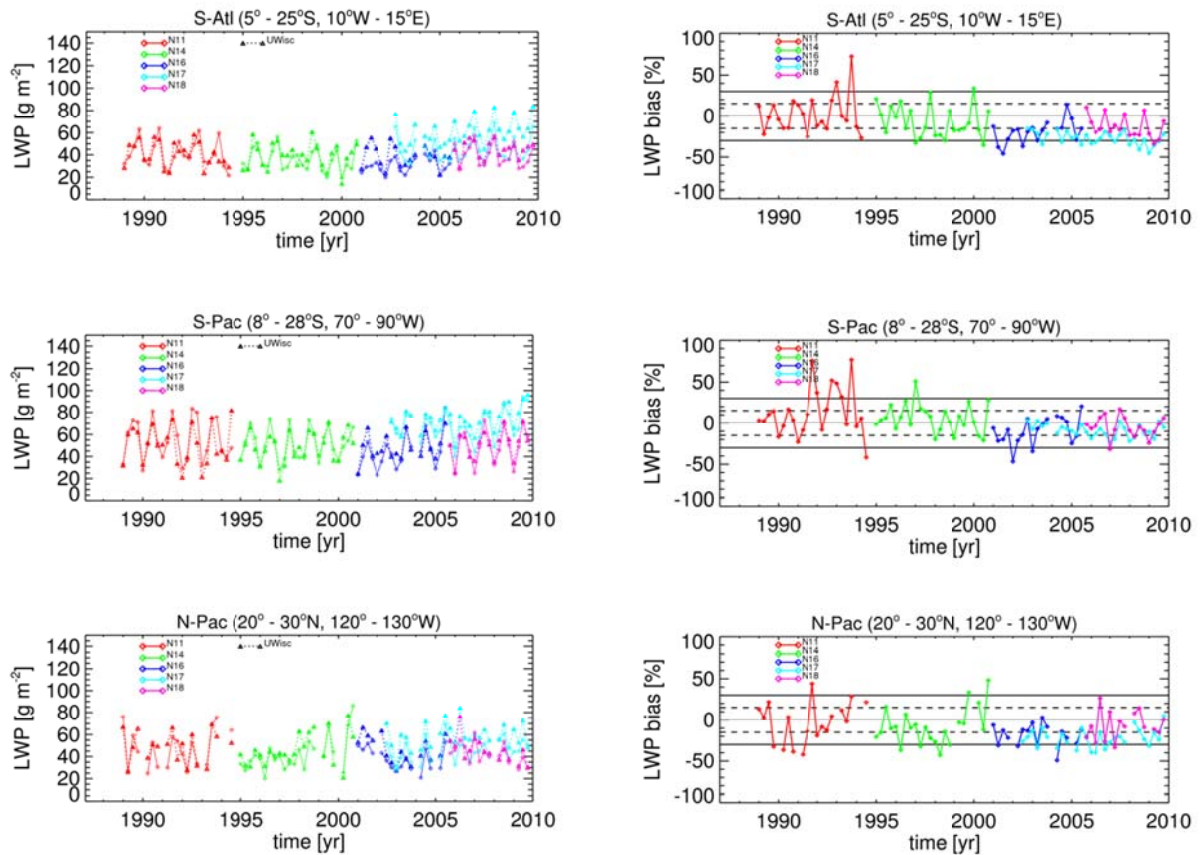


Figure 6.55 GAC (solid coloured lines) and UWisc (dotted coloured lines) monthly mean LWP (left column) for 1989 – 2008 over the S-Atl (upper panels), S-Pac area (center panels), and N-Pac area (lower panels). The relative bias is shown in % in the right column. UWisc values were calculated using the mean diurnal fit parameters for the period 1988 – 2008 (see text for further details). The solid and dashed horizontal lines in the right panels denote threshold and target accuracies, respectively.

It can be seen from Figure 6.55 that the GAC AVHRR and UWisc minimum and maximum LWP for each year correlate well. Over all areas, the GAC AVHRR LWP monthly means for NOAA-11 and NOAA-14 are generally within the 30% threshold accuracy, except for some outliers related to low absolute values for UWisc. NOAA-16 has generally lower average LWP than the earlier satellites, and shows a few months with more than 30% lower values than UWisc. Finally, the results for NOAA-18 are in good agreement with UWisc.

The morning LWP (NOAA-17) is consistently higher than in the afternoon, both for the GAC and the UWisc datasets. This demonstrates that the general thinning of stratocumulus decks during daytime is well captured. For NOAA-17, the bias values over the S-Pac are largely within the target accuracy ($\pm 15\%$), while values over the S-Atl and N-Pac areas are close to the threshold at -30% . As was indicated earlier in this section, the CM SAF retrievals based on the $1.6\text{-}\mu\text{m}$ channel yield generally lower LWP than those based on the $3.7\text{-}\mu\text{m}$ channel. This is also found in the comparisons presented here. It explains the relatively low LWP of

NOAA-16 compared to the other afternoon satellites, as NOAA-16 had the 1.6- μm channel activated during part of its lifetime (see Table 3.2).

Figure 6.56 shows time series of the RMSE of CM SAF LWP with respect to UWisc. The RMSE is close to the target, with a few outliers mostly related to low UWisc mean LWP.

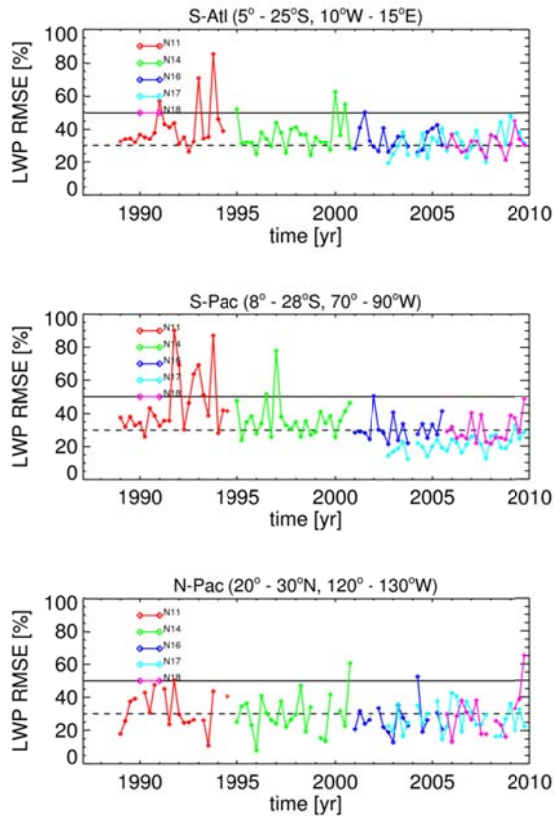


Figure 6.56 As Figure 6.55 but for the RMSE (in %).

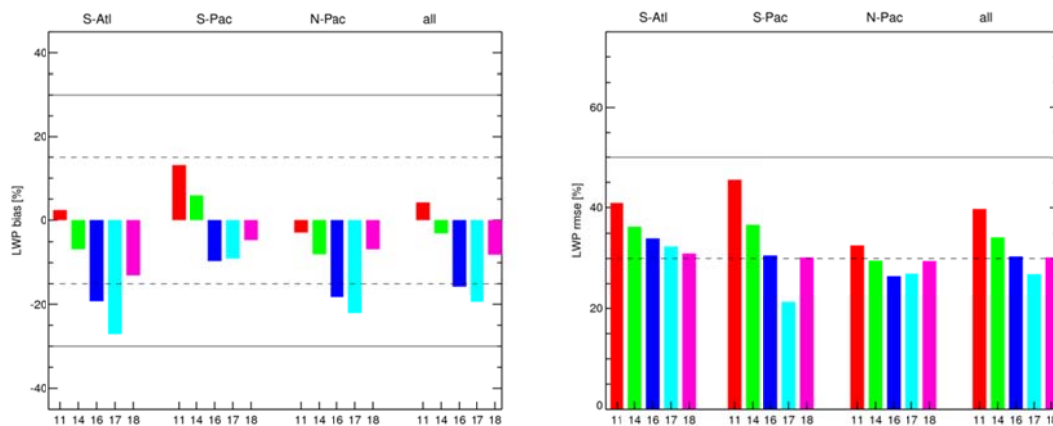


Figure 6.57 Relative bias (left panel) and RMSE (right panel) of CM SAF LWP vs UWisc over the three areas and averaged over all areas. Bar colours correspond to those in Figure 6.55 and Figure 6.56, and the NOAA satellite numbers are given as tick marks on the horizontal axis.

 	<p align="center">EUMETSAT SAF on CLIMATE MONITORING Validation Report Cloud product GAC Edition 1</p>	<p>Doc.No.:SAF/CM/SMHI/VAL/GAC/CLD Issue: 1.1 Date: 30.04.2012</p>
---	--	--

Summary of results

- Figure 6.57 summarizes the LWP evaluation against the UWisc dataset over three areas. It should be noted that – as a consequence of necessary selections of the data – these are all oceanic, stratocumulus-dominated areas.
- For NOAA-11, -14, and -18, bias values are well within the target accuracy, while for NOAA-16 and -17 (using the 1.6- μ m channel) the bias is between the target and threshold.
- The RMSE is generally around the target and in all cases below the threshold.

6.2.3.3 Summary of overall results

Based on the previously described individual studies of the performance of the CM SAF GAC LWP product, we summarize results in the following two tables (one for the Mean Error and one for the RMS error). Here, compliance with requirements is indicated by simple YES or NO statements.

Table 6.32 Overall requirement compliance of the CM SAF GAC LWP product with respect to the Mean Error. Consistency checks marked in blue.

Reference	Mean Error	Fulfilling Threshold requirements 30 %	Fulfilling Target requirements 15 %	Fulfilling Optimal requirements 5 %
UWisc	+/- 15 % (3.7 micron)	YES	YES	NO
	-(20-26) % (1.6 micron)	YES	NO	NO
PATMOS-x	0-30 % (-50 % ?)	YES	NO (?)	NO
MODIS	15 %	YES	YES	NO
ISCCP	30-50 %	NO (?)	NO	NO

	<p align="center">EUMETSAT SAF on CLIMATE MONITORING Validation Report Cloud product GAC Edition 1</p>	<p>Doc.No.:SAF/CM/SMHI/VAL/GAC/CLD Issue: 1.1 Date: 30.04.2012</p>
---	---	--

Table 6.33 Overall requirement compliance of the CM SAF GAC LWP product with respect to the RMS error. Consistency checks marked in blue.

Reference	RMS	Fulfilling Threshold requirements 50 %	Fulfilling Target requirements 30 %	Fulfilling Optimal requirements 10 %
UWisc	30-40 % (3.7 micron)	YES	NO (?)	NO
	20-30 % (1.6 micron)	YES	YES	NO
PATMOS-x	50-140 %	NO (?)	NO	NO
MODIS	35-45 %	YES	NO	NO
ISCCP	70-90 %	NO	NO	NO

We conclude that the CM SAF GAC LWP product generally fulfils threshold requirements even if RMS values are high in some cases. Target requirements are only fulfilled with respect to MODIS and UWisc (3.7 micron) datasets. However, differences are very large if comparing to ISCCP (not even within threshold requirements for neither mean bias nor RMS).

However, consideration of available uncertainty information for the references reveals that current estimations are still rather uncertain (within 15-30 %). Consequently, it is not easy to perform this validation exercise when Target requirements (15 %) are at the very limit of these uncertainties.

6.2.4 Ice Water Path (IWP)

6.2.4.1 Evaluation against PATMOS-x, MODIS, and ISCCP

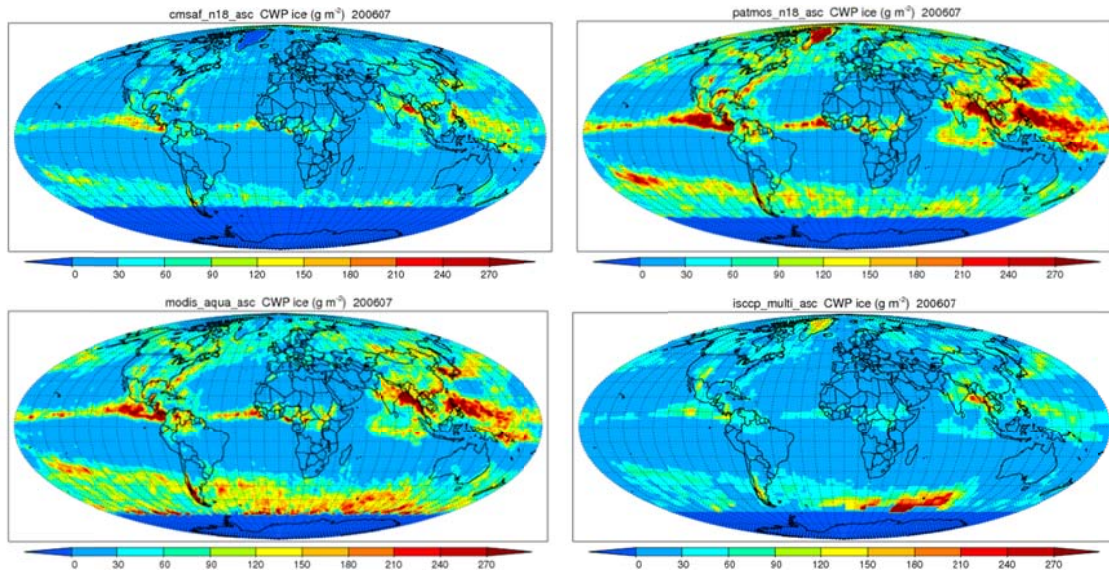


Figure 6.58 IWP for July 2006 for CM SAF (upper left), PATMOS-x (upper right), MODIS Aqua (lower left) and ISCCP (lower right).

Figure 6.58 shows the global distribution of IWP for the four datasets. It is clearly seen that, while the spatial patterns are overall quite similar, the CM SAF IWP is much lower than that of PATMOS-x and MODIS. CM SAF is in closer agreement with ISCCP, but that dataset appears to have a too low COT, thus probably a too low IWP. The CM SAF underestimation of IWP compared to PATMOS-x and MODIS is caused by a generally much lower retrieved effective radius for ice clouds when using the 3.7- μm channel. The explanation of this feature is currently unknown and will be subject of future research.

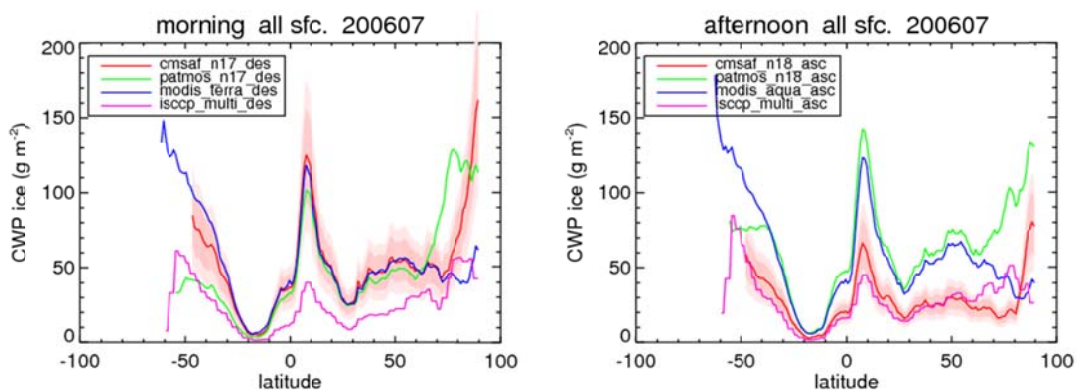


Figure 6.59 Zonal mean IWP for July 2006 for CM SAF, PATMOS-x, MODIS, and ISCCP for morning (left) and afternoon (right) satellites. The lighter and darker shaded areas around the CM SAF curve denote the threshold and target accuracy, respectively.

The zonal means as shown in Figure 6.59, left panel, reveal that for NOAA-17 there is excellent agreement between CM SAF, PATMOS-x, and MODIS-Terra. Between 40°S and 60°N the differences are very small. North of 60°N, the IWP of PATMOS-x increases very sharply, while the difference between CM SAF and MODIS-Terra remains small until 70°N. North of this latitude, the CM SAF IWP exhibits a sharp increase.

The right panel shows the pattern which was already highlighted in Figure 6.58. CM SAF largely underestimates compared to PATMOS-x and MODIS and is very close to ISCCP, which uses a climatological effective radius values rather than retrieved values. PATMOS-x and MODIS-Aqua largely agree within the latitudinal band 40°S - 60°N.

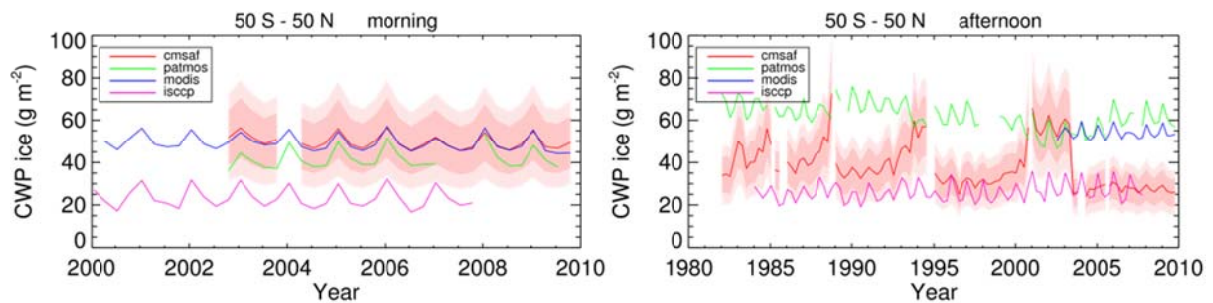


Figure 6.60 Time series of IWP covering 50°S - 50°N for CM SAF, PATMOS-x, MODIS, and ISCCP for the morning satellites (left, 2000 - 2009) and the afternoon satellites (right, 1982 - 2009). The lighter and darker shaded areas around the CM SAF curve denote the threshold and target accuracy, respectively.

Figure 6.60 shows a similar pattern as in Figure 6.59. There is good agreement between CM SAF, PATMOS-x, and MODIS for the morning satellites. However, for the afternoon satellites differences are again considerable. CM SAF has higher IWP than ISCCP, but lower than PATMOS-x (and MODIS-Aqua from 2002 onwards). Further, especially for NOAA-7, -9, and -11 the time series are dominated by the drift in equator crossing times. An interesting feature (which also showed up in the LWP time series) is the good agreement between CM SAF and MODIS/PATMOS-x between 2001 and 2003. This is (again) related to the 1.6- μ m channel which was switched on during that period and which leads to a probably better retrieved effective radius for CM SAF.

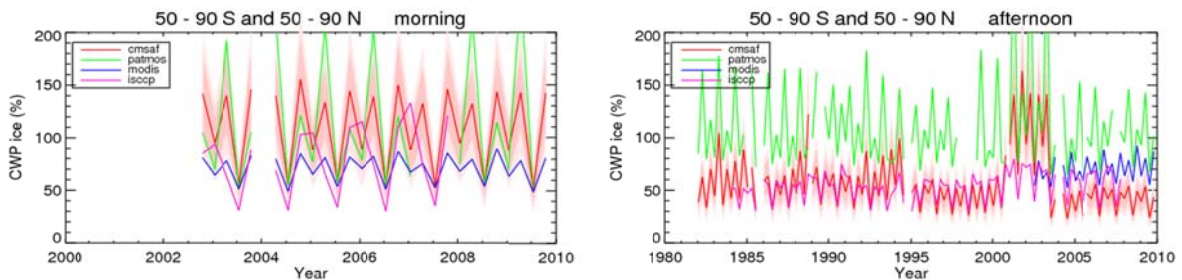


Figure 6.61 As Figure 6.60 but for the area between 50-90°S plus 50-90°N. Averages for each individual dataset were calculated based on those grid cells for which the CM SAF datasets had valid data available.

South of 50 °S and north of 50 °N retrievals are unavailable during part of the year as a consequence of too high solar zenith angles. Therefore, time series for this part of the globe have been compiled separately, using only those grid cells for which the CM SAF dataset had valid retrievals. The result for IWP is shown in Figure 6.61. For the morning satellites the results are overall consistent. For the afternoon satellites CM SAF is close to ISCCP but lower than MODIS and PATMOS-x. Notice again the large impact of the NIR channel 3a or 3b being used for the retrieval (see Table 3.2). Finally, note that – as discussed in Section 6.2.1 – the interpretation of these high-latitude results is difficult.

Summary of results

- The summary of the evaluation of IWP against PATMOS-x, MODIS, and ISCCP is presented in Figure 6.62
- The effect of the problematic effective radius retrieval using the 3.7 μm channel is clearly reflected by the bias plot in the left panel
- Relative to PATMOS-x, all satellites except NOAA-16 and -17 have a bias beyond the threshold
- Relative to MODIS, the same pattern is seen; a too large bias compared to Aqua and an excellent agreement (of NOAA-17) with Terra
- As seen earlier, CM SAF IWP is higher than ISCCP, with bias values larger than the threshold accuracy for both the morning and afternoon satellites
- All RMSE values, except relative to PATMOS-x-NOAA-17 and MODIS-Terra, are larger than the threshold,

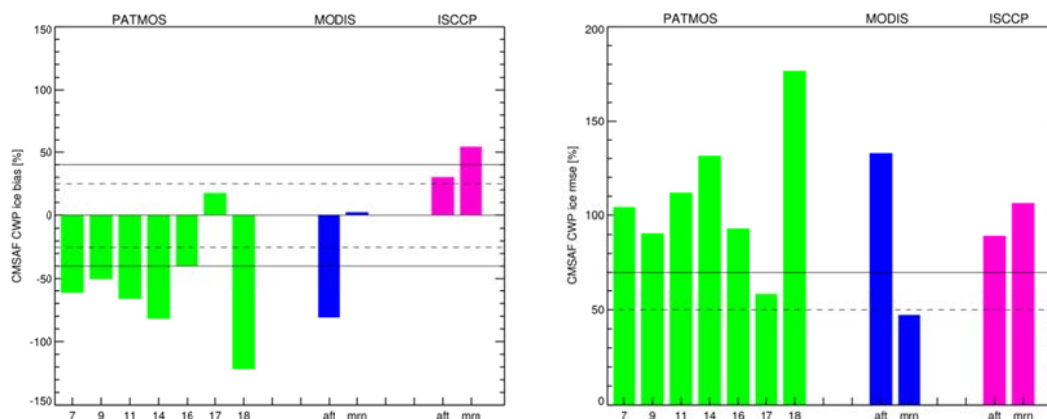


Figure 6.62 CM SAF bias (left panel) and RMSE (right panel) for IWP relative to PATMOS-x, MODIS, and ISCCP, calculated between 50 °S - 50 °N. The numbers refer to the different NOAA satellites. The abbreviations ‘aft’ and ‘mnn’ refer to afternoon and morning, respectively.

Final remark: It should be noted that IWP has a large inherent uncertainty related to the choice of ice crystal model and the parameterization used to calculate IWP from optical thickness and effective radius. This is illustrated in a recent paper by Eliasson et al. (2011). In that light, the differences found here still appear to be acceptable.

	EUMETSAT SAF on CLIMATE MONITORING Validation Report Cloud product GAC Edition 1	Doc.No.:SAF/CM/SMHI/VAL/GAC/CLD Issue: 1.1 Date: 30.04.2012
---	---	---

6.2.4.2 Summary of overall results

Based on the previously described individual studies of the performance of the CM SAF GAC LWP product, we summarize results in the following two tables (one for the Mean Error and one for the RMS error). Here, compliance with requirements is indicated by simple YES or NO statements.

Table 6.34 Overall requirement compliance of the CM SAF GAC IWP product with respect to the Mean Error. Consistency checks marked in blue.

Reference	Mean Error	Fulfilling Threshold requirements 40 %	Fulfilling Target requirements 25 %	Fulfilling Optimal requirements 10 %
PATMOS-x	-(0-120) % (+20 % ?)	NO (?)	NO	NO
MODIS	-(0-80) %	NO (?)	NO	NO
ISCCP	30-50 %	YES	NO	NO

Table 6.35 Overall requirement compliance of the CM SAF GAC LWP product with respect to the RMS error. Consistency checks marked in blue.

Reference	RMS	Fulfilling Threshold requirements 70 %	Fulfilling Target requirements 50 %	Fulfilling Optimal requirements 25 %
PATMOS-x	50-140 %	NO (?)	NO	NO
MODIS	35-45 %	YES	NO	NO
ISCCP	70-90 %	NO	NO	NO

We conclude that the CM SAF GAC IWP product only for one reference (ISCCP) clearly fulfils threshold accuracy requirements (although precision requirements are not fulfilled). For all other references, differences are too large. However, it is clear that all available references have themselves large uncertainties (30-50 %) reflecting the problematic issue of retrieving the ice water path product.

6.3 Multi-parameter product representations

6.3.1 Joint Cloud property histograms (JCH)

6.3.1.1 Evaluation against PATMOS-x

Here, we make only a limited and general investigation of how the CM SAF joint cloud property histograms perform globally in comparison to PATMOS-x results. From the individual Level 2b products, grid points with valid COT and CTP parameters are identified and displayed in joint histograms. Figure 6.63 shows joint COT-CTP histograms for CM SAF (left) and PATMOS-x (right) for January 1982-2008 for all valid grid points. Thus, the distributions here do not take into account the fraction of the observed clouds that are not seen by the other dataset. The corresponding distributions where both agree on cloud occurrence are shown later in Figure 6.64.

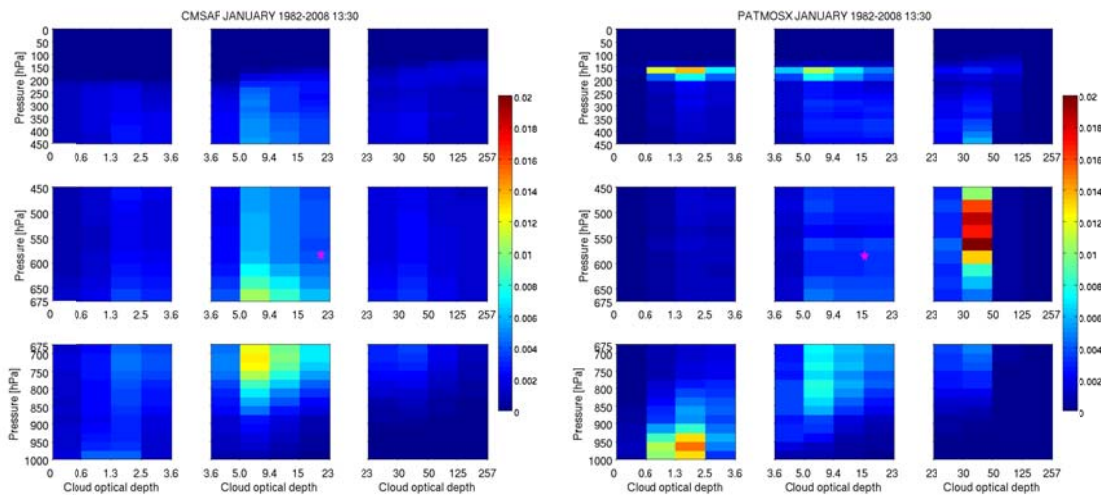


Figure 6.63 Pressure-tau histograms for afternoon 13:30 LT overpasses for January 1982-2008 for CM SAF (left) and PATMOS-x (right). All data, regardless of whether CM SAF and PATMOS-x agree on cloudy pixels, are shown. The magenta star is the arithmetic mean of CTP and COT for the specified month and years.

CM SAF clouds in Figure 6.63 tend to bin primarily into optical thickness ranges between 5 and 15 and cloud top pressures between 800 and 600 hPa. On the other hand, PATMOS-x has a much wider spread in the COT-CTP distribution, covering a wider range of both optical thickness and pressure bins. PATMOS-x does show a similar maximum as the CM SAF but in addition we notice in particular three maxima in the PATMOS-x dataset that are not seen by CM SAF:

1. Low-level optically thin clouds
(COT in range 0.6-2.6, CTP in range 900-1000 hPa)
2. Mid-level optically very thick clouds
(COT in range 30-50, CTP in range 450-600 hPa)
3. High-level optically thin clouds
(COT in range 0.6-15, CTP in range 150-200 hPa)

These results suggest that optically thin high clouds are either missed in CM SAF, and/or they are treated as mid-level clouds and given a geometric height that is lower than PATMOS-x. The significant fraction of optically thick (COT between 30 and 50) mid-level clouds for PATMOS-x (category 2 above) suggests that elevated ice covered surfaces (e.g., over Antarctica or Greenland) may have been falsely sensed as highly reflective clouds and are probably related to the large cloud fractions that PATMOS-x resolves for the northern hemisphere winter (e.g., see Figure 6.14). We also suspect that this group of clouds is linked to the specific peak for COT values close to 40 for PATMOS-x in Figure 6.47.

Clearly the mean of CTP and the mean of COT (stars in the two panels of Figure 6.63) do not give an adequate picture of the cloud top distributions seen in both data sets. The other two categories (1 and 3) of the PATMOS-x distribution are more difficult to judge whether they are realistically described or not.

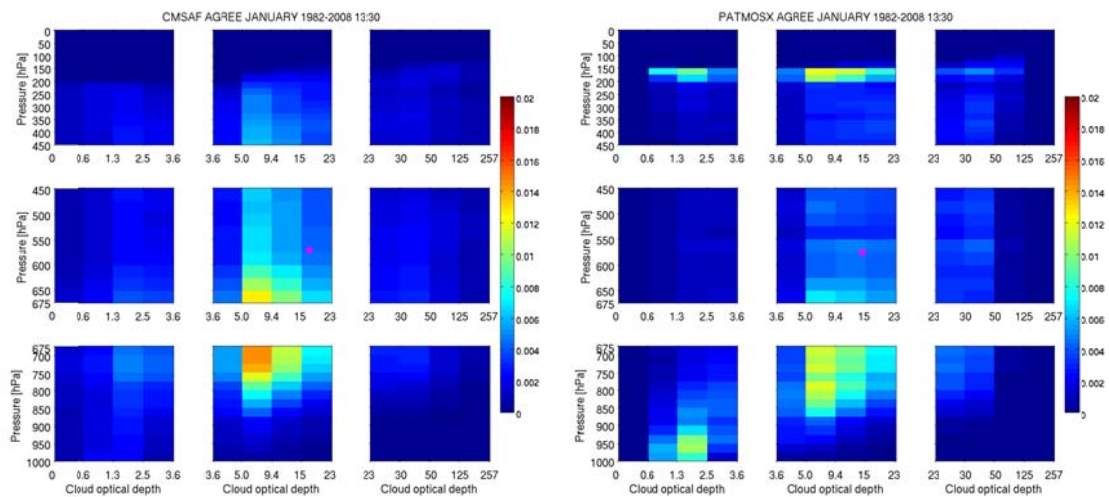


Figure 6.64 Same as Figure 6.63, except distributions are only shown for only observations when CM SAF and PATMOS-x both agree on cloud presence.

For the situation when we require agreement on cloud presence of both datasets in Figure 6.64, the numbers change for CM SAF but the overall distribution patterns remain the same. PATMOS-x tends to have a larger fraction of low-levels clouds in the mid optical thickness range, in closer agreement with CM SAF. There is also a slight increase in the mid-level clouds for PATMOS-x for COT ranging from 3.6 to 23, also in better agreement with CM SAF. However, CM SAF is still missing the large fraction of PATMOS-x identified high clouds. We can also clearly see that the clouds defined as category 2 in Figure 6.63 are now completely absent. Thus, these clouds represent clearly pixels which PATMOS-x registers as cloudy while CM SAF is clearly not cloudy or unable to compute cloud top pressure. There is also a reduction of the frequency of PATMOS-x clouds of the previous category 1 indicating that a large fraction of these clouds are not observed at all by CM SAF.

	<p align="center">EUMETSAT SAF on CLIMATE MONITORING Validation Report Cloud product GAC Edition 1</p>	<p>Doc.No.:SAF/CM/SMHI/VAL/GAC/CLD Issue: 1.1 Date: 30.04.2012</p>
---	--	--

Summary of results

- The visualization of two-dimensional pictures of the global distribution of COT and CTP reveals features that cannot easily be interpreted from pure global averages (i.e., standard Level 3 products)
- When looking at the full dataset (i.e., regardless of if both datasets see the same clouds or not), PATMOS-x show high frequencies for three groups of clouds that are more or less absent in the CM SAF dataset:
 1. Low-level very thin clouds
 2. Mid-level very thick clouds
 3. High-level very thick clouds
- When looking at the common dataset (i.e., requiring that both datasets see the same clouds), it becomes clear that the second category Mid-level very thick clouds only exists in the PATMOS-x dataset
- Cloud distributions becomes more similar in the common dataset but CM SAF still misses large parts of categories 1 and 3 above

6.3.1.2 Evaluation against MODIS and ISCCP

We also provide a limited comparison of two-dimensional Joint Cloud Property Histograms of CM SAF against MODIS and ISCCP for one particular month (Figure 6.65). The histograms are shown in the available binning of CTP and COT, which are different for all three products. For the ‘all-cloud’ histograms CM SAF AVHRR and MODIS seem to give the similar messages, with having the most clouds as low-level clouds with CTP between 680 and 950 hPa and COT between 2 and 20, while ISCCP has another maximum in the distribution for mid-level clouds (440 to 680 hPa) and COT of 10 to 20. Also in the mid and upper troposphere, the CM SAF does not deviate a lot from MODIS with providing COT of 4 to 20 for clouds at these heights. For a better comparison in the future, the binning of the products is suggested to be adjusted.

The histograms also shown for liquid cloud only and ice clouds only, for CM SAF and MODIS. The agreement of CM SAF to MODIS for liquid clouds is very good. Ice clouds seem to be more frequent at higher altitudes in MODIS.

In general, these comparisons show the good quality of the Joint Cloud property Histograms, when comparing to MODIS, which can be assumed to be a more reliable reference for this product than ISCCP.

6.3.1.3 Discussion

No specific requirements have been defined for this product because it is just a different representation of already existing products. However, we took the opportunity here to illustrate the advantages of this product approach compared to the use of traditional Level 3 values at each grid point. Clearly, a user gets additional value from this type of product which has already been demonstrated by the frequent use of joint histograms for evaluation of climate model information (see <http://cfmip.metoffice.com/COSP.html>).

The CM SAF JCH product is delivered as distributions for each grid point – thus, any user may compose cloud distribution statistics for any region size on the globe by simple aggregation of grid point values.

For the next GAC Edition, we will inter-compare existing JCH products more extensively.

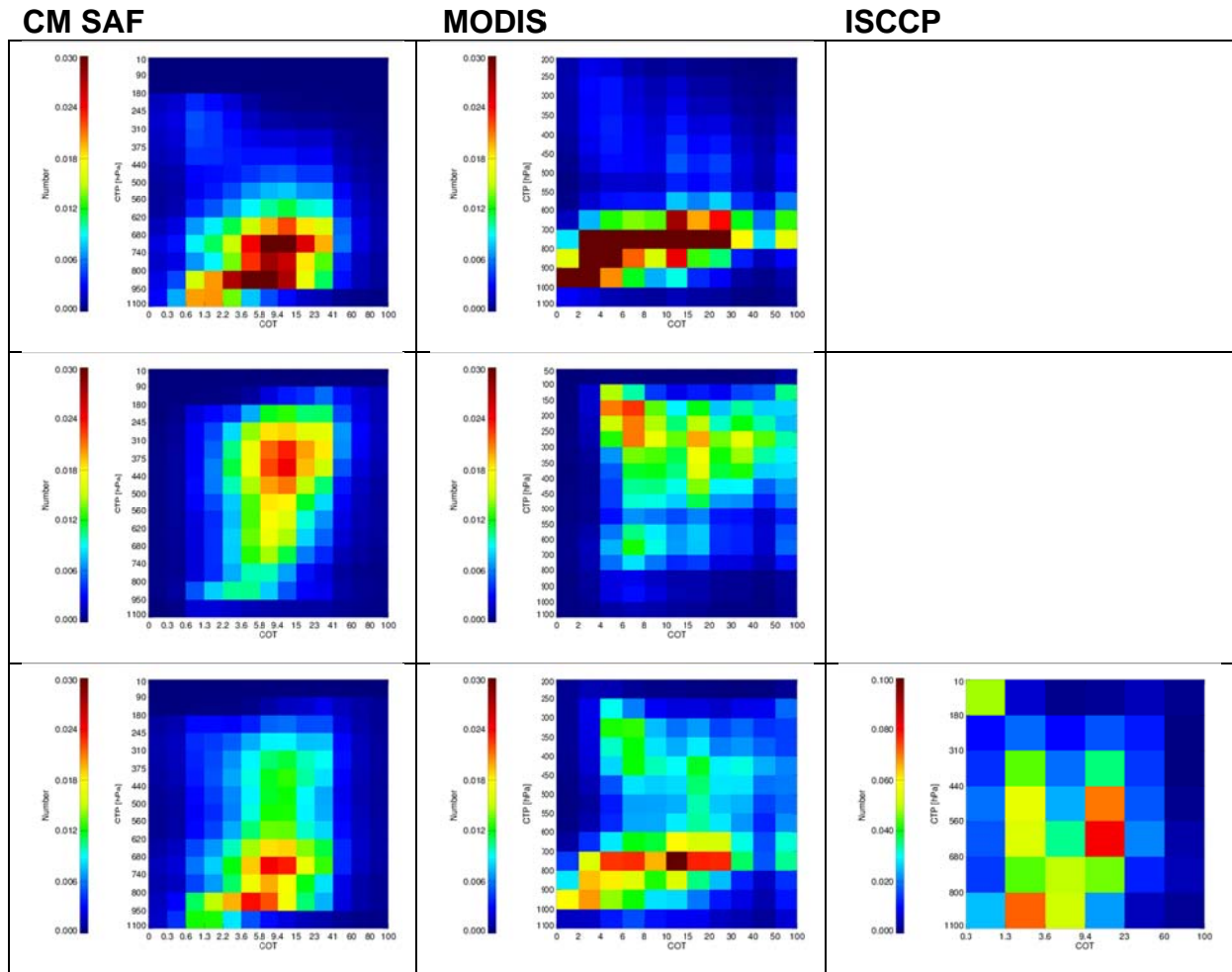


Figure 6.65 Pressure-tau histograms of CMSAF (left column), MODIS-AQUA (middle column), and ISCCP (right column) for liquid clouds (upper row), ice clouds (middle row) and all clouds (bottom row), all for March 2007. The histograms are presented in relative numbers.

7 Decadal stability

In the PRD (*AD 1*) there are also requirements for the stability of results for some (but not all) of the cloud parameters. Here, stability refers to if cloud parameter accuracy changes over time (not to be misinterpreted as the stability of the parameter itself which is directly related to potential climate trends). These are listed in Table 7.1.

Table 7.1 *Target requirements on stability of product accuracies as expressed in the PRD (AD 1).*

Product	Stability requirement (target)
Cloud Fractional Cover (CFC)	Not defined
Cloud Top Height (CTH)	Not defined
Cloud Top Pressure (CTP)	Not defined
Cloud Optical Thickness (COT)	10 % per decade
Cloud Phase (CPH)	3 % per decade
Liquid Water Path (LWP)	10 % per decade
Ice Water Path (IWP)	5 % per decade
Joint Cloud Histogram (JCH)	n/a

It is clear that for evaluating stability requirements the demands on the available reference observations are very strict: Error characteristics for the reference observation must be well-specified and known and should not exhibit any internal trend (i.e., be homogeneous). Our judgement is that none of the available reference datasets are actually suitable in this context (i.e., all of them include inherent variability in quality related to numerous and different kind of problems, especially sampling problems). Thus, the task to evaluate stability requirements is immense and hardly achievable.

Nevertheless, we will try here to at least give some statements on our impressions based on the previously described evaluation results for each individual product. For the CFC product, we also first present some specific results addressing the stability question and which also illustrate the specific problems associated with the analysis of product stability.

In order to evaluate the temporal stability of the AVHRR-GAC CFC product, the SYNOP matchup dataset (described earlier in Section 6.1.1.1) was reduced to only those stations for which monthly mean values are available throughout the entire time period. 165 stations were found to fulfil this criterion (see Figure 7.1). As to be expected these stations are spatially limited to Europe and the U.S. The resulting time series of the cloud cover for both AVHRR GAC and SYNOP observations as well as the mean error and the bias-corrected RMS error are shown in Figure 7.2. The typical Northern Hemisphere seasonal cycle of CFC with a maximum cloud amount in winter and a minimum in summer is clearly depicted by both data sets. Both bias and bias-corrected RMS stay in general well below the target requirements on accuracy and precision of 10 % and 20 % cloud amount respectively, except for several months in 1983 when the bias temporarily increases up to 15%.

SYNOP stations covering 1982–2009

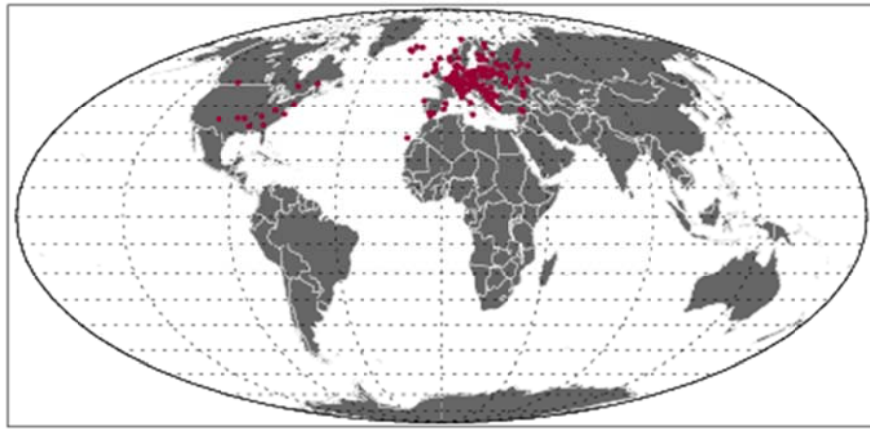


Figure 7.1 Availability of SYNOP stations (red spots) with observations made during the entire AVHRR GAC period 1982-2009.

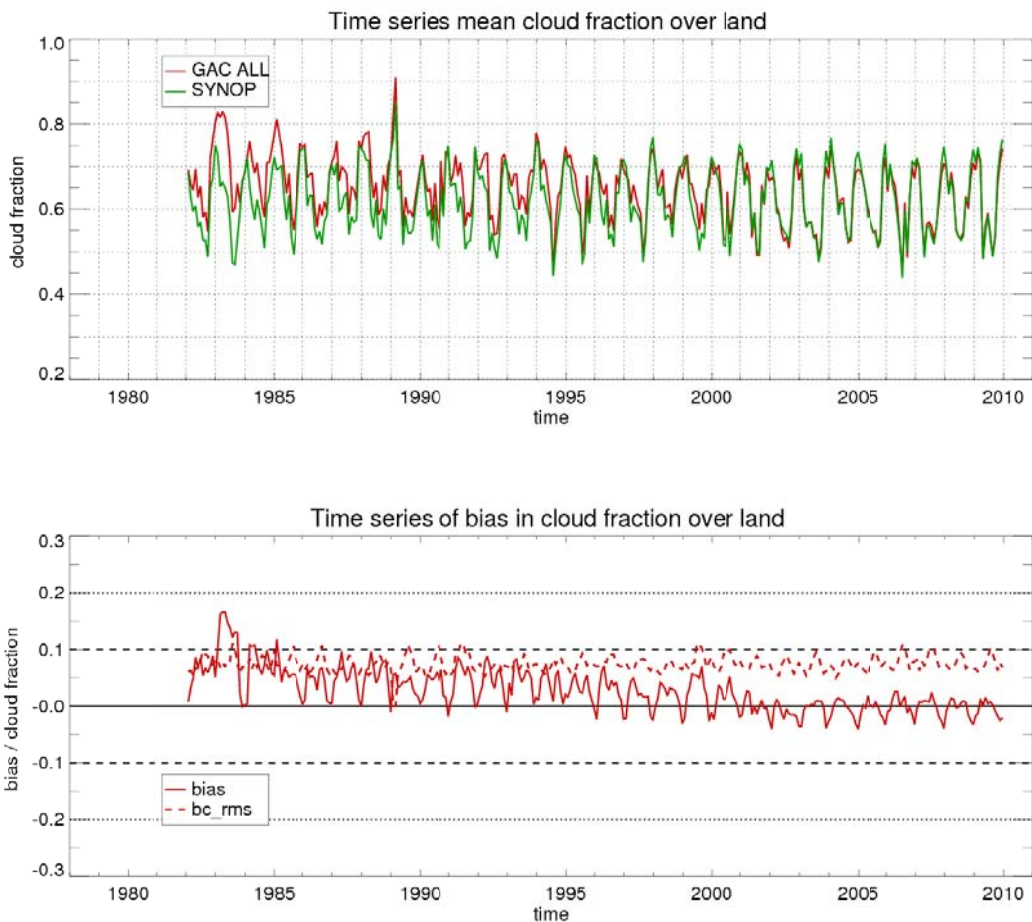



Figure 7.2 Time series of cloud fraction (CFC, top panel) and the mean error and the RMS error (bottom panel) compared to observations from SYNOP stations available for the full period 1982-2009 (see Figure 7.1).

	EUMETSAT SAF on CLIMATE MONITORING Validation Report Cloud product GAC Edition 1	Doc.No.:SAF/CM/SMHI/VAL/GAC/CLD Issue: 1.1 Date: 30.04.2012
---	---	---

The bias-corrected RMS stays stable over time whereas the CFC bias decreases with time from about 10 % in the beginning of the period to about 3 % at the end of the period. This indicates a decadal trend of about 2-3 % regarding the CFC mean error. So, is this a representative and true stability estimate? We would say unfortunately not since the results seem very well correlated with the changes in the availability of polar satellite data. This availability was restricted to one afternoon-night satellite in the beginning of the dataset period but changing to 3-4 satellites in both afternoon-night and morning-evening orbits at the end of the period (as previously illustrated in Figure 6.12). Since the cloud detection capability apparently is tightly linked to the time of day (e.g., see Table 6.5 in Section 6.1.1.2) such changes in the observation setup will influence total accuracy levels. Thus, a representative value of decadal stability measures seems still very difficult to achieve.

Some further clues could be achieved if trying to separate results to be valid for only afternoon-night satellites or morning-evening satellites. However, this reduces then the available SYNOP dataset seriously which make inter-comparisons even more difficult. But, we can at least try to plot the CM SAF GAC results as separated into daytime and night-time portions to see if the trends we have seen in results come from a changed distribution of observations over the day. These specially selected results are shown in the following two figures.

Figure 7.3 shows CM SAF GAC results for exclusive daytime conditions (solar zenith angles below 80 degrees) compared to the reference (full-day) datasets from ISCCP and MODIS. In Section 6.1.1.5 we noticed in Figure 6.23 that the Mean Deviation showed a clear trend over the full period, especially when compared with ISCCP results. However, when only comparing with CM SAF daytime results, this trend is practically gone as shown in Figure 7.3 for the global results. The same is actually true for the night-time only results as seen in Figure 7.4. The only difference between the two cases is that for daytime we have almost zero bias compared to ISCCP while for night-time results the bias is clearly negative. For the MODIS comparisons the bias is nearly zero for daytime and slightly negative for night time, but rather stable for both over time.

From this specific investigation we conclude that the CFC accuracy trends seen for the full dataset over time, when compared to various reference sources (including also SYNOP as shown in Figure 7.2), are largely explained by changes in the frequency of observations during the day. Because of the different quality characteristics day and night, such changes in observation frequencies make it very difficult to make realistic estimations of the stability of accuracy and precision parameters. This does not only affect the CFC product. For example, the same kind of trends seen for the CTO product in Figure 6.36 is likely to be explained in a similar way.

Finally, for the CPP products, which are only retrieved during daytime, the situation is different but in no way easier to handle. Previous results in Section 6.2 show rather stable results over time but since accuracies themselves are very different depending on the chosen reference (especially for the LWP and IWP parameters) it seems rather impossible to discuss and make conclusions about the true stability of corresponding accuracy parameters. Also here we have sampling aspects that complicate the analysis further (i.e., differences caused by retrievals made using either the 1.6 micron or the 3.7 micron channel).

Consequently, we support the idea that stability requirements are important but in reality it is clear that the analysis of such properties is very difficult, if even possible at all. We welcome a further discussion of this topic.

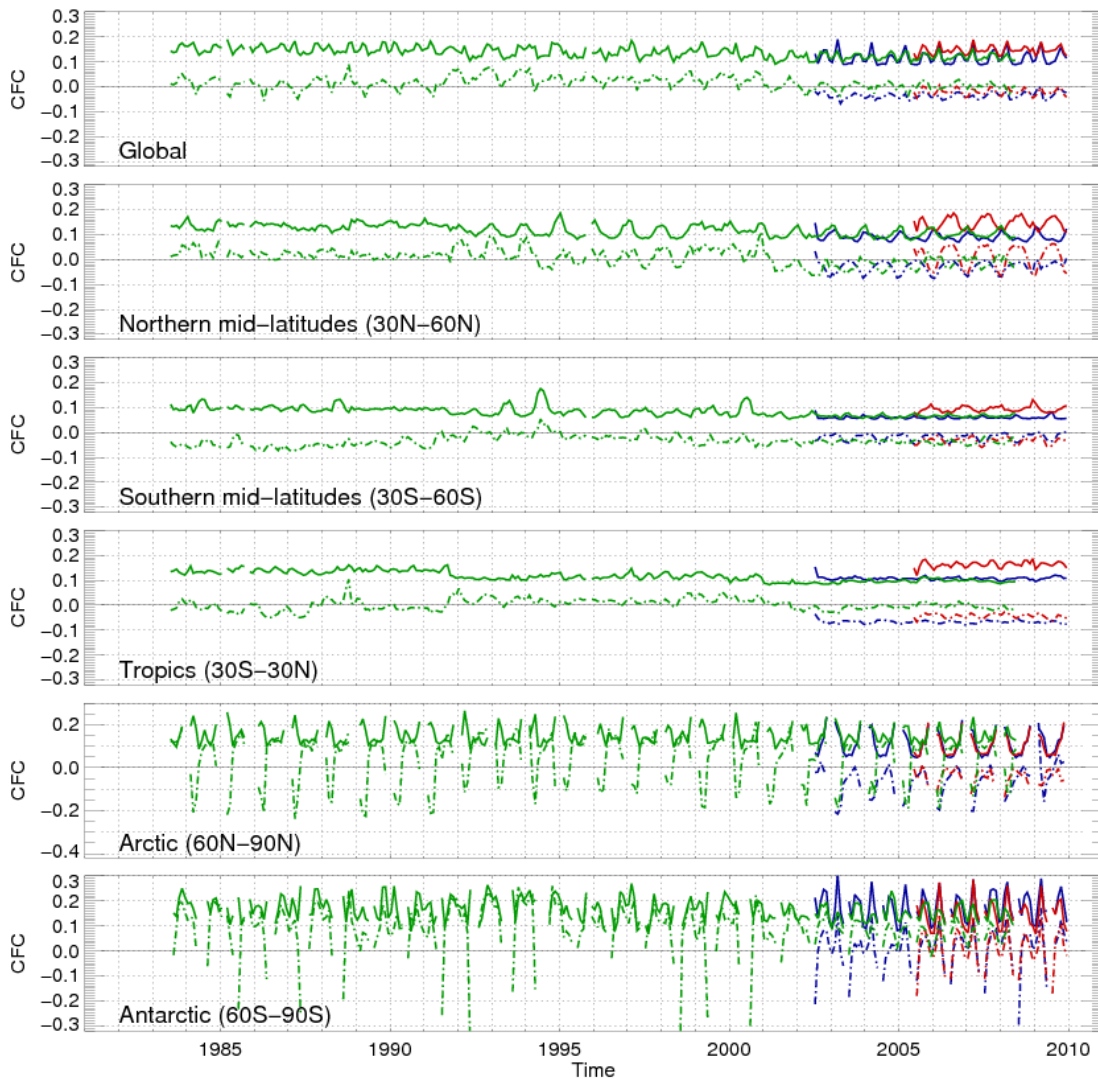


Figure 7.3 Time series (same representation as in Figure 6.23) of relative mean (dashed lines) and standard deviation (solid lines) of CFC of CM SAF compared to ISCCP (green), MODIS/Terra (blue) and MODIS/Aqua (red) but only for daytime CM SAF results. Shown are the global values (upper panel) and the separation into various latitude-bands.

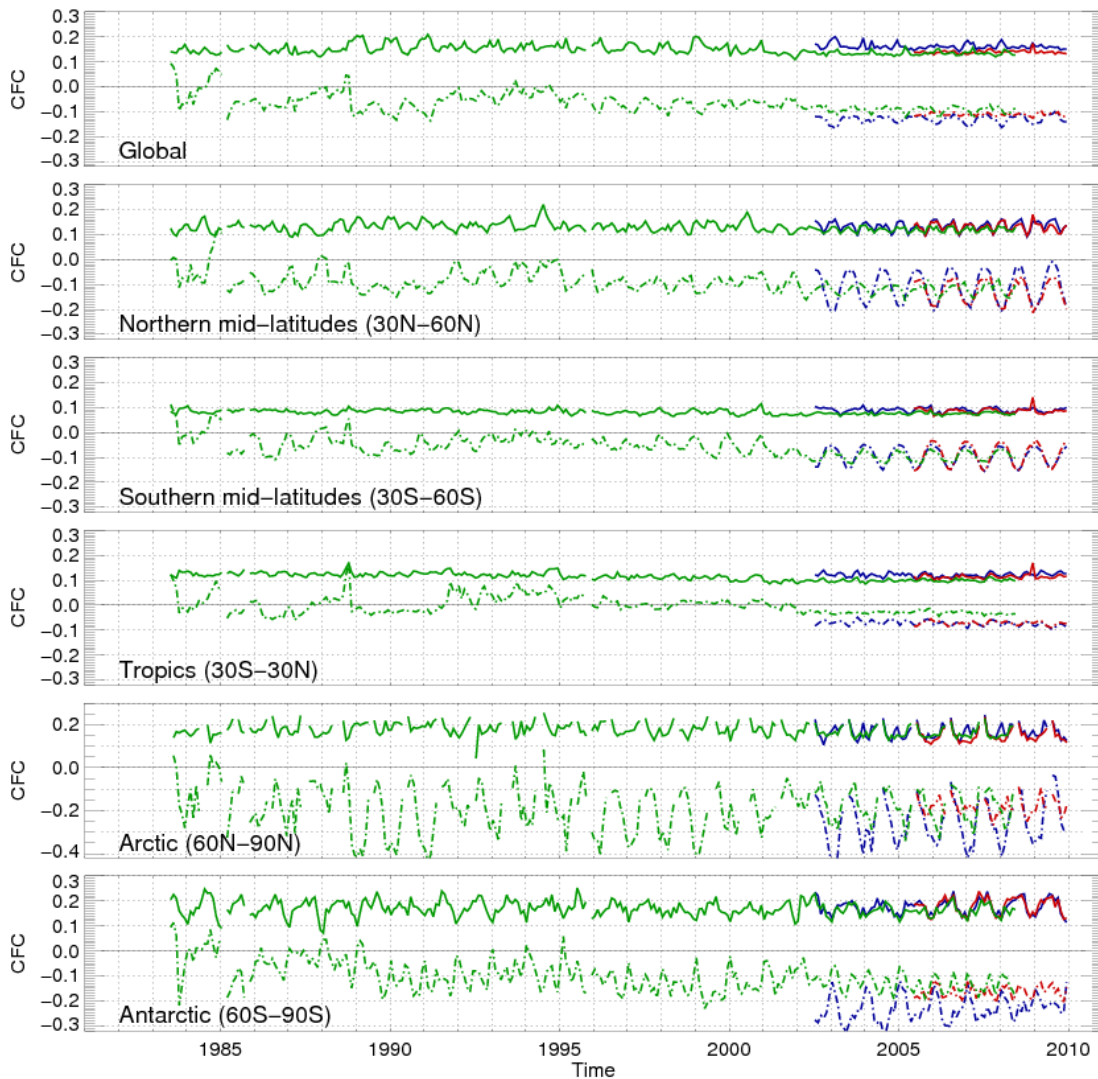



Figure 7.4 Time series (same representation as in Figure 6.23) of relative mean (dashed lines) and standard deviation (solid lines) of CFC of CM SAF compared to ISCCP (green), MODIS/Terra (blue) and MODIS/Aqua (red) but only for night-time CM SAF results . Shown are the global values (upper panel) and the separation into various latitude-bands.

 	<p align="center">EUMETSAT SAF on CLIMATE MONITORING Validation Report Cloud product GAC Edition 1</p>	<p>Doc.No.:SAF/CM/SMHI/VAL/GAC/CLD Issue: 1.1 Date: 30.04.2012</p>
---	--	--

8 Conclusions

An extensive validation of cloud products from the CM SAF GAC Edition 1 dataset has been presented in this report. The reference datasets were taken from completely independent and different observation sources (e.g. SYNOP, CALIPSO-CALIOP, SSM/I and AMSR-E) as well as from similar satellite-based datasets from passive visible and infrared imagery (MODIS, ISCCP and PATMOS-x). Studies were made based on a mix of Level 2 and Level 3 products, also addressing some specific aspects affecting inter-comparisons (e.g., cloud detection capabilities for very thin clouds). More in depth inter-comparisons were also made with the PATMOS-x dataset because of the close relation (being also based on AVHRR GAC data). A limited study inter-comparing several global datasets simultaneously utilizing datasets prepared within GEWEX was also accomplished for the period 2005-2009.

Table 8.1 and 8.2 below give an overview of all results with respect to the target accuracies and precisions in AD 1. More information about relations to threshold and optimal requirements in *RD 1* is given in each individual product section (i.e., sections 6.1-6.3).

Validation results can be summarized as follows for each individual cloud product in the CM SAF GAC dataset (see Table 8.1 and 8.2 for details):

- **Fractional Cloud Cover (CFC)**
 - The CM SAF GAC CFC product fulfils the Threshold requirements when compared with all references
 - The product also fulfils the Target requirement in most cases (the only exception occurs when comparing with MODIS results)
 - Optimal requirements are fulfilled when comparing with SYNOP results, with CALIPSO results and with PATMOS-x results

- **Cloud Top level (CTO)**
 - The CM SAF GAC CTO product, expressed and evaluated as CTP, fulfils all levels of requirements for all references
 - However, one exception occurs when comparing with unfiltered CALIPSO results when none of the requirements is fulfilled
 - The latter result is explained by the fact that for the thinnest detected clouds (with $COT < 0.3$), corrections for the semi-transparency effect is still a major issue

- **Cloud Thermodynamic Phase (CPH)**
 - The CM SAF GAC CPH product fulfils threshold requirements against most references except against ISCCP
 - Target or Optimal requirements are generally not fulfilled (except if comparing against the MODIS IR method)

- **Cloud Optical Thickness (COT)**
 - The CM SAF GAC COT product fulfils threshold and target requirements when compared to PATMOS-x and to MODIS
 - However, differences are very large if comparing with ISCCP (not even within threshold requirements)



 	<p align="center">EUMETSAT SAF on CLIMATE MONITORING Validation Report Cloud product GAC Edition 1</p>	<p>Doc.No.:SAF/CM/SMHI/VAL/GAC/CLD Issue: 1.1 Date: 30.04.2012</p>
---	---	--

Table 8.1 Summary of validation results compared to target accuracies for each cloud product. Notice that accuracies are given as Mean errors or Biases (both terms being equivalent) valid for both negative and positive deviations. Consistency checks marked in blue.

Product	Accuracy requirement (mean error or bias)	Achieved accuracies
Cloud Fractional Cover (CFC)	10 % (absolute)	3.6 % (SYNOP) -10 % (CALIPSO) -4.1 % (PATMOS-x) -10 % to -20 % (MODIS) 0 % to -12 % (ISCCP)
Cloud Top Height (CTH)	1200 m	-2661 m (CALIPSO)
Cloud Top Pressure (CTP)	110 hPa	-20 to 60 hPa (PATMOS-x) -40 to -50 hPa (MODIS) -20 to 60 hPa (ISCCP)
Cloud Optical Thickness (COT)	15 %	3-20 % (PATMOS-x) -5 % to -10 % (MODIS) 50-60 % (ISCCP)
Cloud Phase (CPH)	5 % (absolute)	7-15 % (PATMOS-x) 3-20 % (MODIS) 12-15 % (ISCCP)
Liquid Water Path (LWP)	15 %	+15 % to -26 % (UWisc) 0-30 % (PATMOS-x) 15 % (MODIS) 30-50 % (ISCCP)
Ice Water Path (IWP)	25 %	0 % to -120 % (PATMOS-x) 0 % to -80 % (MODIS) 30-50 % (ISCCP)
Joint Cloud Histogram (JCH)	n/a	n/a




 	<p align="center">EUMETSAT SAF on CLIMATE MONITORING Validation Report Cloud product GAC Edition 1</p>	<p>Doc.No.:SAF/CM/SMHI/VAL/GAC/CLD Issue: 1.1 Date: 30.04.2012</p>
---	---	--

Table 8.2 Summary of validation results compared to target precisions for each cloud product. Consistency checks marked in blue.

Product	Precision requirement (RMS)	Achieved precisions
Cloud Fractional Cover (CFC)	20 % (absolute)	11 % (SYNOP) n/a (CALIPSO) 2.6 % (PATMOS-x) 20-27 % (MODIS) 10-20 % (ISCCP)
Cloud Top Height (CTH)	2000 m	n/a (CALIPSO)
Cloud Top Pressure (CTP)	130 hPa	40 hPa (PATMOS-x) 80 hPa (MODIS) 90 hPa (ISCCP)
Cloud Optical Thickness (COT)	30 %	25-45 % (PATMOS-x) 30 % (MODIS) 80-90 % (ISCCP)
Cloud Phase (CPH)	10 % (absolute)	15-20 % (PATMOS-x) 12-25 % (MODIS) 25 % (ISCCP)
Liquid Water Path (LWP)	30 %	25-40 % (UWisc) 50-140 % (PATMOS-x) 35-45 % (MODIS) 70-90 % (ISCCP)
Ice Water Path (IWP)	50 %	60-180 % (PATMOS-x) 45-90 % (MODIS) 90-110 % (ISCCP)
Joint Cloud Histogram (JCH)	n/a	n/a

	<p align="center">EUMETSAT SAF on CLIMATE MONITORING Validation Report Cloud product GAC Edition 1</p>	<p>Doc.No.:SAF/CM/SMHI/VAL/GAC/CLD Issue: 1.1 Date: 30.04.2012</p>
---	--	--

- **Liquid Water Path (LWP)**

- The CM SAF GAC LWP product generally fulfils threshold requirements even if RMS threshold values are exceeded in some cases
- Target requirements are fulfilled with respect to MODIS and UWisc datasets (for the latter when evaluating LWP products based on the 3.7 micron channel)
- Differences are very large if comparing to ISCCP (not even within threshold requirements for neither mean error nor RMS error)

- **Ice Water Path (IWP)**



- The CM SAF GAC IWP product only fulfils threshold accuracy requirements for one reference (ISCCP) (although precision requirements are not fulfilled)
- For all other references, differences are too large.

- **Joint Cloud property Histograms (JCH)**

- This product is excluded from specific requirement testing because of being composed by two already existing products (COT and CTP)
- Nevertheless, a demonstration of the product in inter-comparisons with PATMOS-x, MODIS and ISCCP products shows that it provides added value to the products by giving important clues on the statistical distribution of the involved parameters
- It is believed that the access to this product representation would greatly enhance the usefulness of the CM SAF GAC products in some applications (e.g., climate model evaluation)


Final Remarks

It should be emphasized that this report describes results from the first global processing of AVHRR GAC data in the CM SAF (GAC Edition 1). The technical feasibility of producing such a dataset has been demonstrated. Furthermore, the actual content of the dataset is in some aspects rather advanced (e.g., products are available for every satellite, results are separated into day and night portions, results are also available in two separate polar grids and for each individual grid point Joint Cloud property Histograms are provided - as described in RD 1). However, it is evident that some problems were encountered in the preparation of the dataset which is reflected in a degraded quality for some products and for some regions. The most evident problem is related to cloud detection over semi-arid areas where a systematic mis-classification of cloud-free land surfaces as being cloudy has resulted. The problem is understood as being caused by an insufficient dynamical adaptation of visible thresholds in a region changing from being completely dry to completely vegetated. This problem will be solved for the next GAC Edition. More problematic is the systematic underestimation of cloud amounts found during night (especially over the Polar Regions) and the systematic biases in cloud top levels for both low-level and high-level clouds. The study also reveals some discrepancies for CPP products (especially the IWP product) which need to be addressed further. All these aspects will have to be studied carefully when preparing the next edition of the GAC dataset in the CDOP-2 phase.

 	<p align="center">EUMETSAT SAF on CLIMATE MONITORING Validation Report Cloud product GAC Edition 1</p>	<p>Doc.No.:SAF/CM/SMHI/VAL/GAC/CLD Issue: 1.1 Date: 30.04.2012</p>
---	--	--

References

- Chepfer H., S.Bony, D. M. Winker, G. Cesana, J.L. Dufresne, P. Minnis, C.J. Stubenrauch, S. Zeng, 2010: The GCM Oriented CALIPSO Cloud Product (CALIPSO- GOCCP), *J. Geophys. Res.*, 105, D00H16, doi:10.1029/2009JD012251.
- Eliasson, S., S. A. Buehler, M. Milz, P. Eriksson, and V. O. John, 2011: Assessing observed and modelled spatial distributions of ice water path using satellite data, *Atm. Chem. Phys.*, 11, 375-391, doi:10.5194/acp-11-375-2011.
- GCOS, 2006: SYSTEMATIC OBSERVATION REQUIREMENTS FOR SATELLITE-BASED PRODUCTS FOR CLIMATE
<http://www.wmo.int/pages/prog/gcos/Publications/gcos-107.pdf>
- Karlsson, K.-G., 2003: A ten-year cloud climatology over Scandinavia derived from NOAA AVHRR imagery. *Int. J. Climatol.*, 23, 1023-1044.
- Karlsson, K-G. and A. Dybbroe, 2009: Evaluation of Arctic cloud products from the EUMETSAT Climate Monitoring Satellite Application Facility based on CALIPSO-CALIOP observations, *Atmos. Chem. Physics D.*, 9, acp-2009-298.
- Heidinger, A.K., W.C. Straka, C.C. Molling, J.T. Sullivan and X.Q. Wu, 2010: Deriving an inter-sensor consistent calibration for the AVHRR solar reflectance data record. *Int. J. Rem. Sens.*, 31(24), 6493-6517.
- Heidinger, A.K., M.J. Pavolonis, 2009: Gazing at Cirrus Clouds for 25 Years through a Split Window. Part I: Methodology. *J. Appl. Meteor. Climatol.*, 48, 1100–1116. doi: 10.1175/2008JAMC1882.1
- Heidinger, A.K., M.D. Goldberg, A. Jelenak and M.J. Pavolonis, 2005: A new AVHRR cloud climatology, *Proc. SPIE 5658*, 197, doi: 10.1117/12.579047.
- Heidinger, A.K., A.T. Evan, M. J. Foster and A. Walther, 2012: A Naïve Bayesian Cloud Detection Scheme Derived from CALIPSO and Applied within PATMOS-x, *J. Appl. Met. and Clim.*, doi: <http://dx.doi.org/10.1175/JAMC-D-11-02.1>
- Ignatov, A., I. Laszlo, E.D. Harrod, K.B. Kidwell, and G.P. Goodrum, 2004: Equator crossing times for NOAA, ERS, and EOS sun-synchronous satellites. *Int. J. Remote Sensing*, 25, 5255–5266, doi:10.1080/01431160410001712981.
- Mittaz, P.D. and R. Harris, 2009: A Physical Method for the Calibration of the AVHRR/3 Thermal IR Channels 1: The Pre-launch Calibration Data. *J. Atmos. Ocean. Tech.*, 26, 996-1019, doi: 10.1175/2008JTECHO636.1
- Pavolonis, M.J., A.K. Heidinger, T.Uttal, 2005: Daytime Global Cloud Typing from AVHRR and VIIRS: Algorithm Description, Validation, and Comparisons. *J. Appl. Meteor.*, 44, 804–826. doi: 10.1175/JAM2236.1
- O'Dell, C.W., F.J. Wentz, and R. Bennartz, 2008: Cloud Liquid Water Path from Satellite-Based Passive Microwave Observations: A New Climatology over the Global Oceans. *J. Climate*, 21, 1721–1739, doi:10.1175/2007JCLI1958.1
- Rossow, W.B., and R.A. Schiffer, 1991: ISCCP cloud data products. *Bull. Amer. Meteorol. Soc.*, 71, 2-20.

 	EUMETSAT SAF on CLIMATE MONITORING Validation Report Cloud product GAC Edition 1	Doc.No.:SAF/CM/SMHI/VAL/GAC/CLD Issue: 1.1 Date: 30.04.2012
---	---	---

- Rossow, W. B., and R. A. Schiffer, 1999: Advances in understanding clouds from ISCCP, *Bull. Amer. Meteorol. Soc.*, 80, 2261-2287.
- Rossow, W.B., A.W. Walker, D.E. Beuschel, and M.D. Roiter, 1996: International Satellite Cloud Climatology Project (ISCCP) Documentation of New Cloud Datasets. WMO/TD-No. 737, World Meteorological Organization.
- Shupe, M.D., V.P. Walden, E. Eloranta, T. Uttal, J.R. Campbell, S.M. Starkweather, and M. Shiobara, 2011: Clouds at Arctic Atmospheric Observatories. Part I: Occurrence and Macrophysical Properties, *J. Appl. Meteorol. Climatol.*, **50**, 626-644.
- Stubenrauch, C., W.B. Rossow and S. Kinne, 2012: Assessment of Global Cloud Datasets from Satellite – A project of the World Climate Research Programme Global Energy and Water Cycle Experiment (GEWEX), draft report, pp 173.
- Thomas, S.M., A.K. Heidinger, M.J. Pavolonis, 2004: Comparison of NOAA's Operational AVHRR-Derived Cloud Amount to Other Satellite-Derived Cloud Climatologies. *J. Climate*, **17**, 4805–4822. doi: 10.1175/JCLI-3242.1